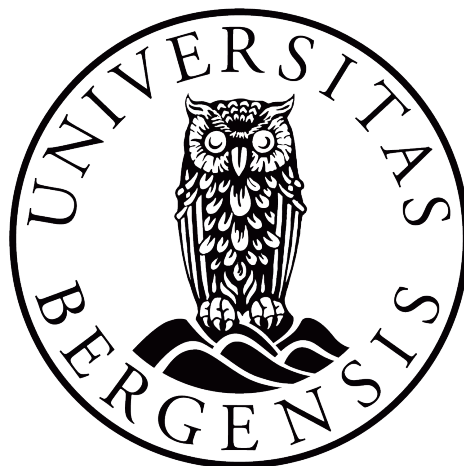


Microplastic in naturally exposed cod from a plastic polluted coastal ecosystem

An investigation of the evidence of microplastic
bioaccumulation



Master thesis

by

Emilie Hæggernes

Department of chemistry

University of Bergen

2022

Acknowledgement

Finally, it is my turn to deliver my master thesis. Many people deserve a big thank you for the help and support during these two years. Firstly, I would like to thank my supervisors Marte Haave from NORCE and Department of chemistry at the university of Bergen and Alessio Gomiero from NORCE.

Marte Haave, thank you for guiding me through my master thesis. Your passion and commitment for microplastic research is extraordinary and have rubbed off on me. Thank you for allowing me to deep dive into an area never investigated and provided me with a place in the world of microplastic research. I'm very honored to have worked with you during these two years.

Alessio, thank you for giving me 6 educational months in NORCE Stavanger. Your knowledge in the microplastic field of research is unique. Thank you for sharing knowledge about your own developed methods and always being available for questions and help in the Plastlab.

In addition, thank you to the people working in NORCE Stavanger for including me and sharing your knowledge on research and the important work that you do. Especially, a big thank you to Veslemøy and Adrián for general contribution and assistance during lab work.

I would also like to thank Kenneth Bruvik from Norwegian Hunters and Anglers' Association/NJFF for providing samples and essential knowledge and pupils from NJFF/TAM for catching cod for the study.

I feel the quote "it takes a village" is an appropriate description for my amazing support system of friends and family. Lotte and Saron, thank you to for the well needed lunch breaks at NORCE Bergen, for reading through my thesis and supporting me through this, at times, stressful period in my life. Nadwa and Renate, thank you for being great friends and support in good times and bad. Finally, a big thank you to my family for being a safe haven and providing that unique support only a family can give.

Emilie Hæggernes
Bergen, September 2022

Abstract

Microplastic (MP) ingestion by marine organisms has been well documented the last decade, including in coastal Atlantic cod (*Gadus morhua*). Bioaccumulation of MP has however not been well investigated. If bioaccumulation occurs, one expects older individuals to have an accumulation of the contaminant in one or several tissues, provided exposure to the contaminant. The study area was a heavily plastic polluted area in the Sotra region in western Norway. These areas receive and trap large amount and long-transported marine debris with the coastal current. The cod is a central species in the Norwegian coastal food chain, and spends its life in this region, eating polychaetes and crabs in the sediments as well as fish, and is being exposed to plastic through water and food.

Muscle tissue (93.50 ± 21.82 g) of 23 healthy cod (k -factor = 1.05 ± 0.18) with a length of 40-73cm and estimated age of 3-5 years old was used. The dissection, extraction by gentle enzymatic and oxidative treatments, and chemical identification of MP ($>20\mu\text{m}$) were performed in NORCE PlastLab based on previously published methods. Particle size and polymer types were determined using μFTIR . 36 MP particles ($175.11 \pm 197.53\mu\text{m}$) were observed in nine of the 23 examined fish, dominated by fragments. Six polymers were detected, PP and PE being the most dominant with 33.3% and 30.6%, respectively. MP particles were found in fish from 40 to 56 cm and zero MP was also observed in fish of all sizes. This study did not find evidence of MP bioaccumulation in cod muscle tissue after 3-5 years in a plastic polluted area suggesting either that bioaccumulation does not occur or that there may be other primary target organs for MP bioaccumulation in cod. Wet traps showed low levels of MP particles ($n=2$), suggesting the PlastLab is sufficient to reduce airborne contamination.

Table of content

Acknowledgement	ii
Abstract	iii
1. Introduction	1
1.1 Background for this study	1
1.2 Aim, hypothesis and objectives of the thesis	3
2. Theory	4
2.1 What is plastic?	4
2.1.1 A short introduction to plastic history	4
2.1.2 Types of plastic	4
2.1.3 Fabrication processes	5
2.1.4 Plastic in society	7
2.2 Microplastic	9
2.2.1 Definition	9
2.2.2 Microplastic behaviour	10
2.2.3 Microplastic ingestion, uptake and translocation	14
2.2.4 Microplastic status as a persistent pollutant	16
2.3 Spectroscopy	18
2.3.1- Infrared radiation (IR)	18
2.3.2- Vibrational modes	20
2.3.3- Absorbance and transmittance	22
2.3.4- Using μ FTIR in MP analysis	27
2.3.5 SiMPLe software	28
2.4 The complexity of microplastic- A challenge in microplastic analysis	29
2.4.1 Purification and isolation methods	31
2.5 Quality assurance (QA) and Quality control (QC) in microplastic analysis	32
3. Materials and Methods	33
3.1 Selected sites	33
3.2 Sampling	34
3.3 Contamination control and QA/QC	34
3.4 Tissue sampling	36
3.5 Purification and removal of organic content.....	37
3.5.2 Multi-enzymatic digestion treatment	37
3.5.3 Strong oxidative purification treatment.....	38
3.5.4 Evaporation treatment	38
3.7 Statistics and calculations	40
3.7.1 Fulton’s condition factor (k)	40
3.7.2 MP particle concentration per kilo muscle tissue.....	40
3.7.3 Standardized MP particle count	40

3.7.4 Statistics	40
4. Results	41
4.1 Description of the cod caught in the two locations.....	41
4.2 Identified MP dimensions and shape in muscle tissue.....	44
4.3 Identified polymer types in muscle tissue.....	44
4.4 QA/QC	44
4.5 Investigation of MP bioaccumulation.....	47
4.6 Microplastic identification by μ FTIR analysis	49
5. Discussion.....	52
5.1 Summary of the study	52
5.2 Larger MP particles and higher MP concentration compared to previous findings	52
5.3 Polymer types.....	54
5.3- Reasons for no MP accumulation in relation to age in cod muscle tissue.....	55
5.3.1 Exposition to lower MP concentrations	55
5.3.2- Target organ	56
5.3.3 Loss of material.....	57
5.3.4 QA/QC considerations	58
5.3.5 Little age variation	59
5.3.6 Is bioaccumulation a suitable term for assessing ecological risk of MPs?	59
5.4 Microplastic analysis with μ FTIR	60
6. Conclusion	61
7. Future work.....	62
8. References	63
Appendices.....	72
Appendix A - Material and suppliers.....	72
Appendix B- Filter images, heat maps and spectra maps	75

List of figures

Figure 1- Polymerization process of Polystyrene from monomer to polymer.....	6
Figure 2- Polymer distribution of the plastic demand in Europe in 2020 (PlasticsEurope, 2021).	8
Figure 3- Illustration of the main degradation process (photodegradation) and fragmentation of plastic in the environment (Booth et al., 2017).	12
Figure 4- Illustration of exposure routes for persistent pollutants, and bioconcentration, bioaccumulation and biomagnification of a persistent pollutant up the food chain (Provencher et al., 2019)	17
Figure 5- Illustration of the intensity of light expressed as a wave (Henshaw & O'Carroll, 2009). Wavelength and frequency are inversely proportional by equation 2.2, meaning long wavelengths provides low frequency (A) and short wavelengths provides high frequency (B).	18
Figure 6- The electromagnetic spectrum with a range of wavelength with various of frequencies from gamma waves (10^{-16} m) to long radio waves (10^8 m) (Henshaw & O'Carroll, 2009).	19
Figure 7- Illustration of molecular vibrations caused by IR radiation divided by stretching and bending vibrations (Cameron et al., 2020).	20
Figure 8- Illustration of transmittance and absorbance in relation to the sample concentration.	23
Figure 9- Simple sketch of the components of FTIR spectroscopy (Subramanian & Rodriguez-Saona, 2009) (left) and illustration of constructive and destructive interference (right).	24
Figure 10- Transformation of signals recorded by interferogram. By applying Fourier transformation mathematical equations, the interferogram can be transferred to an IR spectrum (Bhargava et al., 2003).	25
Figure 11- Simple sketch of the ATR-FTIR principle (left), where the IR source generates evanescent waves that penetrates the sample. The reflective beam is collected by a detector. Right picture illustrates the transmission mode (Liu & Kazarian, 2022).	26
Figure 12- Acquisition of multiple spectra by linear array mapping (Aglient, 2020).	28
Figure 13- Location of the two sampling sites, Nordre Hola and Vindkjeften in the Sotra-region, Rabbarosen, west of Bergen.	33
Figure 14- NORCE PlastLab used during sample preparation and dissection, to limit contamination from surfaces, airborne particles, and other plastic materials.	35
Figure 15- Left: Equipment used for dissection, such as tweezers, scissors, and scalpel. Right: Dissection of muscle tissue from cod.	36
Figure 16- Cod muscle tissue during sample preparation: A= SDS treatment after 12h, B = Protease treatment after 48h, C = Lipase treatment after 24h, D= H ₂ O ₂ (30%) treatment after 12h.	36
Figure 17- Model of the Nicolet™ iN™10 MX Infrared Microscope used in this study (Thermo Fisher 2022).	39
Figure 18- Mean length (cm) per age group for female and male Atlantic cod data from 2000-2004 from Heessen et al. (2006). The estimated age range used in this study is highlighted in green. The estimated age for cod with 40 cm is rounded up to 3 years.	41
Figure 19- Boxplot of the variation in fish mass (g) and fish length (cm) between the two location sites, Nordre Hola and Vindkjeften. The outliers are represented in circles.	42

Figure 20-Graphic summary of standardized MP particle count in cod (nMP/100g). A= Polymers per size class, where PP = purple, PE = turquoise, PS = red, PET = brown, PES = pink, PA = green. B = Polymers per fid ID with same color code as A. C = Size class per fish ID. D = Size class per shape and E = Pie chart of polymer distribution per location site with same color code as A and B. 46

Figure 21- A simple scatter plot illustrating the relationship between standardized particle count and (A) fish length (cm) and (B) body condition factor (k)..... 48

Figure 22- A= Visual image of the filter membrane. B= Heat map where the colors show the probability for PP present in this sample. Blue indicates low probability and red indicated high probability. C = Spectra map. The color codes for the identified MP polymer, with the information on major and minor dimensions (μm). The color codes are shown in figure 20. D= Raw FTIR for PP. Blue = reference spectrum for PP and orange = sample spectrum 49

Figure 23- Polymer groups analyzed using the μFTIR analysis. 50

Figure 24- Filter images and heat maps for cod #2, cod #3 and cod #5 presenting IR absorption. (A) and (D) represent cod #2, (B) and (E) represent cod #3 and (C) and (E) represent cod #5. 51

List of tables

Table 1- Summary of size definition used in this study from nano to macroplastic (Hartmann et al., 2019).	10
Table 2- Overview of different types of plastic degradation in the environment (Andrady et al., 2011).	11
Table 3- Overview of various plastic shapes found in the aquatic environment (Lusher et al., 2020).	13
Table 4- Common applications of plastic polymers found in the marine environment, including their specific gravity in comparison with water density (A. Lusher et al., 2017)....	13
Table 5- The approximate regions where the common functional groups in various frequencies areas absorb IR radiation. Based on (Pavia et al., 2001).	21
Table 6- The logarithmic relationship between the absorbance and the transmittance. If the percentage transmittance is high, more light has passed through the sample. Similarly, if the percentage transmittance is low, the sample have absorbed more light and little light has been transmitted.....	22
Table 7- Characterization of all cod captured in the period 07.05.21-02.11.21 in Nordre Høla and Vindkjefte. The characterization includes fish mass (g), fish length (cm) and body condition factor (k), weight of samples collected during dissection (g). The number of identified MP particles found in the muscle tissue is expressed as standardized number of MP particles per 100 g sample (nMP/100g) and estimated MP concentration per kilo sample ($\mu\text{g}/\text{kg ww}$).....	43
Table 8- Data of detected MP particles from the muscle tissue of cod and their respective blank samples containing MPs by μFTIR and SiMPLe software. The detected MP particles are described by the major and minor dimensions (μm), shape and polymer.	45
Table 9- Mean polymer size (μm , with standard deviation) of detected MP in cod muscle tissue with according to particle shape.	47

List of Abbreviations

ATR	Attenuated total reflectance
FTIR	Fourier transform infrared spectrometers
GI	Gastrointestinal tract
LOD	Limit of detection
LOQ	Limit of quantification
KOH	Potassium hydroxide
MP	Microplastic
NP	Nanoplastic
OCD	Optical path difference
PA	Polyamide
PC	Polycarbonate
PE	Polyethylene
PES	Polyester
PET	Polyethylene Terephthalate
PFTE	Teflon®
PLA	Polylactic acid
POP	Persistent organic pollutant
PP	Polypropylene
PS	Polystyrene
PVC	Polyvinyl chloride
Pyr-GC-MS	Pyrolysis- Gas chromatography- Mass spectrometry
QA	Quality assurance
QC	Quality control

1. Introduction

1.1 Background for this study

An estimated 75-199 million tonnes (Mt) of plastic have entered the marine environment since the start of the mass production in the 1950s (UNEP 2021). With the increasing amount of plastic in the environment, plastic is described by The United Nations Environment Programme as “*one of the fastest-growing threats to the health of the world's oceans*” (UNEP, 2017).

Plastic is well known to be persistent in the environment and can be transported over long distances by winds and currents. This also includes microplastic (<1 mm) (MP). Microplastic have for the last decade received increased attention from governments, public media, and the scientific community due to their widespread presence in the environment and potential physical and toxicological risk to organisms (EFSA, 2016; GESAMP, 2016; UNEP, 2017). Plastic debris and MP in the marine environment are transported to the Norwegian coast by the same currents brought by the Norwegian coastal current and predominant winds from the southwest (Bastesen et al., 2021). As a result, high volumes of floating plastic debris and MP are exposed to fish and other species living along the Norwegian coast. Additionally, marine organisms are also exposed to MPs from local sources released by fish farms along the Norwegian coast, responsible for the release of an estimated 805 tonnes of MPs/year into the environment (Welden & Lusher, 2017).

The MP occurrence in the Norwegian environment has been documented in three preliminary matrices: sediments, water and biota. Sediment has been identified as a sink for MPs and as a good matrix to monitor special and temporal changes (Lusher et al., 2021). Sediment sampling sites have been located offshore (Knutsen et al., 2020), along the coast (Collard et al., 2021; Haave et al., 2019), and in freshwater (Lorenz et al., 2020; Lusher et al., 2018). MP is also present in water, such as surface waters in the polar Arctic ranging between 0 to 131 MP particles per m³ (Lusher et al., 2015), Bergen fjord (0-7 MP particles per m⁻³) (Nerheim & Lusher, 2020) and Oslo fjord (9-217 MP particles per m⁻³) (Albretsen et al., 2018).

Coastal biota is the most studied matrix in relation to MPs in the Norwegian environment. For fish especially, Atlantic cod is a species known to ingest various sizes of plastic. Large pieces of plastic such as a sex toy (Summers, 2014) and a coca cola can (Andersson, 2004) have previously been found in the gastrointestinal (GI) tract of cod. Bråte et al. (2016) found plastic items in the micro to macro plastic size range in 3% of 302 cod and up to 27% in urban hotspots in Bergen, western Norway. Foekema et al. (2013) found that 13% of 80 stomachs of cod contained plastic items all less than 5mm.

Cod is an important species in the world's ocean systems from both an ecological, cultural, and economical point of view (Garcia & Newton, 1995; Link et al., 2009) and has a high commercial value. In Europe, over 103 597 tons of cod were landed in 2019, with a market price of 1,5 billion EUR (EC 2021). Cod is also the most common fish species in Norway with its spread from the coastline to the inner parts of Norway's fjords (Bråte et al., 2016). The coastal cod is a stationary type of cod, with its entire life cycle in the same region, it plays a role as both a predator and prey in the food web. The coastal cod is also a generalist, which means it has a range of prey, from polychaetes, crabs, and other crustaceans to fish in different parts of the water column (Link et al., 2009).

Although the MP ingestion of cod has been well documented the knowledge about the behaviour of MP in the food chain is less known. MP particles down to 10µm have been detected in edible tissue and organs of fish such as Atlantic cod and Atlantic Salmon (*Salmon salar*) (Gomiero et al., 2020a; Haave et al., 2021). However, studies on MP accumulation in organs over time (bioaccumulation) have not been investigated. According to recent field studies, MP bioaccumulation in fish has been difficult to observe (chapter 2.2.5). A recent study by McIlwraith et al. (2021) studied the potential MP bioaccumulation in the liver and muscle tissue from freshwater fish in Canada, such as Smallmouth bass (*Micropterus dolomieu*), Lake whitefish (*Coregonus clupeaformis*), and Northern pike (*Esox Lucius*) and found no trend in accumulated MP in of the organs over time and could therefore not confirm MP bioaccumulation in either of the species. A review by Miller et al. (2020) also confirmed the difficulties to identify MP bioaccumulation. An investigation into the behavior of MP in relation to cod, an important species in the Norwegian ecosystem, is important for the understanding of potential problems related to continuous exposure of MP.

1.2 Aim, hypothesis and objectives of the thesis

The overall aim for this study was to investigate if MP particles in muscle tissue of cod are increasing over time by using length of the cod as an estimation for age.

Hypothesis

The hypothesis for this study were:

1. Accumulation of MP in the muscle tissue is observed in cod that are continuously exposed to MPs.
2. Older cod will have a higher number of accumulated MP particles in the muscle tissue than younger cod.

Objectives

The objectives for this study were to:

- Identify the presence of accumulated MP particles in the muscle tissue of cod by using Micro-Fourier Infrared Spectroscopy (μ FTIR)
- Investigate the correlations between accumulated MP particles in the muscle tissue and length as a proxy for age.

2. Theory

2.1 What is plastic?

2.1.1 A short introduction to plastic history

Plastic is a relatively new material which has existed for nearly two centuries (Napper & Thompson, 2020). The start of plastic is considered to be in the mid-1800s, using camphor, cellulose, and nitrate to create Celluloid. The first fully synthetic plastic was invented in the 1900s by Leo Hendrick Baekeland (Meikle, 1995). The benefits of plastic became quickly evident as it is a low-cost, easy forming, lightweight, durable, and highly versatile material (Napper & Thompson, 2020). As a result of the second world war, traditional material such as wood, stone and metal were short in supply. This shortage led to a rise in plastic production, where the qualities of plastic were put to good use. Plastic production continued after the war and a strong economic expansion combined with the emergence of the modern consumer society led to a rapid increase in global plastic production (Geyer, 2020). The start of mass production of plastic is considered to be in the 1950s. Since then, the global production has reached 367 million tonnes (Mt) in 2021 and is increasing yearly (PlasticsEurope, 2021).

2.1.2 Types of plastic

Plastic consists of long chained molecules known as polymers. These polymers are made of synthetic, semi synthetic, or organic monomers derived from fossil resources (coal, natural gas, crude oil) and organic products such as cellulose, salt and renewable compounds (corn, potatoes, starch, seaweed and vegetable oils) (McKeen, 2014). Plastic can often be categorised into at least two groups: thermoplastics and thermosets. Thermoplastic refers to plastic material that can be formed into different shapes by the application of heat and pressure (Andrady et al., 2003). Thermoplastic products are often easy to recycle and mould into different products by remelting (e.g., Polypropylene (PP), polyethylene (PE), polyethylene terephthalate (PET), polystyrene (PS), polyvinyl chloride (PVC) and polyamide (PA)). Thermoset plastics, however, will not be able to change form when heated. Such products include polyurethane (PU), polyester resins, Bakelite, and Epoxy resins and polyester composites (GRP). These types of plastic are mostly used in vessel fabrication and rubber tires (Andrady, 2017).

As fossil resources are not considered sustainable, there are advanced developments by using hydrocarbons from renewable sources. This introduces a new category of plastic: bioplastic (Iwamoto & Tokiwa, 1993). Bioplastic can be produced from biomass sources and include biodegradable and bio-based plastic. Some of the biodegradable polymers are for example polylactic acid (PLA), a type of polyester made from fermented plant starch from corn, sugarcane, or maize. The sugar is fermented and turned into lactic acid (Sintim & Flury, 2017). PLA is a thermoplastic, it is renewable and biodegradable, which are applied in biological and medical applications (Mekonnen et al., 2013). Biodegradable plastic can be broken down by microorganisms into water and CO₂ (or methane) under specific conditions. Currently, bioplastic represent less than one percent of the total plastic production annually and are now used in an increasing number of markers such as packaging, electronics, and textiles (european-bioplastics.org).

2.1.3 Fabrication processes

Monomers (e.g. propylene, ethylene and styrene) are the building blocks of polymers and consist of simple molecules containing a double bond or active functional groups (Chanda & Roy, 2006). Longer molecules allow for stronger Van der Waals forces, which obtains their structural properties such as strength and toughness (Andrady, 2017). The process of transforming monomers to polymers is called polymerization (Figure 1). There are two fundamental mechanisms behind polymerization: addition polymerization and condensation polymerization. In the addition polymerization process, which is initiated by a catalyst, the monomer (possessing a double bond), is opened up and the free valences join other molecules to form a polymer chain (Chanda & Roy, 2006). PE, PVC, PP and PS are polymers produced by this mechanism and the reaction does not form side products. The condensation polymerization is the reaction between the monomer and polymer chain end group releases a side product often water (McKeen, 2014). Polymers such as PES, and PA are made using this condensation polymerization process.

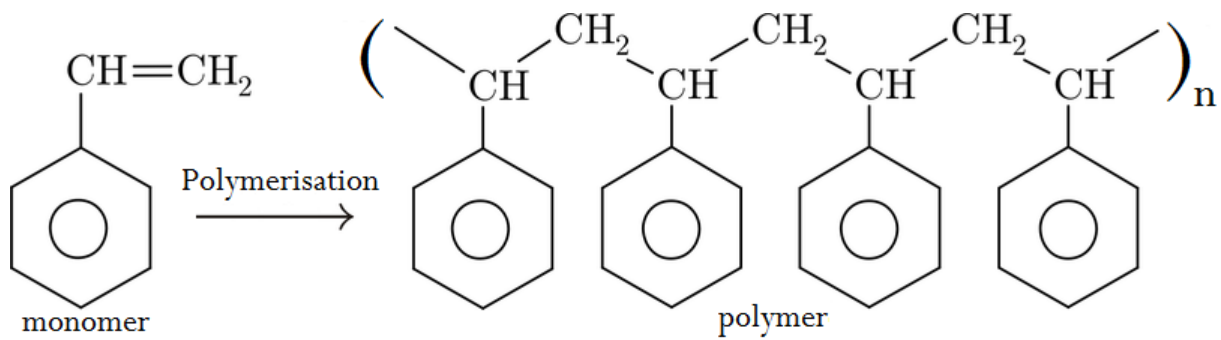


Figure 1- Polymerization process of Polystyrene from monomer to polymer.

Depending on the final product and requirements, additives may be added to enhance polymer properties. These additives include for example plasticizers, hardeners, ultraviolet stabilisers, flame retardants, pigments, fillers, and colourants (Lithner et al., 2011). It is important to understand the polymerization process of a plastic polymer to know its nature and behaviour. Plastic made from polycondensation for example, can degrade when exposed to water at high temperatures. A type of polyester, such as PET can degrade when exposed to an acidic or basic environment. This degradation can damage the polymer chain and alter its chemical integrity, which can lead to difficulties in the process of isolating MP during digestion and purification (McKeen, 2014).

2.1.4 Plastic in society

Plastic is now utilised in every aspect of society and our daily lives (Lebreton & Andrady, 2019). Approximately 15% of the global production is produced in Europe, where plastic is highly demanded in packaging (40,5%), construction (20,4%), electrical and electronics (6,2%), household, recreation, and sports (4,3%), agriculture (3,2%), household, leisure and sports (4,3%), agriculture (3,2%), and a combined category of “others” (16,7%) containing medical applications, furniture, machinery and technical parts (PlasticsEurope, 2021). This demand is reflected by polymer production of PP (19,7%), low-density PE (17,4%), and high-density PE (12,9%) account for the largest share, followed by PVC (9,6%) and PET (8,4%). Their application area is illustrated in Figure 2.

Plastic also facilitates benefits for the society such as the supply and storage of clean drinking waters, thus improving consumer safety and health (Andrady & Neal, 2009). Food packaging applications enable food (vegetables, meat, fish) to remain fresh long after they are produced, and the quality of the food can be monitored by using gas-flush packaging and oxygen scavenger technology (Andrady & Neal, 2009). Plastic has also provided better sterile healthcare products, such as surgical equipment, syringes, medical packaging, goggles, and single-use gloves for preventing infection of bacteria and/or viruses (de Sousa, 2021). During the Covid 19 pandemic, the demand and use of single-use products increased, especially face masks and gloves. Urban and Nakada (2021) have estimated that in Brazil more than 85 million face masks was disposed per day in 2020. This increase in single use face masks and gloves can become a major problem for the environment in the future when improperly disposed.

EU27+3 converters plastics demand

BY SEGMENTS & POLYMER 2020

**Total:
49.1 Mt**

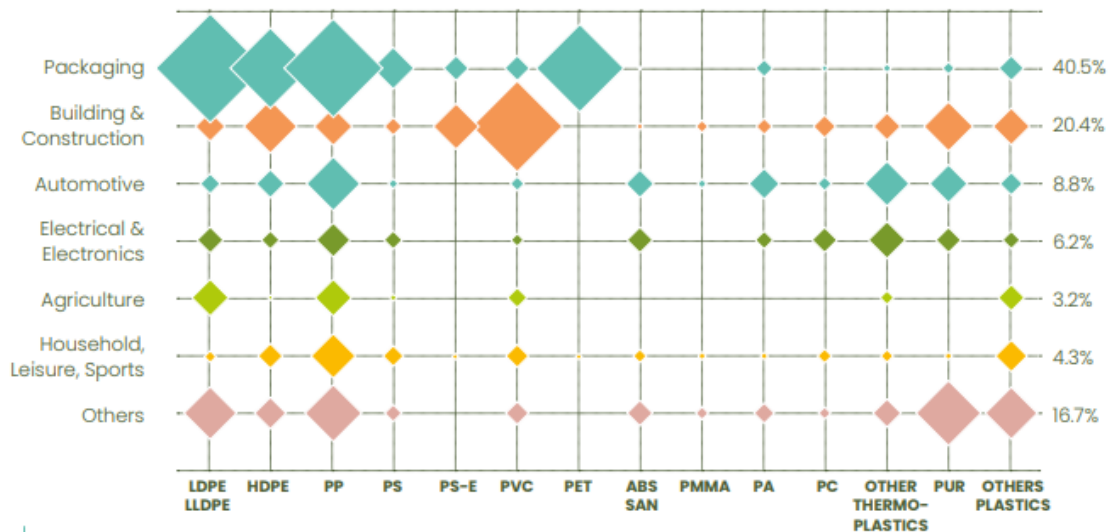


Figure 2- Polymer distribution of the plastic demand in Europe in 2020 (PlasticsEurope, 2021).

With a rapid consumption of plastics which generates large amounts of plastic waste, the world is unequipped to handle it. WWF estimates that 37% of the global plastic waste is managed ineffectively (Hamilton et al., 2019). In 2021, only 23.4% of plastic post-consumer waste was recycled and 42% sent to energy recovery operations in Europe (PlasticsEurope, 2021). Although plastic recycling in Europe has increased 117% since 2006, it is far below global recycling rates recycling products such as iron and steel (70-90%) and paper (58%) (Agenda, 2016). The most prevalent system of managing plastic waste is landfilling, and 24% of plastic waste generated in Europe was disposed of in landfills in 2021 (PlasticsEurope, 2021). Mismatched waste is material left uncontrolled, openly dumped in nature or managed through uncontrolled landfills, taking centuries to decompose (Agenda, 2016; Hamilton et al., 2019). By escaping waste streams, mismatched waste would enter the environment and eventually reach the ocean (Geyer et al., 2017).

2.2 Microplastic

2.2.1 Definition

Two decades after the mass production of plastic started in the 1950s, numerous reports of plastic debris interacting with marine wildlife appeared in the scientific literature. These reports include albatrosses ingesting “indigestible matter” and seals entangled in plastic debris (Fowler et al., 1989; Kenyon & Kridler, 1969) to name a few. In the 1970s, the first report of small pieces of floating plastic fragments and pellets on the ocean surface also appeared in the scientific literature (Carpenter & Smith, 1972). However, the term “microplastic” in relation to the marine environment did not appear in the scientific literature until 2004 by Thompson et al. (2004). Microplastic was defined to an upper limit of 5mm which has become the most frequently used definition (GESAMP, 2015). Lately, the adoption of 1mm as threshold has been proposed, excluding plastics in the millimetre range 1-5mm from the MP definition (Table 1), and allowing only the micrometre sized to be included in the term (Hartmann et al., 2019). The requirement for an “upper size limit” size was needed to focus on the possible ecological effects as particles of this size were more likely to be ingested (Arthur et al., 2009). The inclusion of 5mm particles meant that plastic resin pellets were also included in the microplastic term, undoubtedly important to increase awareness of this source of plastic pollution. To distinguish the origins of MP in the environment they are divided into two groups: primary or secondary MP. This distinction is based on whether MP is intentionally produced in this size (primary) or as a result of the breakdown of large plastic items (secondary) (GESAMP, 2015). Primary MPs include scrubbing agents in cosmetics and toiletries, such as shower gel and facial scrubs (Boucher & Friot, 2017), virgin plastic production (resin) pellets and exfoliants and plastic particles used for abrasion in air-blasting (Arthur et al., 2009). Secondary MPs result from larger plastic items being broken down into smaller parts in the environment. Breakdown of secondary MPs happen through different weathering processes such as sunlight, winds, ocean currents, microbial activity, mechanical wear and tear (Andrady, 2011; Andrady et al., 2003).

Table 1- Summary of size definition used in this study from nano to macroplastic (Hartmann et al., 2019).

	Size
Nanoplastic	1 to <1000 nm
Microplastic	1 to <1000µm
Mesoplastic	1 to <10mm
Macroplastic	1 cm and larger

2.2.2 Microplastic behaviour

2.2.2.1 Degradation

Defined by ISO 472:2013, degradation is an “irreversible process leading to a significant change in the structure of the material, typically characterised by a change of properties and/or fragmentation affected by environmental conditions” (International Organization for Standardization, 2013). The most prevalent type of plastic degradation is photodegradation (Table 2), which facilitates oxidative degradation (Andrady et al., 2011; Andrady et al., 2003). This oxidative degradation process is initiated by sunlight (UV-radiation) and the kinetics depends on the combination of conditions such as oxygen concentration, temperature, water chemistry, and presence of other chemicals (Booth et al., 2017). UV radiation is causing a degradation of the polymer chain, resulting in cracks on the surface of the polymer and weakening the plastic. This weakening is causing the plastic to become brittle, resulting in a generation of secondary MP fragments of different sizes (Andrady et al., 2011; GESAMP, 2015; Lassen et al., 2012). Not only is the kinetics of the polymer degradation dependent on environmental conditions, but also the chemical composition. Polymers such as PE, PP, and PS consist of a pure carbon-carbon backbone, whilst polymers such as PET consist of a heteroatom in the backbone, mainly oxygen (Lambert & Wagner, 2016). UV-radiation initiates the production of radicals by oxidation and these radicals lead to a breakage of the polymer chain (Yousif & Haddad, 2013). With a heteroatom present in the polymer chain, the strength is weakened and plastic is therefore more sensitive to oxidation.

The temperature also plays a significant role in terms of degradation rate. Studies have shown more efficient weathering degradation of plastic debris in the beach zones, compared to floating plastic debris in the ocean. This is mostly due to lower temperatures and lower oxygen levels in the water compared to the sand in the beach zone (Andrady et al., 2011; Andrady et al., 1998). Once in the marine environment, the lack of solar UV-light, (to initiate the photo-oxidation process), lower temperature, and oxygen concentration make extensive degradation far less likely for plastic debris. Plastic debris present in the beach zone, are exposed to higher UV-light, higher temperature and have more access to oxygen. It is therefore the majority of secondary MPs are generated in the beach zone and translocated to the sea (Andrady, 2017). Other types of degradation such as biodegradation do also occur but have a significantly slower degradation rate compared to photo-oxidative degradation. Clearly, the nature of the polymers also plays an essential role in determining their environmental fate and potential impact on the ecosystem (Andrady, 2017). There are some ways to control degradation by using additives such as UV stabilisers which will reduce the degradation. The additives are added in for example the PA-polymer used in mainly fishing nets, reducing the degradation when exposed to sunlight.

Table 2- Overview of different types of plastic degradation in the environment (Andrady et al., 2011).

Type of degradation	Source
Biodegradation	Action of living organisms
Photodegradation	Action of light (usual sunlight in outdoor exposure)
Thermooxidative degradation	Slow oxidative breakdown at moderate temperatures
Thermal degradation	Action of high temperatures
Hydrolysis	Reaction with water

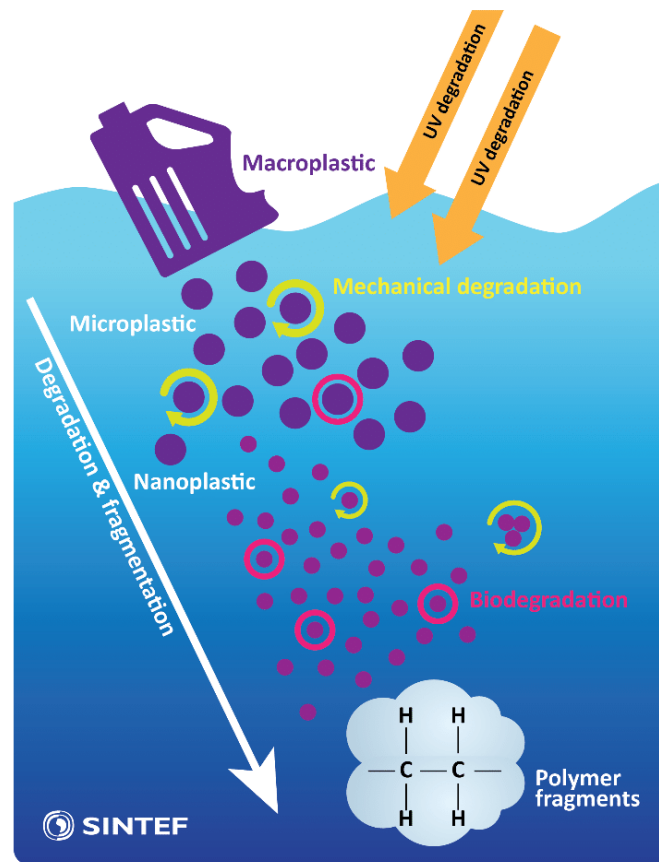


Figure 3- Illustration of the main degradation process (photodegradation) and fragmentation of plastic in the environment (Booth et al., 2017).

2.2.2.2 Size, shape, and density

Size, shape, and density are important factors for determining the fate of plastics in the marine environment (GESAMP, 2016; A. Lusher et al., 2017). The shape of MP varies between irregular to long, from thin fibres to spherical. Pellets can have ovoid, cylindrical, disk and spherical shapes whilst particles with irregular shapes affected by degradation in the environment are underlying the wide category of “fragments” (Hidalgo-Ruz et al., 2012). The most abundant shape category of MPs in the water are fibres (48,5%), followed by fragments (31%), beads (6,5%), films (5,5%), and foam (3,5%) (Table 3) (Kooi & Koelmans, 2019). The specific density of plastic particles can vary, depending on the polymer and manufacturing process. These values for plastic range from $<0.05 \text{ g cm}^{-3}$ for polystyrene foam to $2.1\text{-}2.3 \text{ g/cm}^{-3}$ for Polytetrafluorethylene (PTFE/Teflon®) as listed in Table 4 (Chubarenko et al., 2016).

Given the seawater density ($>1,027 \text{ g/cm}^3$), low-density plastic such as PE ($0.91\text{-}0.94 \text{ g/cm}^3$) will float when present in water and high-density plastic such as PVC ($1.35\text{-}1.39 \text{ g/cm}^3$) will sink and accumulate in sediments (Lobelle & Cunliffe, 2011). The continuous degradation including its polymer properties gives a variety of different MP particles in the water column, making them available for a range of various organisms (Wright et al., 2013).

Table 3- Overview of various plastic shapes found in the aquatic environment (Lusher et al., 2020).

Shape classification	Other terms used
Fragments	Irregularly shaped particles, crystals, fluff, powder, granules shavings, films
Fibres	Filaments, microfibers, strands, threads
Beads	Grains, spherical microbeads, microspheres
Foams	Polystyrene, EPS
Pellets	Resin pellets, nurdles, pre-production pellets, nibs

Table 4- Common applications of plastic polymers found in the marine environment, including their specific gravity in comparison with water density (A. Lusher et al., 2017).

Plastic polymer	Common applications	Specific gravity (g/cm^3)
PE	Plastic bags, storage containers	0.91-0.95
PP	Rope, bottle caps, fishing gear	0.90-0.92
PS	Cool boxes, cups, containers	1.01-1.09
PVC	Film, pipe, containers	1.16-1.30
PA (Nylon)	Fishing nets, rope	1.13-1.15
PET	Bottles, strapping, textiles	1.34-1.39
PES	Textiles, boats	>1.35
PFTE	Cookware, paint	2.1-2.3
Pure water		1.000
Sea water		1.027-1.035 (depending on salinity)

2.2.3 Microplastic ingestion, uptake and translocation

MP ingestion by marine organisms happens either through direct ingestion by mistaking MP for prey items or indirect ingestion from plastic-contaminated prey, called trophic transfer (Watts et al., 2016). When ingesting MP particles there are two possible pathways from the gastrointestinal tract into the internal organs of the fish. This mode of uptake happens either through the intestinal epithelium or by an endocytic process followed by a transportation in the circulatory fluid system (Wright & Kelly, 2017). A more likely route of larger MP particles to translocate is by paracellular diffusion, or so-called persorption. Translocation and persorption are two terms frequently used to describe the mechanism of the uptake process. Translocation is used to describe the specific particle that has passed through the intestinal tract and transferred via blood to other organs and tissues. In comparison, persorption is used to describe the passage of an intact particle through the wall of the intestinal tract. Volkheimer (1993) tested a variety of substances (e.g., pollen, cellulose, crab and lobster shells, PVC, hair fragments and soot) in the microparticle range to study the mode of uptake of in vertebrates.

Volkheimer (1993) stated that the microparticles up to 150 μm can pass through the biological barrier through the intestinal wall by persorption and translocate to the liver and other organs via the portal vein system. As MP lies in the size range available for persorption, these two terms have been adapted by the MP literature to describe the potential uptake.

Exposure studies on MP uptake shows contradictory results and the mechanism behind the process of translocation is poorly understood (Chain, 2016; GESAMP, 2015; Maes et al., 2021; van Raamsdonk et al., 2020). By feeding European sea bass (*Dicentrarchus labrax*) with a diet containing fluorescent MP particles (1-5 μm) for 16 weeks, the fillets contained a mean estimated MP concentration of 0.36 ± 0.29 nMP/g (Zeytin et al., 2020). A recent exposure study used even smaller sizes by feeding rainbow trout (*Oncorhynchus mykiss*) palladium doped polystyrene nanoplastic (PS-Pd NPs $\sim 200\text{nm}$) and identified NP-particles in liver ($1.1 \pm 0.1\text{ng/g}$) and kidney (65.6 ± 25.4 ng/g) (Clark et al., 2022). These findings support the persorption size limit established from Volkheimer (1993). However, recent studies have also observed MP particles of 200-600 μm in the liver (Avio, Gorbi, Milan, et al., 2015; Collard et al., 2017; Jovanović, 2017) suggesting an even higher size limit of MP persorption and translocation.

Exposure studies have also investigated potential target organ(s) for MPs. From a toxicological point of view, a target organ means the organ(s) that is most affected from the exposure to a contaminant of concern (Heywood, 1981). The fish liver is normally the primary target organ for many organic pollutants due to various metabolism and different processes (Hedayati, 2016). Other organs such as brain, kidney and muscle tissue are also known target organs. Muscle tissue has for example shown to be the target organ for methyl mercury in Atlantic cod (Kwaśniak & Falkowska, 2012).

Recent field studies have investigated the presence of MP in organs such as liver and muscle tissue of fish. Haave et al. (2021) studied the presence of MP in the muscle tissue (1000µg/kg) and liver (3400µg/kg) of naturally exposed cod in the Sotra region west for Bergen. McIlwraith et al. (2021) detected zero to 84 particles in muscle tissue of various freshwater fish species ranging from 100µm to 5000µm in lakes in Canada. Furthermore, Gomiero et al. (2020a) observed MP particles from 11-240µm in muscle tissue and liver of farmed and wild salmon and mountain trout in western parts of Norway.

2.2.4 Microplastic status as a persistent pollutant in the environment

Bioaccumulation is a term primarily applied for dissolved chemicals present in the environment, known as POP (Persistent Organic Pollutant) and metals. Examples of POPs include polychlorinated biphenyls (PCBs), polybrominated diphenyl ethers (PDBEs) and polyaromatic hydrocarbons (PAHs). Bioaccumulation refers to the net uptake of contaminants in the tissues of organisms through any route such as respiration, ingestion or direct contact with contaminated water or sediments, leading to a higher concentration in the organism over time (Simpson, 2005). The solubility of organic compounds in lipids (fat, oils) tends to determine to what extent they bioaccumulate. Bioaccumulation and trophic transfer of a contaminant may result in biomagnification at higher trophic levels (Figure 4) (Miller et al., 2020).

POPs can stem from improper use and/or disposal of industrial chemicals and unwanted by-products of industrial processes or combustion (Maes et al., 2021). POP was classified by the Stockholm convention in 2004 with the aim to reduce the release of these chemicals on a global scale (Hagen & Walls, 2005). In comparison, plastic production and subsequent release into the environment are still continuously increasing (Kershaw et al., 2019; Maes et al., 2021; Worm et al., 2017). Plastic and MPs share similar behaviour to POPs as they are also persistent, stable substances, meaning there is risk for remaining in the environment for a long time and long-time exposure for wildlife. In contrast POPs and metals have shown evidence for bioaccumulation and biomagnification across trophic levels such as cod (Amlund et al., 2007; Ruus et al., 2012; Shaw et al., 2009), seal (Letcher et al., 2009; Shaw et al., 2008) and polar bears (Boisvert et al., 2019; Muir et al., 2006; Sørmo et al., 2006), which have not been observed for MPs (Miller et al., 2020).

For MP to be classified as a persistent pollutant they also need to show a pattern of bioaccumulation and toxicity. By assessing whether MP concentration increases over time within organisms and from lower to higher trophic levels are based on the classical definition of bioaccumulation and biomagnification applied to POPs and metals (Alexander, 1999; Bernes, 1998; Miller et al., 2020). Physical items such as MPs, presented as fragments or fibres, do interact with marine organisms in different ways compared to POPs. In contrast, MPs also makes for an even broader category of combinations of polymers, additives, and their degradation state (Worm et al., 2017). Once MP particles have entered the body, their mode of uptake is more limited compared to POPs. MP has the potential to pass biological tissue and translocate via phagocytosis by either the gills of the gastrointestinal tract and therefore size dependent. POPs, that are already dissolved chemicals, have a greater chance to be taken up by the organism. It is therefore a discussion about whether these concepts are suitable for assessing ecological risk for MP concentration in marine organisms, but this needs to be further investigated (Miller et al., 2020).

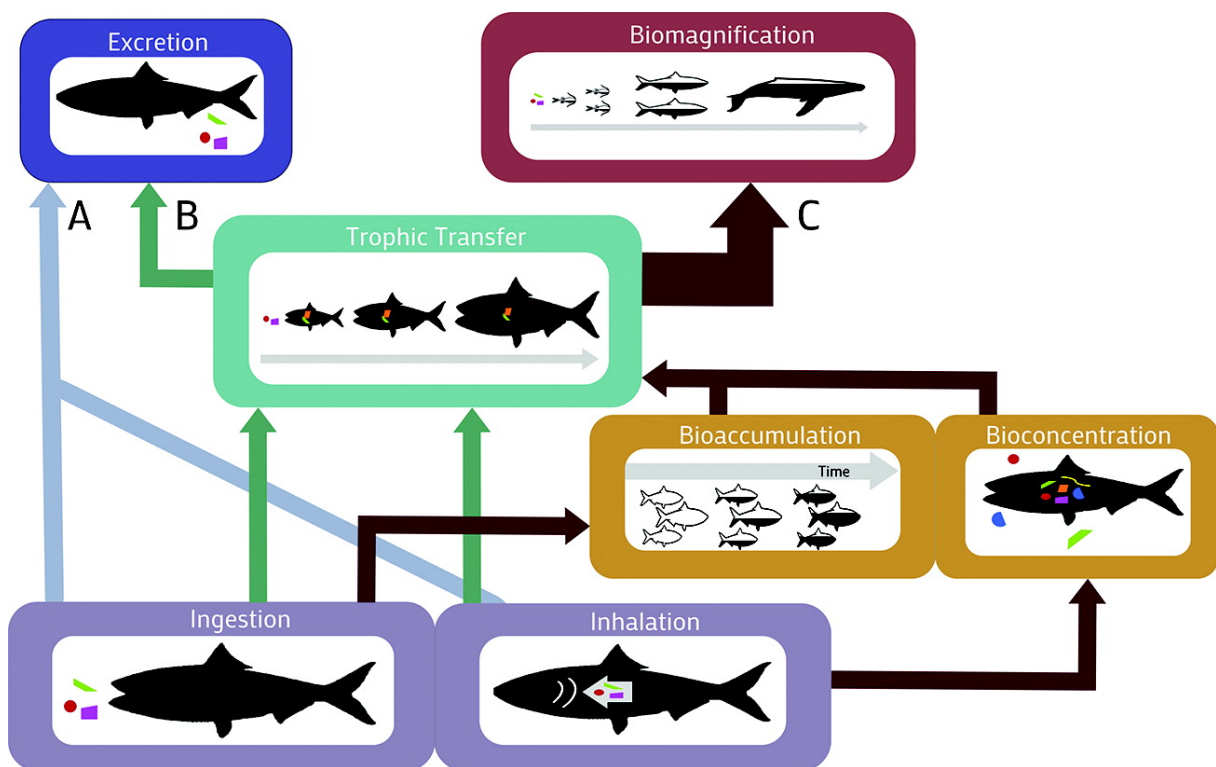


Figure 4- Illustration of exposure routes for persistent pollutants, and bioconcentration, bioaccumulation and biomagnification of a persistent pollutant up the food chain (Provencher et al., 2019)

2.3 Spectroscopy

2.3.1- Infrared radiation (IR)

In the electromagnetic spectrum, IR radiation (700nm-1mm) lies between the microwave radiation range (30cm-1mm) and visible light (400nm-700nm) (Figure 6). Electromagnetic radiation (light) is defined as either a particle or a wave. By expressing light as particles, each particle carries energy E:

$$E = h\nu \quad 2.1$$

Where h = Planck constant ($=6.626 \times 10^{-34}$ J*s) and ν = frequency.

A wave by comparison is defined by frequency and wavelength (λ). Frequency is the number of waves that passes through a given point per second (s^{-1}), commonly known as Hertz (Hz). Wavelength is the distance between two corresponding positions of head-to head waves (Figure 5). The relationship between frequency and wavelength is given in equation 2.2:

$$c = \nu\lambda \quad 2.2$$

Where c = speed of light ($=2.998 \times 10^8$ m/s in vacuum).

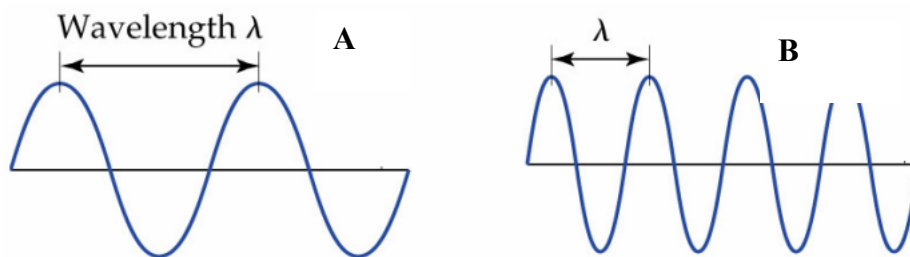


Figure 5- Illustration of the intensity of light expressed as a wave (Henshaw & O'Carroll, 2009). Wavelength and frequency are inversely proportional by equation 2.2, meaning long wavelengths provides low frequency (A) and short wavelengths provides high frequency (B).

Since energy is directly proportional to frequency, equation 2.1 and 2.2 can be combined:

$$E = \frac{hc}{\lambda} = hc\tilde{\nu} \quad 2.3$$

Where $\tilde{\nu} = 1/\lambda$ is called wavenumber (cm^{-1}).

As equation 2.3 express, energy is inversely proportional to wavelength and directly proportional to wavenumber. This relationship is illustrated in figure 6. An increase in wavenumber corresponds to an increase in energy. Red light for example has longer wavelength than blue light indicating that red light is less energetic compared to blue light.

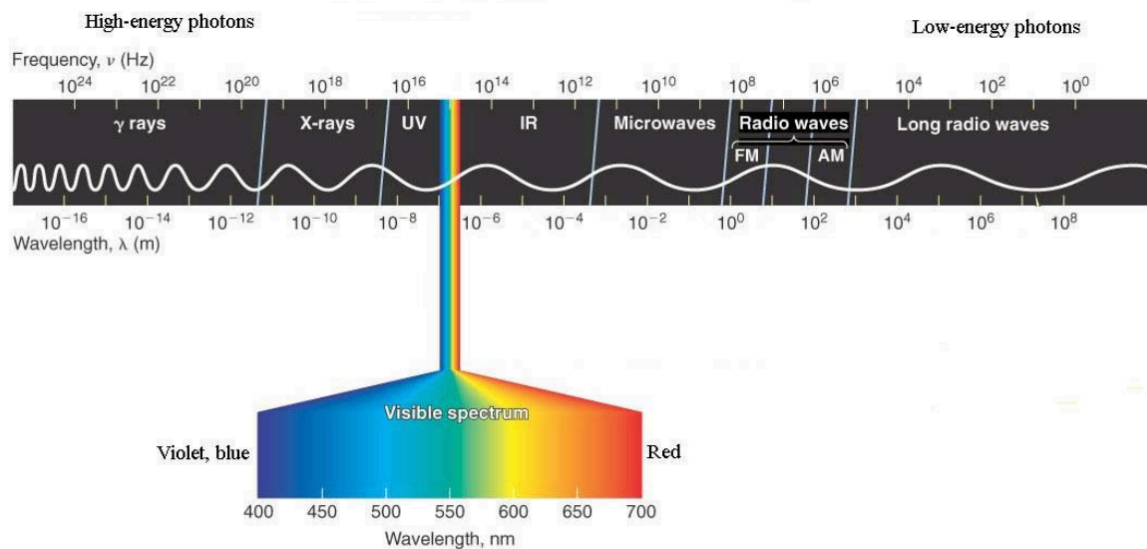


Figure 6- The electromagnetic spectrum with a range of wavelength with various of frequencies from gamma waves (10^{-16} m) to long radio waves (10^8 m) (Henshaw & O'Carroll, 2009).

2.3.2- Vibrational modes

Depending on the energy, radiation can interact with molecules in various ways. Ultraviolet radiation and visible light for example, contains enough energy to make electrons in the molecule excite to a higher orbital level, called electronic transition. In contrast, IR radiation does not contain enough energy to induce electronic transitions (Harris, 2010). IR radiation can only stimulate molecular vibrational motions. However, only molecules with a dipole moment are capable of absorbing IR radiation. Symmetric molecules such as H_2 , N_2 and O_2 are IR-inactive as the vibrations causes no change in the dipole moment. Vibrations can cause a change in either bond length (stretch) or bond angle (bending). The bending vibrations are often divided by scissoring, rocking, wagging and twisting (Figure 7).

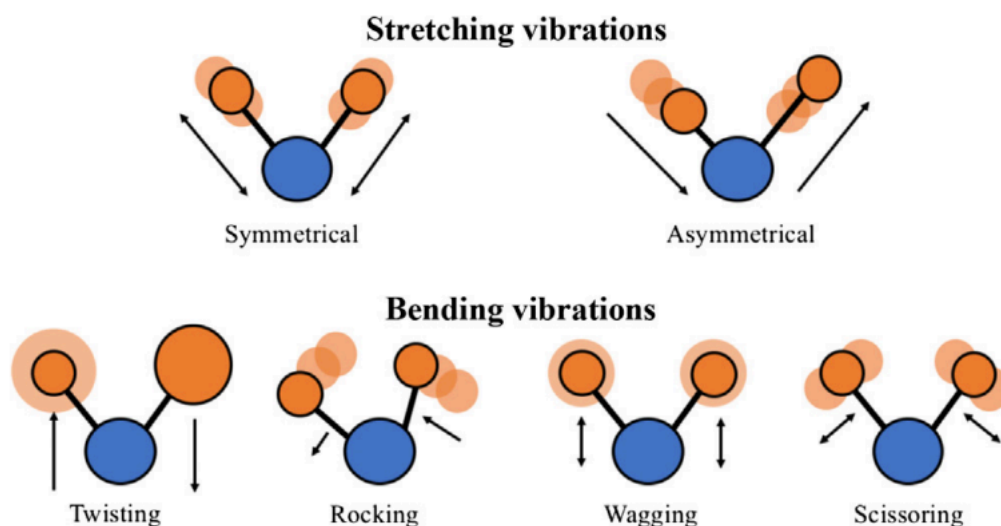


Figure 7- Illustration of molecular vibrations caused by IR radiation divided by stretching and bending vibrations (Cameron et al., 2020).

The various vibrations of the compound are expressed in an IR spectrum. The IR spectrum is a plot of %Transmittance vs the wavenumber of the radiation. The wavenumber used in IR spectroscopy lies normally between 4000-400 cm^{-1} , because most compounds show characteristic absorption in this region range. This region can be divided into the functional group region (4000-1400 cm^{-1}) and the fingerprint region (1400-400 cm^{-1}).

Table 5- The approximate regions where the common functional groups in various frequencies areas absorb IR radiation. Based on (Pavia et al., 2001).

Frequency (cm^{-1})

4000	2500	2000	1800	1650	1500	650
O-H C-H N-H	C≡C C≡N X=C=Y	Very few bands	C=O	C=N C=C N=O		C-Cl C-O C-N C-C N=O

2.3.3- Absorbance and transmittance

Absorbance and transmittance are two related, but differently used quantities. Absorbance refers to the substance capacity of absorbing radiation and transmittance measures how much light that passes through the sample (Figure 11) (Harris, 2010).

Transmittance of any sample equals the relationship of the radiation from the sample I, over the radiation before the sample I_0 :

$$T = \frac{I}{I_0} \quad 2.4$$

Where I_0 = the intensity of the radiation striking the sample and I = Transmitted light (the remaining light that have passed through the sample). Transmittance is mostly expressed in T%:

$$T\% = \frac{I}{I_0} * 100\% \quad 2.5$$

Absorbance and transmittance are related through equation 2.5 and illustrated in table 5:

$$A = \log \frac{I_0}{I} = -\log T \quad 2.6$$

Table 6- *The logarithmic relationship between the absorbance and the transmittance. If the percentage transmittance is high, more light has passed through the sample. Similarly, if the percentage transmittance is low, the sample have absorbed more light and little light has been transmitted.*

Absorbance	Transmittance
0	100%
1	10%
2	1%
3	0.1%

The relationship between absorbance and transmittance can be expressed by Beer-Lambert law, the fundamental law of quantitative absorption spectroscopy (Li-Chan et al., 2010). This law states that the absorbance of a sample with a thickness l (cm) is given by:

$$A = \log \frac{I}{I_0} = \epsilon lc \quad 2.7$$

Where ϵ = molar absorptivity ($M^{-1} \text{ cm}^{-1}$) and c = molar concentration (M).

Equation 2.6 states that the absorbance is proportional to the concentration in the sample and transmittance is inversely proportional (Li-Chan et al., 2010). This relationship is illustrated in Figure 8.

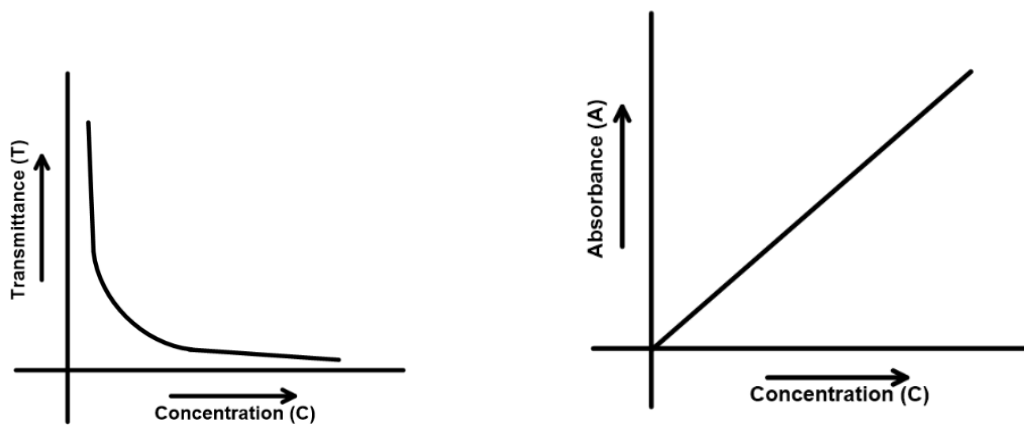


Figure 8- Illustration of transmittance and absorbance in relation to the sample concentration.

2.3.3 Fourier transform infrared radiation spectroscopy

Spectroscopy is the study between electromagnetic radiation and matter (Harris, 2010). Fourier transform infrared radiation (FTIR) spectroscopy is a non-destructive and well established method for identifying chemical compounds (Ismail et al., 1997). The components of FTIR spectroscopy are based on the components in IR spectroscopy. These components are traditionally a light source, a monochromator, a sample cell, and a detector that produces a single spectrum from one sample. By applying more advanced components such as interferometer (Figure 7), Linear array (LA) mapping (Figure 11) and sensitive detectors, the FTIR method has developed into a more reliable identification technique (Tagg et al., 2015).

By applying an interferometer, the radiation from the light source is split into two optical beams by a beam splitter. The beam is reflected by a mirror of a fixed length and a moving mirror, providing beams in various frequencies. This can either cause constructive or destructive interference (Figure 9). When the two mirrors are at the same distance, there is no optical path difference (OPD) and the beams are in phase (constructive interference). Constructive interference occurs when the two mirrors is an integer (n) multiple of the wavelength (Subramanian & Rodriguez-Saona, 2009). In contrast, destructive interference occurs at $(n + \frac{1}{2})$ multiple of the wavelength. The intensity of the beam for constructive interference is higher in contrast to destructive interference. The resulting light intensity varies in form of a cosine wave. When the two beams reflected by the two mirrors collide, they are added together to form a single wave.

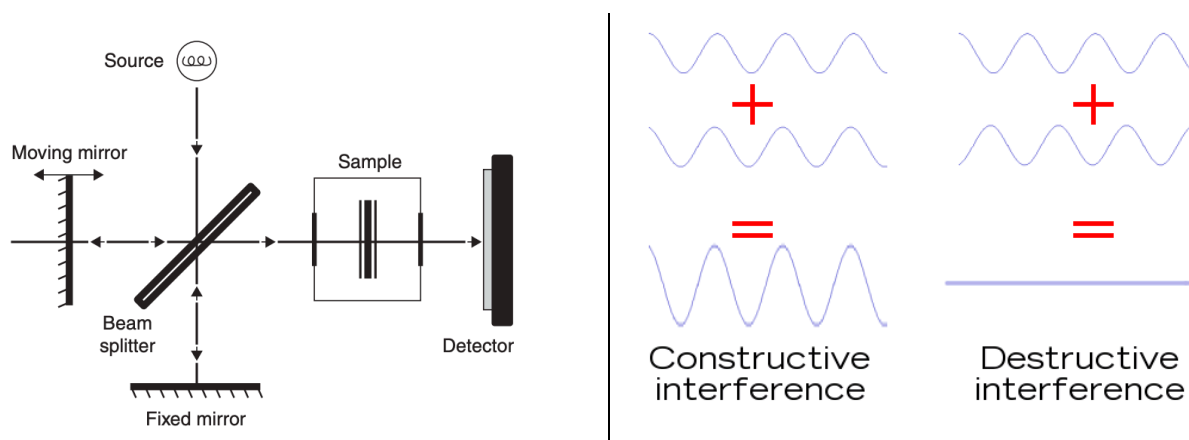


Figure 9- Simple sketch of the components of FTIR spectroscopy (Subramanian & Rodriguez-Saona, 2009) (left) and illustration of constructive and destructive interference (right).

The plot of the light intensity (in volt) and OPD is called an interferogram and contains every recorded wave. The interferogram is a function of time and is not recognizable as a spectrum. By applying a mathematical procedure, called Fourier transformation, the component frequencies can be extracted from the interferogram and create an IR spectrum (Figure 10).

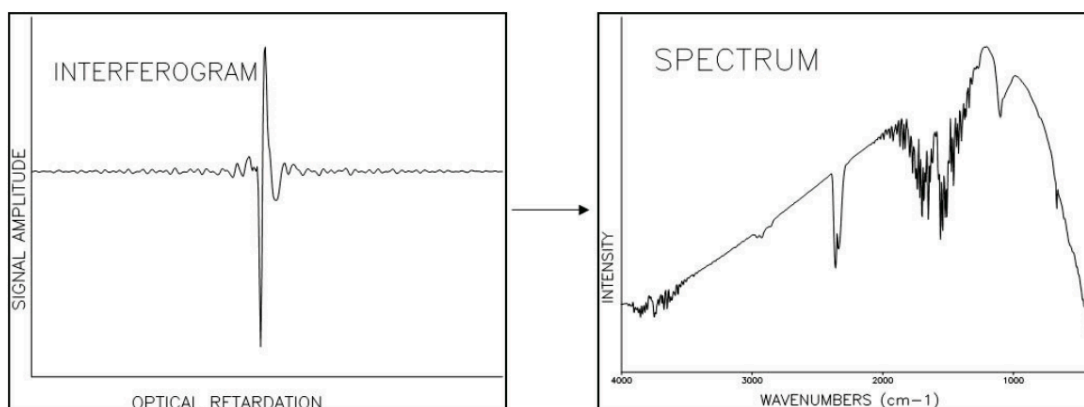


Figure 10-Transformation of signals recorded by interferogram. By applying Fourier transformation mathematical equations, the interferogram can be transferred to an IR spectrum (Bhargava et al., 2003).

2.3.3.1- Sampling modes

In FTIR there are two operating modes which are commonly used for FTIR; Transmission, attenuated total-reflectance (ATR) (Xu et al., 2019). In Transmission mode the IR light passes through the sample and the transmitted light is measured. This mode requires the filter to be IR transparent and the sample to be sufficiently thin to avoid total absorption of the IR spectrum (Käppler et al., 2016). In contrast, ATR sampling uses an optical crystal (with a high refractive index at a specific angle, θ) to provide a total internal reflection of the IR beam when in contact with the sample. An IR beam is sent into the crystal at a certain angle, called the critical angle. Information about the sample is gathered through the interaction of evanescent waves and the sample (Figure 11). After the reflected IR beam have interacted with the sample, it carries the chemical information to the detector. The evanescent wave is key to how ATR can provide the use of vibrational or chemical information about the sample of interest. The evanescent wave penetrates the sample on a given intensity of the IR beam and the penetration depth is dependent two variables. When a sample is in contact with the sample, the evanescent wave will lose energy at frequencies identical to the absorption of the sample. The resulting beam registered by the detector can be used to generate the absorption spectrum of the sample.

Based on Beers law, the larger the pathlength (l), the higher absorbance (chapter 2.3.3). The pathlength in ATR-FTIR is the sum of interactions the IR beam have with the sample through the crystal and these interactions is dependent on the depth of penetration, which increases with lower wavenumber. The angle between the refractive index of the crystal and the sample is also related to the depth of penetration. Germanium crystal, with a refractive index around 4.0 will have a lower penetration depth compared to diamond with a refractive index of 2.4 (Subramanian & Rodriguez-Saona, 2009). The ATR sampling mode is developed to enhance the surface sensitivity

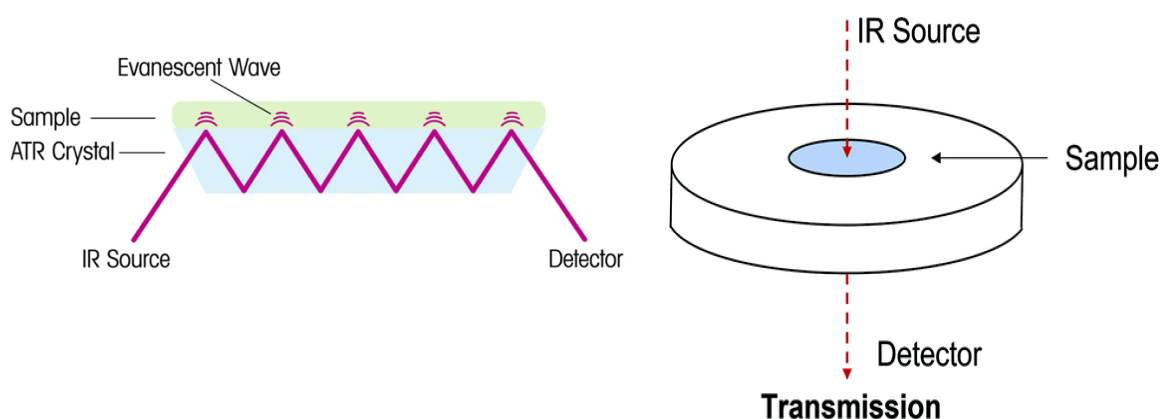


Figure 11- Simple sketch of the ATR-FTIR principle (left), where the IR source generates evanescent waves that penetrates the sample. The reflective beam is collected by a detector. Right picture illustrates the transmission mode (Liu & Kazarian, 2022).

2.3.4- Using μ FTIR in MP analysis

FTIR has been widely used in world wide MP research since 2004 (Veerasingam et al., 2021) and have shown to be efficient method used for the identification, quantification and characterization of MPs in air (Catarino et al., 2018), the aquatic environment (Bergmann et al., 2017; Cunningham et al., 2020; Enders et al., 2019; Gomiero et al., 2019; Lorenz et al., 2019; Peeken et al., 2018), food (Catarino et al., 2018; Gomiero et al., 2020a; Haave et al., 2021; Woods et al., 2018) and drinking water (Gomiero et al., 2018; Kirstein et al., 2021; Novotna et al., 2019; Weisser et al., 2021). Because each polymer contains a unique constellation of atoms, their chemical structure can be determined and identified by FTIR (Chalmers, 2006). Detecting MP on filters using transmission mode is the most promising technique in MP research for MPs $<500\mu\text{m}$, whilst ATR-FTIR is more suitable for plastic particles $>500\mu\text{m}$ (Käppler et al., 2016). The analysed particles need to be covered by the ATR crystal and particles with smaller size might be unable to produce a desirable spectrum.

The FTIR instrument requires high selectivity in terms of resolution and a sensitive quantum detector to identify the MP particles present in complex organic matrices. Selectivity refers to the capability the method has to distinguish between a given analyte and other substances. Sensitivity refers to the instrument's capability to detect the small amount of the analyte (Prichard and Barwick 2007). A major limitation in terms of sensitivity of FTIR spectroscopic measurements is the signal-to-noise ratio (SNR), especially when the absorbance of the component is weak (Chan 2006). The SNR compares the wanted signal with the levels of background noise. SNR can be affected by the quality of digestion treatment of organic matrices in terms of background and possible interferences (Ivleva, 2021). To reduce this ratio, an interferometer (Figure 9), LA-mapping (Figure 12), and a sensitive quantum detector such as mercuric cadmium telluride detector (MCT, HgCDTe) can be applied. By also coupling FTIR with a microscope, it can provide better sensitivity and resolution for chemical imaging of MP particles. This chemical imaging by using LA mapping can detect MP particles down to $10\mu\text{m}$. In the μ FTIR spectra of MP, not all segments contain relevant information, so the spectrum can be reduced to a smaller and more characteristic sub spectrum. This can increase the selectivity of the reference database in SiMPLE (chapter 2.4.4).

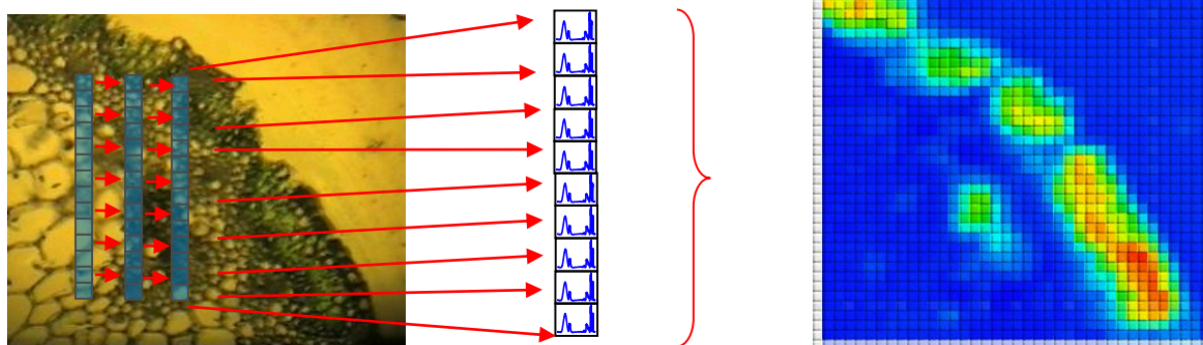


Figure 12- Acquisition of multiple spectra by linear array mapping (Aglient, 2020).

2.3.5 SiMPLe software

SiMPLe software (Systematic identification of Microplastic Particles in the environment) is a post-processing imaging analysis software that counts, identifies, and quantifies measured particles analysed by μ FTIR. The software allows for two types of data analysis. First, by comparing the IR spectra of detected particles analysed by μ FTIR to a reference database (containing both plastic polymers and natural materials), and second by analysing the filter area of the sample (Primpke et al., 2017). The algorithm for detecting particles applies to the two thresholds of probability scores expressed by values 0 and 1 by using Pearson correlation calculations (<https://simple-plastics.eu/>). These calculations can be used to mathematically filter away unwanted tops when comparing spectra and increasing the selectivity. The software also applies a raw dataset, with information about the dimensions, estimated volume and mass, and a max AAU score. This score indicates how well the spectrum from the analysed particle fits the reference material. Values around 1 are considered a perfect match. as to values below 0.5 indicate not a good match. Applying the SiMPLe software to the analysis, provides for a simpler quality QA/QC compared to other commercial software used for identification (Primpke et al., 2020). Not only is it a more sensitive software, detecting and identifying organic material (protein, cellulose), but it can also separate the organic material from the specific polymer.

2.4 The complexity of microplastic- A challenge in microplastic analysis

Visual identification has been one of the most frequently used methods for identifying MPs by using the criteria of type, shape, and colour for identification (Lusher et al., 2020). There is however a limitation with this identification method as particles below a certain size cannot be discriminated from other materials in the sample matrix (Bergmann et al., 2015). Colours of the MP particle that are similar to the colour of the matrix, can also be a challenge to identify when MP particles are below a certain size (Haave et al., 2019). Hidalgo-Ruz et al. (2012) suggested in 2012 that visual identification should be applied for MP particles $<500\mu\text{m}$, as misidentification for MP particles below $500\mu\text{m}$ is very high and suggested an even higher size limit of 1mm. The use of techniques that facilitates the proper identification of MP particles is still recommended since visual sorting depends on 1) the analyst counting the MP particles, 2) the quality of the microscope, and 3) the sample matrix (Bergmann et al., 2015; Hidalgo-Ruz et al., 2012). The need for more sensitive methods for the identification, quantification, and characterization of MPs in complex matrices was addressed and there have been a developing with sensitive identification methods for MP analysis such as FTIR, Raman and Pyr-GS-MS (Bergmann et al., 2015; Hidalgo-Ruz et al., 2012; Lusher et al., 2020).

Currently, MP can either be expressed by the number of particles present in the sample or by the mass concentration of the respective polymer (Primpke et al., 2020). This is conducted by two analytical approaches, either spectroscopic or thermal degradation. For spectroscopic methods, FTIR (μFTIR or ATF-FTIR) and Raman spectroscopy are mainly used, primarily due to their ability to determine polymer type (identification), as well as number and size (quantification) and shape of the MP particles (characterization) (Ivleva, 2021). For a spectrometry method, either Pyrolysis Gas Chromatography-Mass Spectrometry (py-GC-MS) or Thermo-extraction desorption GC-MS (TED-GC-MS) are used. In contrast to spectroscopic methods, the thermal degradation uses mass spectrometry for detection methods. The thermal degradation method is destructive and the analysed sample will no longer be available for potential follow-up analysis. With thermal degradation methods, the isolated particles are decomposed and pyrolyzed at temperatures up to 600 degrees (Pipkin et al., 2021; Zarfl, 2019).

The specific degradation products are then measured by the gas chromatography-mass spectrometry part of the instrument. The European Marine Strategy Framework Directive (MSFD) technical subgroup on Marine litter recommends FTIR or Raman methods for MP particles smaller than 100µm (Gago et al., 2016). As recent studies on biota indicate, most MPs located in tissues are smaller than 100 making spectroscopic methods suitable for these types of samples.

There are currently no accredited methods for MP analysis, which makes it difficult to compare and harmonize results obtained by other studies (International Organization for Standardization, 2013). Comparability across laboratories, as well as the need for background control for contamination to avoid false positives, are important for developing standard protocols to generate accurate and reproducible results. An established framework of standards will enhance the quality of meta-analysis across laboratories, resulting in a more accurate assessment of the global risk of MP (Brander et al., 2020). The development of standard protocols are in the starting phase as Wageningen Evaluating Programmes for Analytical Laboratories- Quality Assurance of Information for Marine Environmental Monitoring in Europe (WEPAL-QUASIMEME) and Network of reference laboratories, research centres and related organisations for monitoring of emerging environmental substances (NORMAN) have set up a worldwide development exercise to assess harmonization of laboratory results for MP analysis (Van Mourik et al., 2021). The study reports large RSD (Relative Standard Deviation) of reported MP particles and highlights the difficulties of analysing small MP particles and the need for harmonization and comparability (Van Mourik et al., 2021). The study of Van Mourik et al. (2021) did however not include complex matrices such as biota or sediments.

2.4.1 Purification and isolation methods

Before MP particles can be identified and characterised, either visually or chemically by FTIR, the MP particles need to be isolated from its organic matrix. For biota matrix, isolation can be done by a purification step, a process of breaking down biological tissue (plankton or tissue). This breakdown is traditionally done by applying reagents such as strong acidic and/or alkaline solutions (Cole et al., 2015; Enders et al., 2015; Foekema et al., 2013; Löder et al., 2017). MP exposed to the environment have been subject to weathering, abrasion, and photodegradation and as a result the MPs may have reduced structural strength and resistance against chemicals (A. Lusher et al., 2017). These traditional purification methods are therefore potentially harmful to the MP as the reagents, depending on their pH, can have a negative effect on the polymers and the MP integrity could be damaged or may be lost during purification (Löder et al., 2017). PA and PES for example have a low resistance to acids, even at low concentrations (Amy. Lusher et al., 2017).

In contrast, enzymatic digestion is more biologically specific and has a moderate temperature. The enzymes can therefore purify the organic material without damaging plastic particles (Cole et al., 2014). Protease and lipase are enzymes recommended for the digestion of biota samples (Gomiero et al., 2020a; Gomiero et al., 2019; Löder et al., 2017). Protease is used for the purpose of degrading proteins and does so efficiently in buffers with a pH between 5.0 and 11.0. Since biota samples usually contain high levels of lipids, lipase is applied for splitting the lipids into glycerol and fatty acids, most efficiently in buffers with pH between 2.0 and 5.0 (Löder et al., 2017).

2.5 Quality assurance (QA) and Quality control (QC) in microplastic analysis

One of the most important element in QA/QC practice regarding MP analysis is the control and documentation of contamination (Brander et al., 2020). Compared to other organic pollutants, MP is now present in every surrounding and samples are constantly exposed to secondary contamination. Secondary contamination can stem from air deposition on samples or equipment, sampling equipment and tools made of plastic, water used for cleaning equipment and samples, working solutions, reagents, and synthetic clothing worn by staff (Brander et al., 2020). Therefore, precautions must be made in every step during the study from sampling, processing to analysis in order to prevent or reduce the presence of secondary contamination.

Air contamination is a major concern when working with MPs (Dris et al., 2016; Prata, 2018; Vianello et al., 2019). Previous studies on airborne MP particles show that the dominating polymer in indoor air is PES (Vianello et al., 2019). It is therefore necessary to quantify this secondary contamination from the lab by using background checks and procedural blanks, as it can lead to an overestimation of results (Prata, 2018). To limit secondary contamination, good laboratory practice (GLP) needs to be implemented. The most basic GLP considerations suggested by Brander et al. (2020) are to limit any plastic equipment wherever possible and glass or metal should be used instead, regardless of the matrix. In situations where plastic cannot be avoided a procedural blank should be required to quantify and correct any contribution from the equipment. Secondly, working solutions and reagents used should also be pre-filtered and stored in glass bottles. Third, personnel wear when working in the lab should be non-synthetic attire and the laboratory coat should be made of cotton.

3. Materials and Methods

3.1 Selected sites

The study area is located on the west coast of Norway, in the Sotra region (Rabbarosen) outside of Bergen, Norway (Figure 13). Rabbarosen was chosen for this study because it is known to be a highly plastic polluted area, due to the permanent northward bound ocean current (Norwegian Coastal Current) and south-westerly winds that lead to an accumulation where the plastic is deposited onshore (Bastesen et al., 2021; Bastesen et al., 2020). There have been over 800 documented plastic accumulation sites in this area with an estimated mass of 500-1000 tonnes of marine plastic litter (Bastesen et al., 2020). A study area with large quantities of documented marine plastic litter is important for this study, since we assume MP accumulation in cod occurs with continuous exposure to MPs.

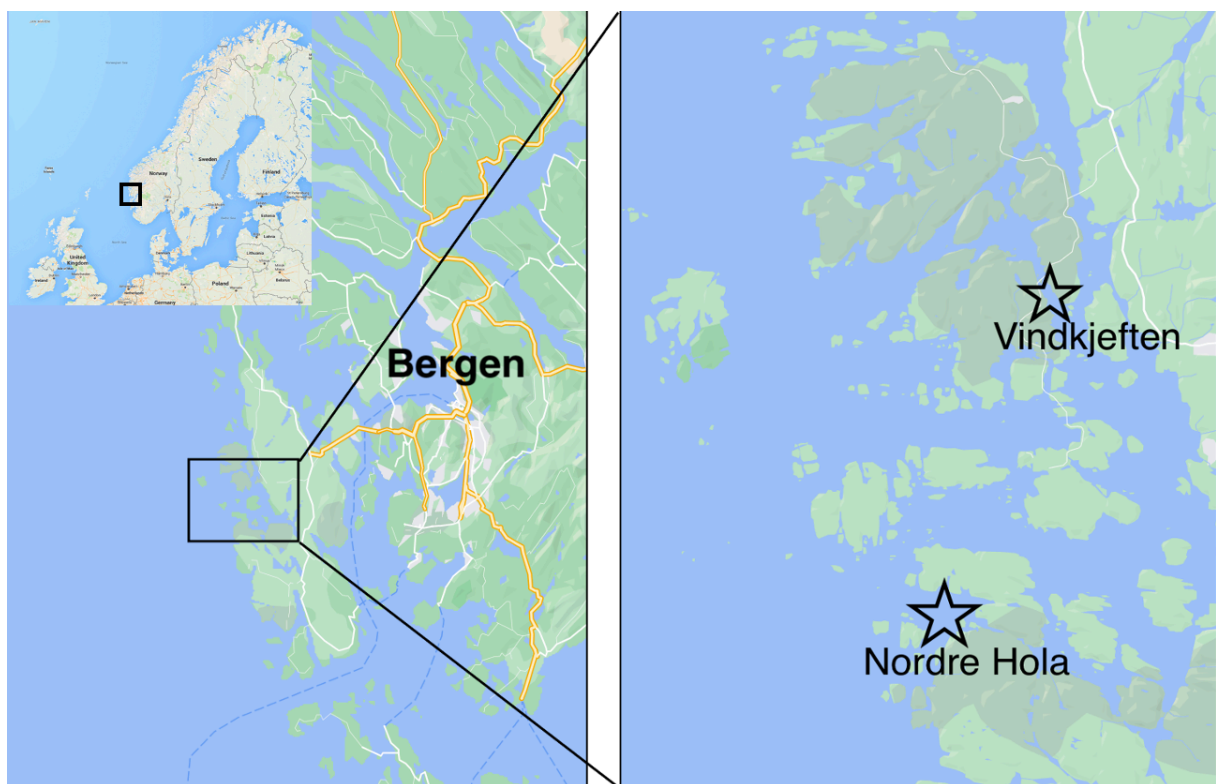


Figure 13- Location of the two sampling sites, Nordre Hola and Vindkjeften in the Sotra-region, Rabbarosen, west of Bergen.

3.2 Sampling

23 fish from Nordre Hola (n=10) and Vindkjeften (n=13) were caught by volunteers from the Norwegian Hunters and Anglers' Association during the period of 07.05.2021- 02.11.2021. By Norwegian regulations, fish below the minimum size of 40cm were not collected for this study but were set free. The fish collected from the sites were either caught by fishing nets or fishing rods, euthanized by a blow to the head, wrapped in aluminium foil, and frozen at -20°C until further dissection and chemical analysis at NORCE PlastLab, Mekjarvik. This sampling method was based on previously published studies (Haave et al., 2021).

3.3 Contamination control and QA/QC

To prevent contamination during dissection and sample processing, the procedures were done in the NORCE PlastLab, located in Mekjarvik, Stavanger (Figure 14). This lab is specially designed to reduce exposure to contamination such as indoor air during sample preparation and secure reliable results in MP analysis. The air through the ventilation system is filtered through HEPA filters, trapping particles 0.3-0.5µm. All samples and blanks were prepared in this lab. Glass equipment, such as funnels, glass tubes, glass petri dishes, glassware used for wet traps, glass beakers, and glass containers were covered in aluminium foil and burned in a muffle oven at 500 °C before use. The top of the glass beaker was always covered with aluminium foil during sample preparation to reduce exposure of air borne contamination.

To enter the lab, only cotton lab coats, cotton personal wear and specialised footwear such as clogs were used to minimise the sources of contamination from clothing and shoes. The lab outfit would be in an isolated sluice section before entering the plastic lab. The plastic lab is equipped with steel benches to prevent contamination from bench surfaces such as linoleum. These surfaces were rinsed with water and tissue paper before and after the dissection of the fish and sample preparation. Filters, tweezers, and other equipment that was in contact with samples during dissection or preparation were rinsed x3 and burned by a gas burner, FLAMEBOY™ (propane gas, 1350°C) before using it on another sample. It was also important to limit the use of plastic in the lab. Some plastic products were however used in the lab, such as squeeze bottles made of PFTE (Teflon®) containing Milli-Q water or EtOH/water (50%). PFTE is a rare polymer to find in the environment. If present in the sample, PFTE would be identified as contamination rather than MP particles from the sample.

For quality assurance purposes and to secure reliable results, a wet trap was used for background checks, containing Milli-Q water to collect air-contaminated particles in the lab during dissection and sample preparation. This is important for securing correct results due to the low MP concentration in tissues, recorded from previous studies (Gomiero et al., 2020a; Haave et al., 2021). Solutions used in the preparation were pre-filtered through a glass fibre filter (Whatman GF/A, 0.7 μm) and stored in glass containers. Milli-Q water was triple filtered by a Milli-Q[®] Direct Water Purification System.



Figure 14- NORCE PlastLab used during sample preparation and dissection, to limit contamination from surfaces, airborne particles, and other plastic materials.

3.4 Tissue sampling

All 23 fish were measured, weighed, and dissected in the NORCE PlastLab. Approximately 100 grams of muscle tissue was collected for MP analysis using scalpels and tweezers. The scalpel knife blade was replaced, and the tweezers were thoroughly washed x3 and burned by a FLAMEBOY™ between each dissection. Two replicates of muscle tissue were collected from both sides of the fish (Figure 15). The samples were weighed, packed separately in a double layer of aluminium foil, and frozen at -20°C until further treatment and chemical analysis.



Figure 15- Left: Equipment used for dissection, such as tweezers, scissors, and scalpel. Right: Dissection of muscle tissue from cod.

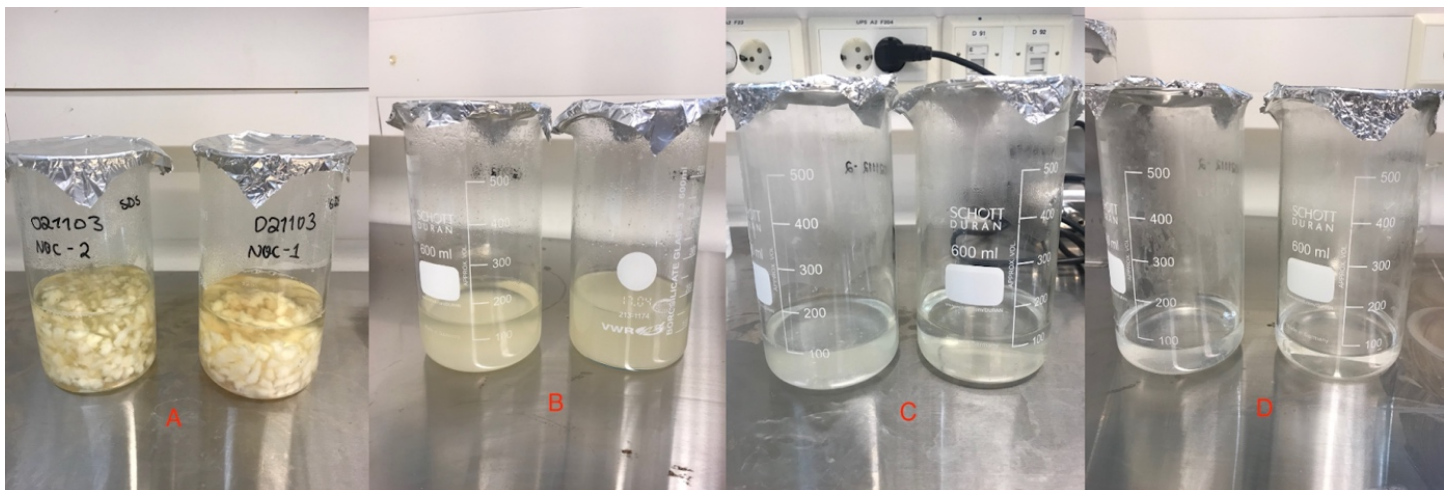


Figure 16- Cod muscle tissue during sample preparation: A= SDS treatment after 12h, B = Protease treatment after 48h, C = Lipase treatment after 24h, D= H₂O₂ (30%) treatment after 12h.

3.5 Purification and removal of organic content

All chemicals, enzymes and equipment used for purification are listed in Appendix A. The protocol of extraction of MP particles from organic material was based on previously developed methods (Gomiero et al., 2020a; Gomiero et al., 2019; Haave et al., 2021).

3.5.2 Multi-enzymatic digestion treatment

The first step in the purification procedure was performed using Sodium Dodecyl Sulphate (SDS), an anionic surfactant for the purpose of denaturing proteins and increasing the contact surface and the enzymes infiltration during enzymatic treatment (Löder et al., 2017). The defrosted muscle tissue was divided into cubes by a clean scissors and placed in a glass beaker (pre-burned at 500 °C). The glass beaker containing the muscle tissue was added 100mL of 5% SDS solution and incubated at 50 °C in minimum 3 hours (Figure 16 A). After incubation, the solution was transferred to a vacuum filtration assembly, using a vacuum flask, glass funnel, graduated funnel, and a pre-burned 10µm stainless steel filter. The SDS-solution was filtered off. EtOH/water was used to clean inside the funnel after completed filtration to include the remaining MP particles sticking to the side of the funnel. The funnel was also cleaned with approximately 2mL Milli-Q water over the glass beaker. The filter containing the remaining sample was transferred to the beaker facing down. The beaker was placed in an ultrasonic bath (B200, 117V, 60Hz, BransonTM Ultrasonic Cleaner) and sonicated for 10 minutes to release any remaining MP particles still sticking to the filter surface. After the ultrasonic bath, the filter was gently scratched by a pre burned, small stainless steel spatula to transfer any remaining sample into the sample beaker and rinsed with approximately 1mL of Milli-Q water on both sides of the filter. The spatula was cleaned with Milli-Q water after scratching over the beaker. The beaker was then added 100mL 0.1 M glycine buffer at pH 10.0 (Appendix A) and 1mL protease concentrated enzyme (P3111, Sigma Aldrich, Germany) and incubated in optimal conditions, 50°C (Figure 16 B). Since the developed method from Gomiero et al. (2020a) is based on salmon tissue, a less protein-rich fish compared to cod, the procedure for cod was set to 48h incubation time for protease degradation instead of 24h.

After the break down of protein in the sample, a new filtration step was needed following the previous description of the procedures for filtration. After filtration and rinsing, the filter containing the remaining sample was transferred to the beaker facing down for an ultrasonic bath for 10 minutes. As previously stated, the filter was washed with approximately 1mL of Milli-Q water on both sides of the filter and scratched with a pre-burned spatula on the surface to transfer remaining MP particles into the sample breaker. After sonication, the beaker was added 100mL of Phosphate buffer saline (PBS) with pH 5.0 and 1mL of lipase enzyme (L0777, Sigma Aldrich, Germany) for enzymatic hydrolysis and subsequent removal of fats and oils. The sample was incubated for 24h under optimal activity conditions at 50°C (Figure 16 C).

3.5.3 Strong oxidative purification treatment

For the final step of purification, a strong oxidative digestion was performed using 50mL hydrogen peroxide (H₂O₂, 30%, VWR International Germany) at 50°C for 12h (Figure 16 D). The final filtration step and sonication step was performed as previous description. After sonication, the filter was thoroughly rinsed on both sides with EtOH/water in a glass tube used for evaporation. The remaining solution with EtOH/water in the sample beaker was also transferred to the glass tube.

3.5.4 Evaporation treatment

A Zymark evaporator was used for evaporating the sample at 59 °C until 1 mL of the sample remained. The glass tube containing 1 mL of sample, was then transferred to a vial for storage. The glass tube was thoroughly cleaned with 1mL EtOH solution x4. After cleaning, a total volume of 5mL EtOH in the vial, was isolated by a top lid for storage. Before μ FTIR analysis, the solution in the vial was filtered onto an anodisc filter ($\phi = 10$ mm; 0.1 μ m, Whatman) and placed in a glass petri dish with a glass lid to dry until μ FTIR-analysis.

3.6 Determination of the size and shape of MP particles using μ FTIR

The μ FTIR analysis was performed in the PlastLab. μ FTIR imaging was performed using a Nicolet™ iN10 MX Infrared Microscope coupled with a 64x64 line array mapping detector and a quantum MCT (Mercury cadmium telluride, HgCdTe) detector to identify MP particles in the muscle tissue samples (Figure 17). By applying an interferometer, the line array detector collected 64 scans per sample and the IR spectra of every MP particle were recorded in the mid-IR range 4000-650 cm^{-1} with a spectral resolution of 4 cm^{-1} in transmission mode. As the MCT detector is temperature sensitive, liquid Nitrogen (N_2 , -196°C) was applied to cool the detector down to detect the vibrations from the MP particles.

The software SiMPLe, characterizes the two dimensions of the MP particle, minor and major dimensions (μm). Major-dimension is defined as the length of the particle (continuous axis in the centre of the particle) whereas minor dimension is defined as the width of the particle (perpendicular to the major axis). The ratio between the two dimensions can give a characterization and distinction to the form of the particle as fibres (length to width ratio > 3) or fragments (length to width ratio ≤ 3).



Figure 17- Model of the Nicolet™ iN™10 MX Infrared Microscope used in this study (Thermo Fisher 2022).

3.7 Statistics and calculations

3.7.1 Fulton's condition factor (k)

Fulton's condition factor (k) is used to describe the two-dimensional weight (W)–length (L) relationship, as a proxy for fish health and physical condition of the cod, using equation 3.1.

$$k = \left(\frac{W}{L^3}\right) * 100 \quad 3.1$$

3.7.2 MP particle concentration per kilo muscle tissue

MP particle concentration per kilo muscle tissue ($\mu\text{g}/\text{kg ww}$) was calculated by the estimated mass of the MP particles performed by SiMPLe in nanograms (ng). The MP particle mass was converted from ng to μg and the estimated MP particle concentration per kilo ww was calculated by equation 3.2.

$$\frac{\text{Particle mass } (\mu\text{g})}{\text{Estimated sample weight (kg ww)}} = \text{Estimated MP particle concentration per kilo ww } \left(\frac{\mu\text{g}}{\text{kg}} \text{ ww}\right) \quad 3.2$$

3.7.3 Standardized MP particle count

To account for differences in sample weight, the number of detected MP particles was standardised to 100g using equation 3.3.

$$\frac{\text{Sample weight (g)}}{100} * n \text{ detected MP particles} = n\text{MP}/100\text{g} \quad 3.3$$

3.7.4 Statistics

The statistical analyses and calculations were performed using IBM SPSS statistics (version 28.0) and Microsoft excel. SPSS was also used for creating graphs. A Shapiro-Wilk normality test was used to test for normal distribution. Nonparametric tests, Mann Whitney test was used to test the comparison of means and Spearman Rho correlation test was used to find correlations between MP particle count detected in cod and the cod length. The statistical significance level was set to $\alpha = 0,05$.

4. Results

4.1 Description of the cod caught in the two locations

The weight and length of the cod are listed in Table 7 and the variation between the two locations are illustrated in Figure 19. As length at maturation increases with age, the length of the cod was used a proxy for age. Based on growth rate curves for stationary cod, the cods length (40-73cm) gives an approximately age 3-5 years (Figure 18) (Heessen et al., 2006). The cod from Nordre Hola (41.4 ± 2.95 cm) were significant smaller in length than the cod from Vindkjeften (51.37 ± 14.77 cm), respectively (Mann-Whitney U-test, $U = 0$, $p < 0.001$). Body condition factor is a proxy for fish health and factor around 1 indicates that the fish is in good condition. The majority of the body condition factors were around this value, with some exceptions. In the upper region, cod #10 had a k-value of 1.57. In the lower region, cod #6 and cod #7 had a k-value of 0.74 and 0.67 (Table 7). There is no significant difference in body condition factor values between the sites (Mann-Whitney U-test, $U = 53$, $p = 0.475$).

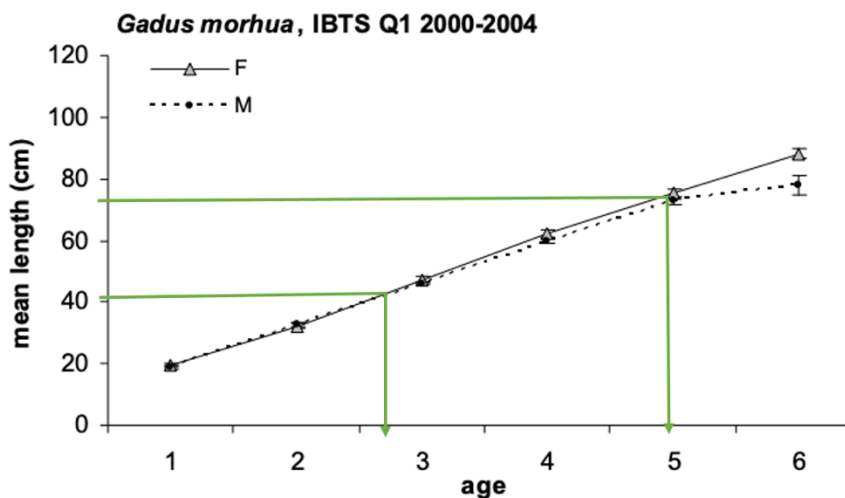


Figure 18- Mean length (cm) per age group for female and male Atlantic cod data from 2000-2004 from Heessen et al. (2006). The estimated age range used in this study is highlighted in green. The estimated age for cod with 40 cm is rounded up to 3 years.

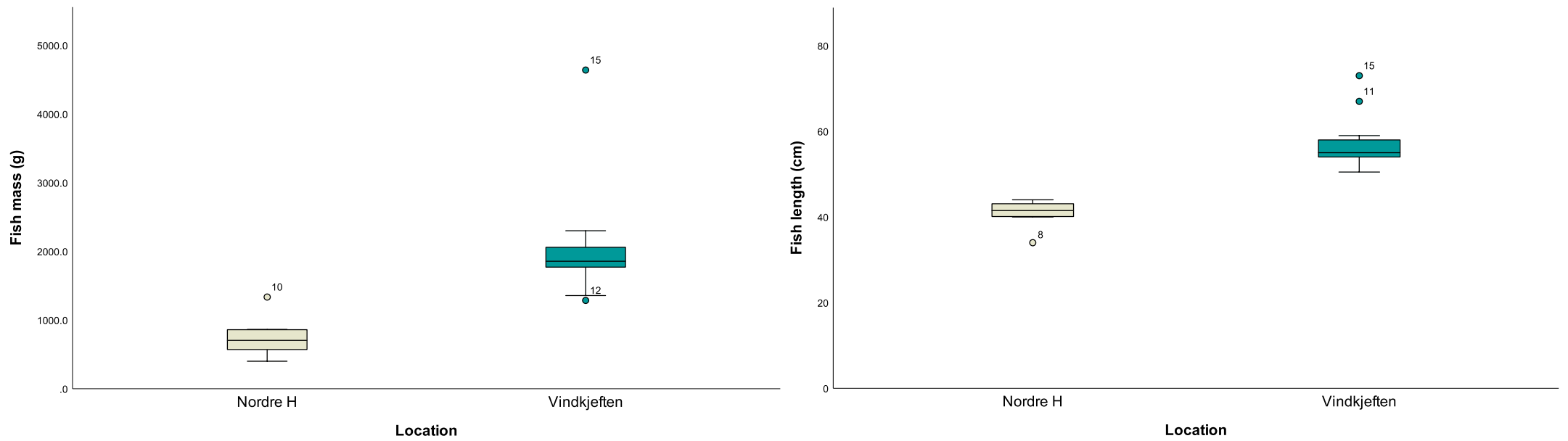


Figure 19- Boxplot of the variation in fish mass (g) and fish length (cm) between the two location sites, Nordre H and Vindkjeften. The outliers are represented in circles.

Table 7-Characterization of all cod captured in the period 07.05.21-02.11.21 in Nordre Hola and Vindkjeften. The characterization includes fish mass (g), fish length (cm) and body condition factor (k), weight of samples collected during dissection (g). The number of identified MP particles found in the muscle tissue is expressed as standardized number of MP particles per 100 g sample (nMP/100g) and estimated MP concentration per kilo sample ($\mu\text{g}/\text{kg}$ ww).

Fish ID	Capture date	Fish mass (g)	Fish length (cm)	Body condition factor, k	Sample weight (g)	n validated MP particles per 100g sample (nMP/100g)	Estimated MP concentration per kilo sample ($\mu\text{g}/\text{kg}$ ww)
Spring							
Nordre Hola							
#1	07.05.21	855	43	1.08	71.41	2.80	0.1
#2*	19.05.21	859	43	1.08	42.13	nd	nd
#3*	19.05.21	637	40	1.00	69.20	nd	nd
#4	19.05.21	698	40	1.09	67.96	10.30	637.62
#5*	30.05.21	863	42	1.17	83.53	nd	nd
#6	30.05.21	550	42	0.74	72.89	nd	nd
#7	30.05.21	570	44	0.67	85.02	nd	nd
#8	07.06.21	400	44	1.02	94.34	nd	nd
Autumn							
#9	27.10.21	708	42	0.96	78.46	3.82	1.29
#10	27.10.21	1334	44	1.57	91.23	1.10	0.76
Vindkjeften							
#11	02.11.21	2299	67	0.76	103.43	3.87	11.42
#12	02.11.21	1285	51	0.97	95.21	9.45	9.55
#13	02.11.21	2059	58	1.06	108.59	nd	nd
#14	02.11.21	1855	55	1.11	91.30	nd	nd
#15	02.11.21	4639	73	1.19	152.78	nd	nd
#16	02.11.21	2229	59	1.09	95.20	nd	nd
#17	02.11.21	1459	53	0.98	97.90	nd	nd
#18	02.11.21	1823	54	1.16	108.13	4.09	1.75
#19	02.11.21	2023	56	1.15	107.64	0.92	5.31
#20	02.11.21	1959	55	1.18	106.06	nd	nd
#21	02.11.21	1356	51	1.02	103.47	nd	nd
#22	02.11.21	1796	56	1.02	115.50	4.33	6.13
#23	02.11.21	1770	55	1.06	110.21	nd	nd
Mean \pm SD	-	1479.45 \pm 917.52	50.3 \pm 9.42	1.05 \pm 0.18	93.50 \pm 21.82	1.89 \pm 3.10	29.30 \pm 132.65

nd = not detected. * = The results are uncertain due to high interference.

4.2 Identified MP dimensions and shape in muscle tissue

The particle size detected in the muscle tissue of cod had an average size of $175.11 \pm 197.53 \mu\text{m}$ and ranged from 25-830 μm (Table 8). The majority of MP particle size were in size classes below 100 μm (Figure 20 A). There was no significant difference in particle size between the two locations (Mann-Whitney U-test, $U=83$, $p = 0,336$). The size distribution per fish is illustrated in Figure 20 C. Fragments were the dominant particle shape (74%) overall with an average size $100.55 \pm 51.36 \mu\text{m}$. Fragments dominated in sizes below 250 μm and fibres dominated over 250 μm (Figure 20 D).

4.3 Identified polymer types in muscle tissue

In total, six different polymers were identified (PP, PE, PS, PET, PES, PA), and they are all among the most commonly produced polymers worldwide. The polymers PP (33,3%) and PE (30,6%) dominated (Figure 20 E). The cod from both locations contained the same polymer distribution apart from PET which was only identified in Nordre Hola in cod #1. The polymer distribution in each cod is illustrated in Figure 21 B. PP had the largest average size for both fragments ($143.79 \pm 68.83 \mu\text{m}$) and fiber ($570.84 \pm 304.14 \mu\text{m}$) (Table 9) and dominated for MP particles over 200 μm (Figure 20 A).

4.4 QA/QC

Nine of 23 wet traps, corresponding to the samples containing MP particles were analysed by μFTIR . Two wet traps contained MP particles, corresponding to cod #1 ($n=1$) and cod #4 ($n=1$) (Table 8). The particles detected ($n=2$) were PE fibres of 123 μm and 310 μm in size. As the PE fibre in the wet trap was in similar colour to the PE fibres in the cod #1, the two PE polymers were excluded from the result. Cod #4 did not contain PE fibres and a subtraction was therefore not performed. After blank subtraction a total of 36 out of 38 MP particles were included in the result.

Table 8- Data of detected MP particles from the muscle tissue of cod and their respective blank samples containing MPs by μ FTIR and SiMPLe software. The detected MP particles are described by the major and minor dimensions (μm), shape and polymer.

Fish ID	Major dimension (μm)	Minor dimension (μm)	Dimension ratio	Shape	Polymer
#1	49.2	8.5	5.7	Fiber	PET
	25.0	15.9	1.9	Fragment	PS
#4	220.3	86.7	2.5	Fragment	PP
	205.3	89.2	2.3	Fragment	PP
	136.8	58.2	2.3	Fragment	PP
	806	260.6	3.1	Fiber	PP
	234.9	125.4	1.9	Fragment	PP
	701.4	189.5	3.7	Fiber	PP
	830.4	272.1	3.1	Fiber	PP
#9	121.8	23.0	5.3	Fiber	PES
	153.0	28.0	5.5	Fiber	PE
	124	36.0	3.4	Fiber	PE
#10	80.9	49.2	1.6	Fragment	PA
#11	136.8	69.8	1.9	Fragment	PE
	192.7	103.2	1.9	Fragment	PP
	95.7	74.8	1.3	Fragment	PE
	95.7	58.2	1.6	Fragment	PS
#12	180.0	30.8	5.8	Fiber	PP
	179.9	45.3	3.9	Fiber	PES
	155.0	23.8	6.5	Fiber	PE
	131.8	70.0	1.8	Fragment	PES
	60.4	52.7	1.1	Fragment	PES
	110.0	60.7	1.8	Fragment	PE
	135.1	48.4	2.8	Fragment	PES
	70.3	44.1	1.6	Fragment	PA
	101.1	45.9	2.2	Fragment	PA
#17	60.4	39.6	1.5	Fragment	PES
	60.4	39.6	1.5	Fragment	PE
	75.0	42.4	1.7	Fragment	PE
	80.9	49.2	1.6	Fragment	PE
#18	258.2	86.3	2.9	Fragment	PP
#22	258.2	86.3	2.9	Fragment	PP
	60.4	39.6	1.5	Fragment	PP
	60.4	52.7	1.1	Fragment	PE
	50.0	31.8	1.5	Fragment	PES
	60.4	39.6	1.5	Fragment	PE
Mean \pm SD	175.11 \pm 197.53	53.90 \pm 20.11	-	-	-
Corresponding wet traps					
#1	310.0	38.8	7.98	Fiber	PE
#4	123.0	34.0	3.61	Fiber	PE

PA= Polyamide. PE = Polyethylene. PES = Polyester. PET = Polyethylene terephthalate. PP = Polypropylene. PS = Polystyrene.

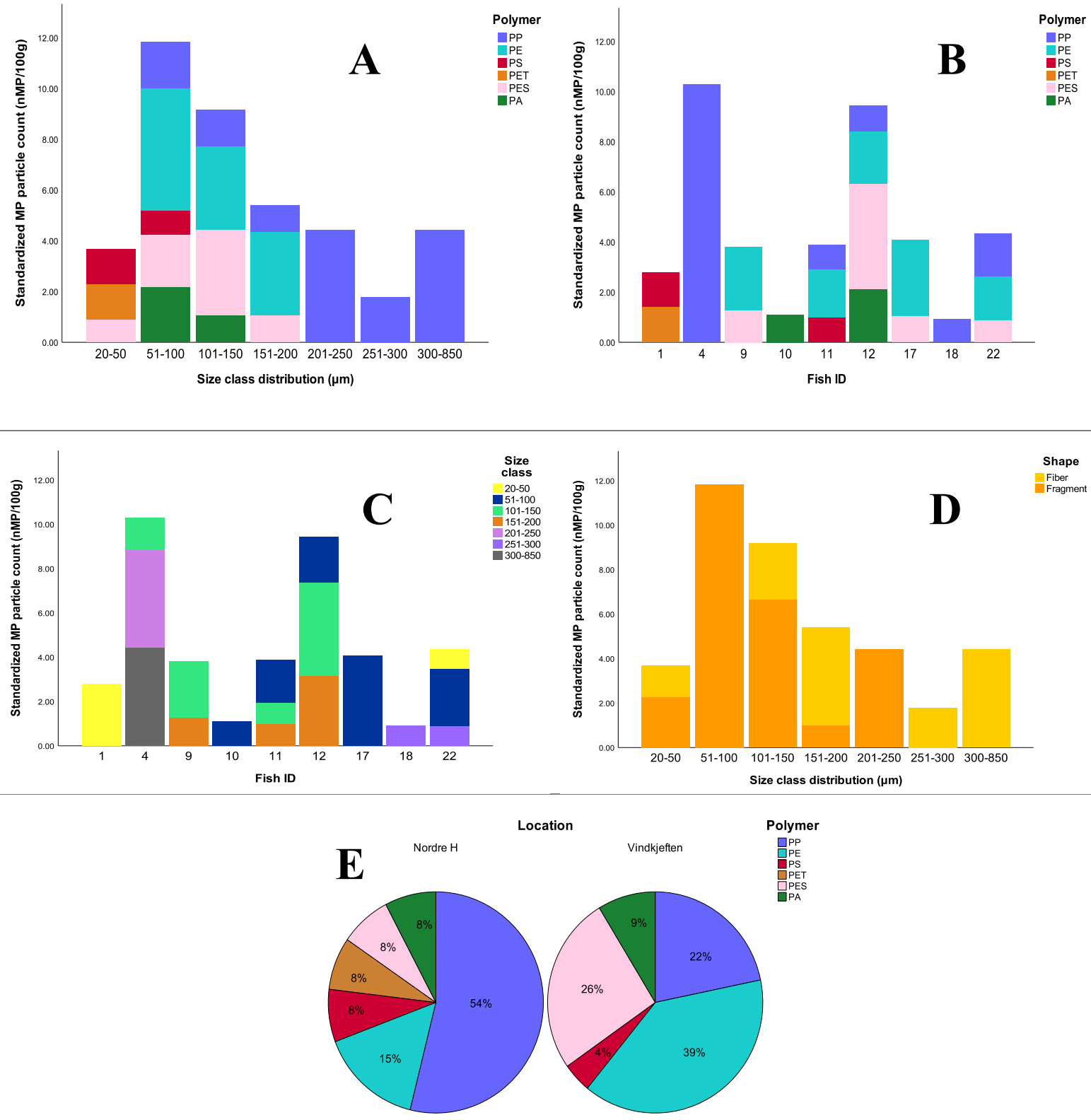


Figure 20-Graphic summary of standardized MP particle count in cod (nMP/100g). A= Polymers per size class, where PP = purple, PE = turquoise, PS = red, PET = brown, PES = pink, PA = green. B = Polymers per fid ID with same color code as A. C = Size class per fish ID. D = Size class per shape and E = Pie chart of polymer distribution per location site with same color code as A and B.

Table 9- Mean polymer size (μm , with standard deviation) of detected MP in cod muscle tissue with according to particle shape.

		PP	PE	PS	PES	PET	PA
Fragment	Mean	143.70	97.08	63.75	87.54	-	87.54
	SD	68.30	48.08	45.18	49.19	-	49.19
Fibre	Mean	570.84	144.0	-	150.85	48.40	-
	SD	304.13	17.35	-	41.08	-	-

4.5 Investigation of MP bioaccumulation

The observations of MP in cod are presented in Table 7. MP particles (n=36) were detected in a total of nine of 23 cod from Nordre Hola (n=4) and Vindkjeften (n=5). The average MP particle count per 100g and average MP particle concentration per kg sample was 1.89 ± 3.10 nMP/100g and 29.30 ± 132.65 $\mu\text{g}/\text{kg}$ ww, respectively. The number of cod containing MP particles were low (n=9) and was therefore not possible to investigate the relationship between the dependent variable (number of particles) and the independent variables such as fish length and location by a linear regression analysis. Instead, a Spearman rank correlation test was done. Spearman rank correlation test show no correlation between N standardized MP particles and length ($r_s = -0.090$). The correlation is also illustrated in Figure 21A ($R^2 = 0.010$), presenting that smaller cod contained as much MP particles as the larger ones. The relationship between N standardized MP particles and body condition factor (k), a proxy for the cod's health was also examined by Spearman rank correlation and shows no correlation ($r_s = -0.183$). This correlation is illustrated in Figure 21 B ($R^2 = 0.012$).

The number of N standardized particle count per 100g between the fish had large variations (0-10.38nMP/100g). The fact that the majority of the cod did not contain MP (n=14) effects the standard deviation for N standardized particle count per 100g and the MP mass concentration per kilo sample ($\mu\text{g}/\text{kg}$ ww) (Table 7).

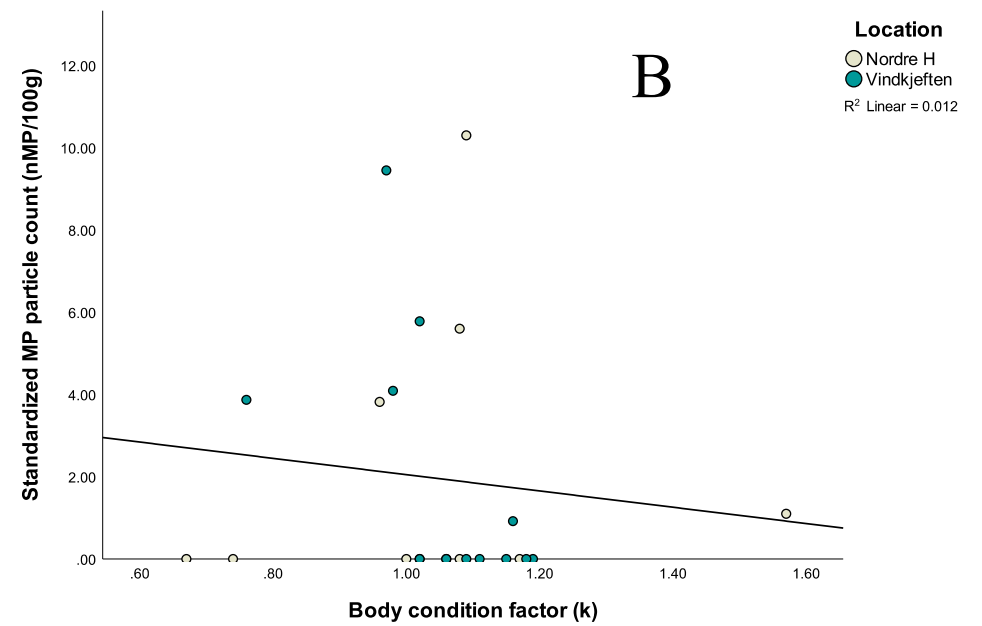
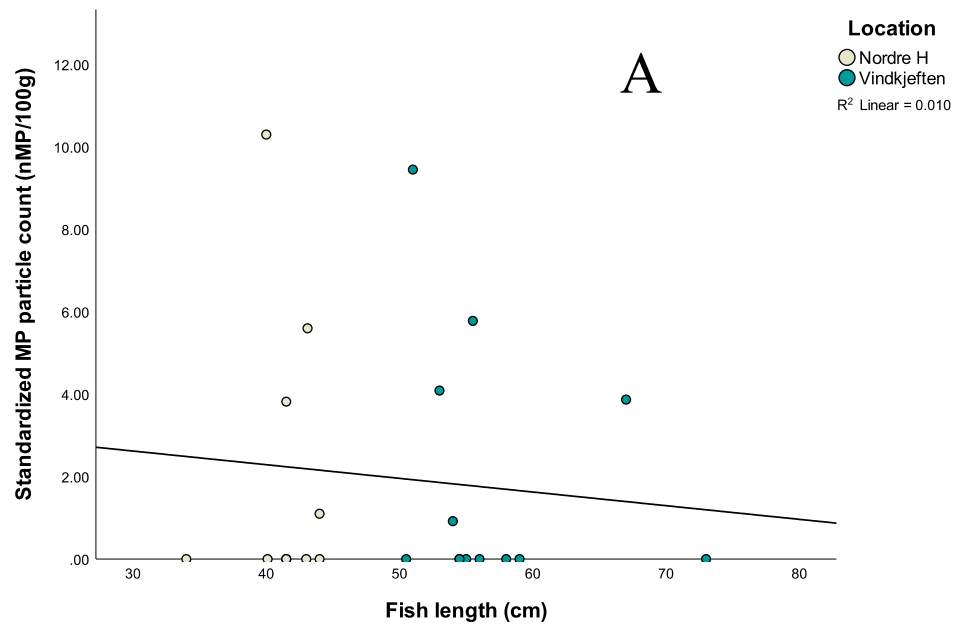


Figure 21- A simple scatter plot illustrating the relationship between standardized particle count and (A) fish length (cm) and (B) body condition factor (k).

4.6 Microplastic identification by μ FTIR analysis

The μ FTIR analysis was time-consuming and therefore not all wet traps were analysed. Only the wet traps corresponding to samples with detected MP particles. The resolution and selectivity of the spectra and images were high and could easily identify particles as either MP particles or organic material, such as protein or cellulose. The μ FTIR analysis provided filter images, heat maps and spectra map for the 23 samples of cod. Figure 22 illustrates the different parts of μ FTIR analysis of cod #4. The remaining filter images and maps for the other samples are listed in Appendix B.

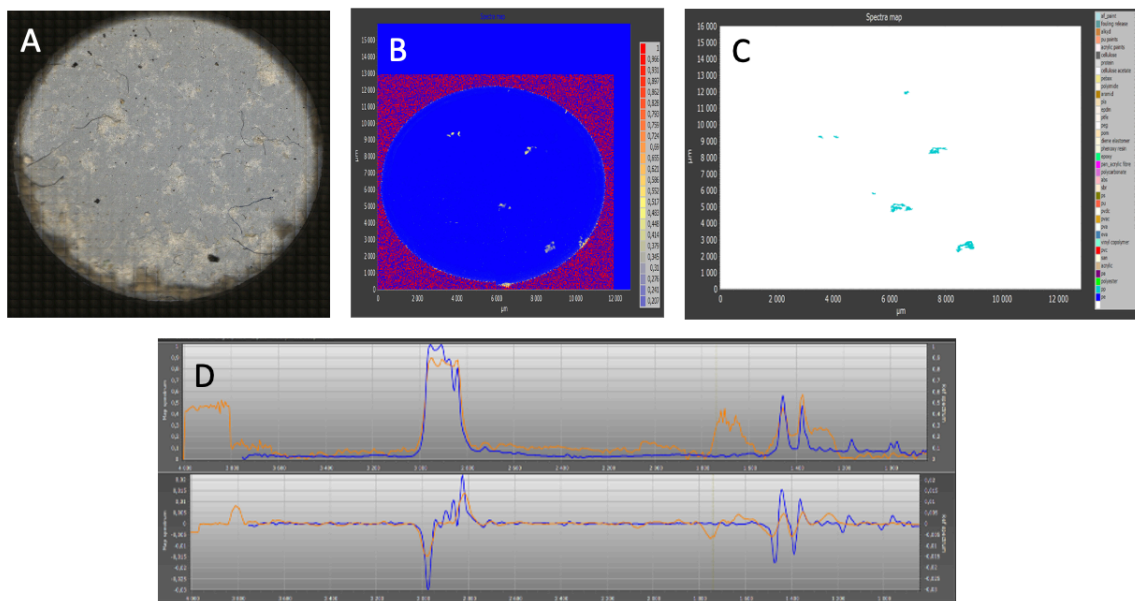


Figure 22- A= Visual image of the filter membrane. B= Heat map where the colors show the probability for PP present in this sample. Blue indicates low probability and red indicated high probability. C = Spectra map. The color codes for the identified MP polymer, with the information on major and minor dimensions (μm). The color codes are shown in figure 20. D= Raw FTIR for PP. Blue = reference spectrum for PP and orange = sample spectrum

	0
	1 Polyethylene
	2 Polypropylene
	3 Polyester
	4 Polyamid
	5 Acrylic
	6 Sand
	7 Polyvinyl chlorid
	8 Vinyl copolymer
	9 eva
	10 pva
	11 pvac
	12 pvds
	13 pu
	14 Polystyrene
	15 sbc
	16 abs
	17 polycarbonate
	18 pan_acrylic fibre
	19 epoxy
	20 phenoxy resin
	21 diene elastomer
	22 pom
	23 peg
	24 ptfe
	25 epdm
	26 pla
	27 aramid
	28 Polyimide
	29 pebax
	30 cellulose acetate
	31 protein
	32 cellulose
	33 acrylic paints
	34 pu paints
	35 alkyd
	36 fouling release
	37 af_paint

Figure 23- Polymer groups analyzed using the μ FTIR analysis.

The filters of cod #2, cod #3 and cod #5 contained excessive organic material. The excessive organic material made it difficult to conduct proper μ FTIR analysis (Figure 24) when the IR radiation is completely absorbed by the filter and causes high interference. After performing a second protease step for samples of approximately 100g, for example cod #17 (97.90 g) and cod #20 (106.06 g) a more purified filter images were observed (Figure 59B and Figure 74B). There were however variations in purifications although a second protease step was included, for example for cod #19 (Figure 71B). Due to the porous nature of the anodisc filter, some sample filters partly broke when transporting the filter to the μ FTIR instrument using tweezers (Figure 77B for example).

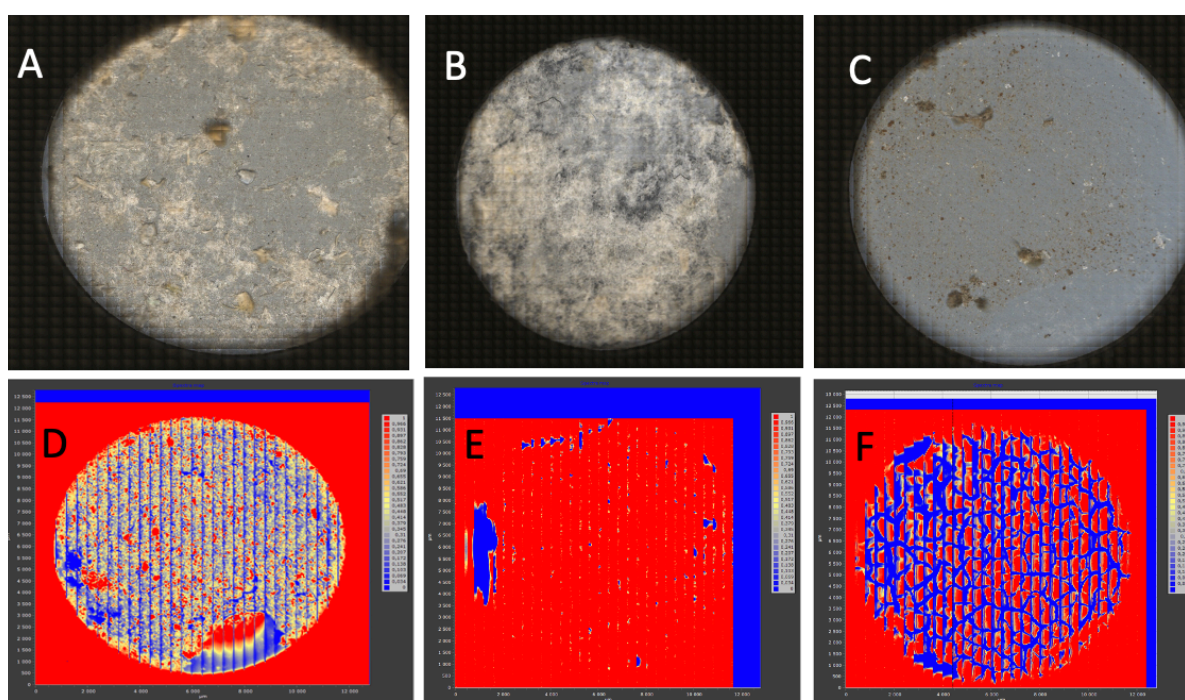


Figure 24- Filter images and heat maps for cod #2, cod #3 and cod #5 presenting IR absorption. (A) and (D) represent cod #2, (B) and (E) represent cod #3 and (C) and (F) represent cod #5.

5. Discussion

5.1 Summary of the study

This study investigated correlation between MP accumulation in relation to fish length (as a proxy for age) in cod from two locations in Sotra. MP particles (n=36) in muscle tissue of nine of 23 cod from the two locations Nordre Hola (n=4) and Vindkjeften (n=5) were observed. The average MP concentration per sample weight was $19.26 \pm 61.90 \mu\text{g}/\text{kg ww}$. The average MP particle count per 100g was $1.89 \pm 3.10 \text{ nMP}/100\text{g}$. μFTIR detected 10 fibres and 26 fragments in total. Six different polymers were identified, PP (33.3%) and PE (30.6%) being the dominating polymers. MP particles were observed in large as well as smaller cod. There was no correlation between length and nMP or k-factor and nMP.

5.2 Larger MP particles and higher MP concentration compared to previous findings

Compared to previous findings of MP in muscle tissue from wild and farmed fish along the Norwegian coast this study has a larger size range (25-830 μm) and estimated MP particle concentration range (0.1-637.62 $\mu\text{g}/\text{kg ww}$) (Gomiero et al., 2020a; Haave et al., 2021). However, it is consistent with previous studies that the majority of the MP particles were below 100 μm . Gomiero et al. (2020a) applied both Py-GC-MS and μFTIR and detected MP particles ranging from 10-240 μm with a mass concentration of 0-79.6 $\mu\text{g}/\text{kg}$ in the muscle tissue of wild and farmed salmon. Haave et al. (2021) quantified 1000 $\mu\text{g}/\text{kg}$ by Py-GC-MS in muscle tissue of wild cod. Reasons for a larger size range and mass concentration range detected in this present study compared to previous studies are composite. One reason could be a higher upper size limit for persorption of MPs trough the GI than previously assumed. As mentioned in chapter 2.2.3, Volkheimer (1993) stated that particles <150 μm are less likely to pass through the GI wall and to be transported via the portal system to other organs such as muscle tissue and liver. This size limit has been proven to be higher in laboratory studies, observing MP particles larger than 150 μm in fish livers, with sizes of 200-600 μm (Avio, Gorbi, & Regoli, 2015) and $323 \pm 101 \mu\text{m}$ (Collard et al., 2017). However, there has not been a specific study that have specifically investigated the persorption size limit in fish (Jovanović et al., 2018).

In this study 12 particles larger than 150 μm were detected by μFITR . Six of these MP particles were PP polymers (Figure 20 B) from the muscle tissue of cod #4. Compared to the other fish containing MPs, cod #4 has the largest size variation from 136,8 μm to 830,4 μm (Figure 20 C) and estimated MP concentration per kilo sample weight (637.3 $\mu\text{g}/\text{kg}$ ww). These large particle sizes (μm) and estimated mass concentration ($\mu\text{g}/\text{kg}$ ww) could stem from contamination. Contamination or cross-contamination is a major challenge in MP research and each step in the preformed method in this study has considered the possibility of contamination. A potential contamination source could be fishing gear used during sampling, such as nets and ropes as they are commonly made from PP polymers. There is a possibility for PP particles to retain in the skin of the fish after sampling. Although the fish was rinsed with Milli-Q-water and wiped with paper tissue before dissecting in the PlastLab, MP particles sticking to the skin could potentially attach to the knife or tweezers and contaminate the samples. Since the MP particles identified in cod #4 was blue, it would therefore be unlikely that the fibres originated from the fishing net equipment as the colour of the fishing net used for sampling was orange. As this study did not include procedural blanks, solutions and chemicals could be potential contamination sources, even though the solutions are filtered before use. However, it is unlikely that such large particles have passed through the filters and were in the reagents and solutions. If the particles originated from airborne contamination HEPTA-filters in the lab would limit this. By only applying wet traps for the detection of airborne contaminants and not including procedural blanks or reference materials from field equipment, there is a greater risk of being unable to confirm or exclude contamination.

It seems more likely that the MP particles larger than 150 μm detected in this study stems from contamination rather than a higher persorption size limit. Contamination can be supported by the shape of the MP particles as the three largest particles found in the muscle tissue of cod #4 for example (701.4 μm , 806.0 μm , 830.4 μm) are fibres. When present in the GI tract and intestines, having a more compact shape (i.e., fragments, films, or pellets) would facilitate the passage through cells by endocytosis process rather than fibres, especially in those large sizes. A persorption of fibres in those sizes detected in cod #4 through the intestinal epithelium is therefore unlikely. This argument can also be supported by the dominance of fragments compared (74%) to fibres observed. However, the largest fragment observed is around 258 μm , which also raises the question if the particles originated from contamination or translocated from the intestine to the muscle tissue.

This study confirms the conflicting evidence around MPs ability to translocate in terms of size and there is still much to understand about the mechanisms of transporting small particles in the body.

5.3 Polymer types

The six different polymers identified are all among the most commonly produced polymers worldwide which also corresponds to the polymers found in the marine environment (GESAMP, 2015). The polymer distribution also supports previous findings in the stomach and muscle tissue of fish along the Norwegian coast (Bråte et al., 2016; Gomiero et al., 2020a; Haave et al., 2021). The same polymer distribution was found in the muscle tissues between Nordre Hola and Vindkjeften, which could indicate a homogeneous distribution of MPs between the two location sites (Figure 20 E). Overall, PP and PE polymers dominated in this study. PP and PE are polymers associated with consumer products such as plastic bags, plastic bottles, films and containers and could originate from the break-down of larger macro plastic items. PP and PE are also dominating polymers in aquaculture and fishing and are used in ropes and fishing nets, buoyancy materials and feeding pipes (Gomiero et al., 2020b; A. Lusher et al., 2017). PA is also a polymer used in fishing ropes and nets and would also be expected to be dominant in this area but only observed in cod #10 (n=1) and cod #12 (n=2). As mentioned in chapter 2.4.1, PA has low resistance to acids. Since the purification treatment involved H₂O₂, a strong oxidative, their low amounts could explain the absence.

A prevalent polymer present in the environment and not observed in this study was PVC. PVC have been detected in stomachs and tissue of fish, including cod (Bråte et al., 2016; Gomiero et al., 2020a; Haave et al., 2021). PVC is a high-density polymer and present in the lower part of the water column and sediments (Table 4). The observation of crabs and sand in the stomach of the cod during dissection supports the statement that the cod also operates in the lower parts of the water column and sediments. PVC is therefore a polymer that would be expected to identify in the muscle tissue. However, previous findings of PVC in sediments along the Norwegian coast show large variations (Haave et al., 2019) and it was not within the scope of this study to analyse MP concentration in sediments. The occurrence of polymers could therefore not be based on only two studies done in the area.

5.3- Reasons for no MP accumulation in relation to age in cod muscle tissue

Our assumptions were that if the cod was continuously exposed to MPs and MP was bioaccumulate, the number of MP particles in muscle tissue of cod would increase over with cod length/age. The cod length varied from 40-73 cm (3-5 years) and based on our assumptions, there would be a larger particle count of accumulated MP particles in the muscle tissue in older cod than younger cod. However as seen in Table 7 and Figure 21, the accumulated MP particles in muscle tissue are present in younger cod as well as older. The reason why there was lower number of cod containing MP particles than expected and why there was no correlation between nMP/100g, and length (cm) are discussed in the chapters below.

5.3.1 Exposition to lower MP concentrations

Considering the cod are very much likely been continuously exposed to MPs and that MP was bioaccumulative, the number of cod containing MP particles (n=9) is lower than expected. However, by comparing the number of cod containing MPs in this present study to the number of the different fish species containing MP from Gomiero et al. (2020a), the number of fish is similar. Gomiero et al. (2020a) detected MPs particles in the muscle tissue of eight farmed salmon, three wild salmon and one mountain trout. In other words, 20% of the analysed fish from Gomiero et al. (2020a) contained MPs and are lower compared to this present study (39%). However, Gomiero et al. (2020a) detected higher amounts of MP particles (0-54 MP particles) in the fish compared to this study (0-36 MP particles).

A reason why this study has documented lower MP particle counts compared to other studies could be that the fish have been exposed to different levels of MP concentrations. Farmed salmon are more exposed to MPs in their aquaculture facilities they live in such as the framework constructed with plastic pipes and fibres from fishing nets covering the cages. Fish feed have also shown to contain PP, PA and PE polymers up to 300µm (Gomiero et al., 2020b). However, farmed salmon are also located along the coast and are exposed to the same MP concentration in the water as the wild cod located in the same area. Gomiero et al. (2020a) was also conducted in different regions compared to this study, so the exposure levels could be different.

Haave et al. (2021) investigated MP in muscle tissue and liver in cod and other species located along the coast such as birds and seals. The cod was also caught in the Sotra region, north off our location sites. Haave et al. (2021) also observed over a 1000 times higher MP concentration with py-GC-MS in the muscle tissue ($1.0 \mu\text{g/g} = 1000\mu\text{g/kg}$) compared to this study ($29.30 \mu\text{g/kg ww}$). A reason why there are so large differences in concentration is that Haave et al. (2021) used only 30g of muscle tissue and standardizing to 1 kg, which can affect smaller samples by multiplying the results as it magnifies the measurement uncertainties. Which study that provides a representative picture for the area is hard to tell, as there are only two studies to compare for cod and the occurrence of MP in muscle tissue need to be further investigated. The presented results in this study are difficult to compare to other studies as well due to the very limited available data in literature, and constantly improving methodology.

5.3.2- Target organ

Another reason for low MP particle count and that the majority of the muscle tissues ($n=14$) did contain zero MPs, could be that the cod muscle tissue is not the primary target organ, and higher levels of MP accumulation occurs in other tissues, such as the liver. Gomiero et al. (2020a) found similar high levels of MPs in both muscle tissue and liver of salmon and could not conclude a definite target organ. Haave et al. (2021) found higher levels of MP in the cod liver ($3400\mu\text{g/kg}$) compared to the muscle tissue. Salmon and cod differ in lipid content in the muscle. Salmon are known to have a higher fat content (10%) in the muscle compared to the cod (1%) which is leaner in the muscle and contains a higher fat content in the liver (Sivertsvik et al., 2004). Since plastic and fatty tissue are both lipophilic, a higher accumulation of MPs in the liver rather than the muscle could explain the lower MP count in the muscle of cod. To analyse the liver as a potential target organ would provide a better picture of MP accumulation as it has shown high levels of MPs in Haave et al. (2021) and Gomiero et al. (2020a), however it was not within the scope of this study to perform analysis of both tissues.

A laboratory study by Clark et al. (2022) exposed rainbow trout to palladium-doped polystyrene nanoplastics (PS-Pd NPs, ~200nm) for seven days and did not observe an NP accumulation in the liver (1.1 ± 0.1 ng/g). In contrast, the study did observe higher MP levels in the kidney (65.6 ± 25.4 ng/g). After the depuration phase, the MP concentration in the kidney had decreased to detection level (3.0 ± 0.5 ng/g). The study observed an interesting NP behaviour as the kidney excretes the accumulated PS-Pd NPs when the rainbow trout was not being continuously exposed. Even though this laboratory study used a different species of fish and used smaller plastic particles compared to this present study, the result may cause doubt that the fatty tissues such as the liver could be a primary target organ for MP accumulation than first assumed. These exposure studies provide important knowledge on the possibility of excretion of NPs in target organs and raises the question if MPs behaves in the similar manner. If so, excretion could be another possibility as to why this study did not observe MP accumulation over time in the muscle tissue and cannot be observed by field studies.

5.3.3 Loss of material

There is also possibility that MP present in the muscle tissue could have been lost or remained on the equipment (e.g., glass funnels, tweezers, glass beakers) in different steps of the sample preparation. As mentioned in Chapter 3-Material and methods, the steps to prevent potential loss were done by thoroughly rinsing (x3) the equipment with pre-filtered EtOH/water to minimize the surface tension and use ultrasonic bath for the filters to release the remaining MP from the filter. Loss of material is therefore an unlikely explanation of the low number of MPs since quantitative transfer of all potential MP particles has been focused on in the steps of sample preparation during this study. Still, as MPs $< 300\mu\text{m}$ are not visible to the naked eye, it is hard to observe if the cleaning has been completely successful and if cleaning did collect potentially lost MP particles. Smaller particles ($< 10\mu\text{m}$) could also have been lost during the filtration steps, potentially not been detected by μFTIR or misidentified as cellulose or protein.

As mentioned, it was difficult to fully digest the protein in the larger pieces of muscle tissue (~100g) with enzymatic treatment. The samples from cod #2, #3 and #5 contained so much organic matter on the filters that a complete $\mu\text{-FTIR}$ analysis was not possible (Figure 23). An incomplete digestion of these samples could have led to potential MP particles have not been detected by μFTIR .

5.3.4 QA/QC considerations

This study is based on methods used and developed by Gomiero et al. (2020a) and Haave et al. (2021). These studies dissected the fish in a MP clean room rather than an isolated lab, making the fish more exposed to secondary contamination. However, the studies report low amounts of airborne MP and MPs from procedure controls. Still, as samples were dissected in open air, it increases the possibility of contamination.

By comparison, this present study used the PlastLab in every sample preparation step, from dissection to analyzing the samples on μ FTIR. By including the PlastLab, could also be a reason why this study detected a lower MP particle count than Gomiero et al. (2020a) and Haave et al. (2021). Both Gomiero et al. (2020a) and Haave et al. (2021) have highlighted the possibility for contamination during the procedure from either reagents or equipment and implies that the results must be considered to have an inherit uncertainty. Uncertainty of the results is not to be avoided in this study either. Not including procedural blank in the study provides the results with a higher uncertainty. However, the reason to question the reliability of the results in this study is rather the MP particle size than the number of MPs (n=36) observed.

Previous studies on airborne plastic particles show that the dominating polymer in indoor air is polyester (Vianello et al., 2019). As PES is a polymer mostly used in clothes and textile fabrics (Table 2), it would therefore be reasonable to expect, that any detected airborne contamination to be PES particles. The detected PE particles, however, are not as common in either clothing or textile. PE is mostly used in single-use products and can originate from sources such as packaging material (Table 2). As the PlastLab contains limited plastic material, especially single-use products it is unlikely it originates from the lab itself. The wet traps detected 2 PE particles from the nine fish that contained MP particles. Some wet traps did detect airborne particles, but μ FTIR did not identify them as plastic (Figure 31B for example). By including the number of muscle tissue samples and wet traps, 39 samples in total were analysed by μ FTIR. 28 samples in total (72%) did not contain MP particles and gives a good indication that an isolated PlasticLab, with limited plastic equipment and with personnel and lab- clothes made of cotton is an important quality assurance step in MP analysis.

5.3.5 Little age variation

The age of the cod were approximately 3-5 years based on the length of the cod and growth rates. Since the age of the cod only differed by a couple of years, it could explain why we cannot see a clear MP accumulation in relation to age. If our assumptions are correct, that more mature cod contains higher MP concentrations compared to younger cod, this could have been observed if more mature cod have been caught. In other words, although this study could not find evidence of MP accumulation with increasing age, it does not mean MP does not accumulate in muscle tissue over time.

5.3.6 Is bioaccumulation a suitable term for assessing ecological risk of MPs?

Bioaccumulation and biomagnification are two classic concepts applied to dissolved chemicals adopted by the MP scientific literature to assess whether the MP concentrations are increasing in the organism over time and from lower to higher trophic levels in the food chain. In general, dissolved chemicals and MPs interact with marine organisms in different ways and the process of MP persorption and translocation have shown to be more complex compared to soluble chemicals such as POPs. The complexity of MP persorption and translocation could explain why it is challenging to find evidence for MP bioaccumulation. However, we know marine organisms in the Norwegian environment ingest MPs and recent studies have observed MPs in the muscle tissue and other organs of fish (Gomiero et al., 2020a; Haave et al., 2021). It is only natural to investigate bioaccumulation as part of understanding which organisms are affected to exposure of MPs and to what extent. This study did not find evidence of MP bioaccumulation as we could not see MP concentration increasing with length. However, as this study only examined muscle tissue to investigate MP accumulation in muscle tissue of cod, it cannot be concluded if MP bioaccumulation do or do not happen at all based on our result, since MP accumulation may occur in other organs. More research is needed to assess whether the classical concepts bioaccumulation and biomagnification are suitable for describing the ecological fate of MP in the environment.

5.4 Microplastic analysis with μ FTIR

This study was originally set to combine μ -FTIR and Py-GC-MS for a more precise and accurate analysis to count, measure and quantify the MP particles. Since only μ FTIR was used, estimated mass concentration ($\mu\text{g}/\text{kg ww}$) was calculated by using the estimated mass (ng) from SiMPLe. The μ FTIR analysis in collaboration with SiMPLe gave a mass estimate for the identified particles, based on which a concentration estimate for the muscle samples were made. As the analysis provides two dimensions for the particle, the third dimension, particle thickness, is an estimate, defined as 0.67 times the minor dimension(μm). As particle thickness varies between particles, there is a possibility for over-and-underestimation of the mass concentration and including a spectrometry analysis such as Pyr-GC-MS would therefore be more accurate. The filter images showed (Appendix B) variation in how much of the muscle tissue that has been fully digested in the samples. The undigested muscle tissue in the samples is identified by SiMPLe as “natural” particles as protein. Cotton or paper present in the sample are identified as cellulose. Some samples have been fully digested which makes it easier to spot detected MP particles and some are not. In some filters there seem to be a fibre in a black shade colour, but this can stem from oxidised fish bones and muscle tissue.

6. Conclusion

Atlantic Cod is an important species in the coastal ecosystem. Identifying whether MP accumulates in cod will provide valuable information regarding MP behaviour in the food web. This study demonstrates that MP particles are present in the muscle tissue of wild-caught cod in the Norwegian environment, which is continuously exposed to MP in its natural habitat. The size of the MP particles is higher than previously reported and suggesting a possible unidentified source of contamination rather than a possible higher size limit of persorption. Low levels of MP particles were found in the wet traps (n=2), suggesting that the PlastLab is sufficient to reduce airborne contamination. In addition, no correlation was found between the MP in the muscle tissue and cod length (as a proxy for age) in this study. These results suggest that MP bioaccumulation does not occur or that there are other primary target organs for MP accumulation such as the liver or kidney. This study supports previous findings that MP bioaccumulation in muscle tissue have not been confirmed, a concept adopted in MP literature used for ecological risk assessment for pollutants in the environment.

Microplastic is a new and emerging field of research and the many environmental and ecotoxicological questions revolving plastic and MP are still unanswered. By identifying MP in edible tissue of cod provides an important insight regarding the status of MP pollution in the coastal ecosystem and potential exposure route for humans. More research is needed to answer these questions, by developing more precise and sensitive methods to identify MPs in complex matrices.

7. Future work

- To get a better perspective on the role of MP translocation within an organism and determine a potential target organ(s), liver and gastrointestinal tract should also be included in the study.
- Species at different trophic levels of the food web should also be included for a better understanding of the transfer of MP up the food web.
- A combined identification and quantification method for MPs consisting of both μ FTIR and py-GC-MS.
- Include procedural blanks and/or reference material from sampling to analysis to exclude and document possible contaminations for more reliable results as a part of quality assurance criteria.
- Include a reference site, a more shielded site for marine plastic litter to compare MP particle count and MP concentration to fish exposed to higher amount of plastic litter.
- To provide more reliable results in terms of establishing bioaccumulation of MP in naturally exposed organisms, water samples from the sampling sites and a more thorough mapping of the sampling area for plastic.
- More research to establish the persorption size limit for MPs through the GI tract of various species for better understanding for the mode of MP uptake.

8. References

- Agenda, I. (2016). The New Plastics Economy Rethinking the future of plastics. The World Economic Forum: Geneva, Switzerland.
- Aglient. (2020). *Introduction to FTIR Microscopy and Imaging* Retrieved May 12, 2022 from https://www.agilent.com/cs/library/eseminars/public/Chemical_Imaging_for_Industrial_Laboratories.pdf
- Albretsen, J., Huserbråten, M. B. O., Lyngvær Mathisen, H., & Naustvoll, L. J. (2018). Marin plast i Skagerrak-Kartlegging og spredningsmodellering. *Rapport fra Havforskningen*.
- Alexander, D. E. (1999). Bioaccumulation, bioconcentration, biomagnification. In Springer.
- Amlund, H., Lundebye, A.-K., & Berntsen, M. H. (2007). Accumulation and elimination of methylmercury in Atlantic cod (*Gadus morhua* L.) following dietary exposure. *Aquatic toxicology*, 83(4), 323-330.
- Andersson, A. (2004). *Fant Colaboks i torske-mage*. Retrieved June 13, 2022 from <https://www.bt.no/nyheter/lokalt/i/WgazQ/fant-colaboks-i-torske-mage>
- Andrady, A. L. (2011). Microplastics in the marine environment. *Marine Pollution Bulletin*, 62(8), 1596-1605. <https://doi.org/10.1016/j.marpolbul.2011.05.030>
- Andrady, A. L. (2017). The plastic in microplastics: A review. *Mar Pollut Bull*, 119(1), 12-22. <https://doi.org/10.1016/j.marpolbul.2017.01.082>
- Andrady, A. L., Hamid, H., & Torikai, A. (2011). Effects of solar UV and climate change on materials. *Photochem Photobiol Sci*, 10(2), 292-300. <https://doi.org/10.1039/c0pp90038a>
- Andrady, A. L., Hamid, H. S., & Torikai, A. (2003). Effects of climate change and UV-B on materials. *Photochem Photobiol Sci*, 2(1), 68-72. <https://doi.org/10.1039/b211085g>
- Andrady, A. L., Hamid, S. H., Hu, X., & Torikai, A. (1998). Effects of increased solar ultraviolet radiation on materials. *J Photochem Photobiol B*, 46(1-3), 96-103. <https://www.ncbi.nlm.nih.gov/pubmed/9894353>
- Andrady, A. L., & Neal, M. A. (2009). Applications and societal benefits of plastics. *Philos Trans R Soc Lond B Biol Sci*, 364(1526), 1977-1984. <https://doi.org/10.1098/rstb.2008.0304>
- Arthur, C., Baker, J., & Bamford, H. (2009). Proceedings of the International Research Workshop on the Occurrence, Effects and Fate of Microplastic Marine Debris. Sept 9-11, 2008. *NOAA Technical Memorandum NOS-OR&R-30*.
- Avio, C. G., Gorbi, S., Milan, M., Benedetti, M., Fattorini, D., d'Errico, G., Pauletto, M., Bargelloni, L., & Regoli, F. (2015). Pollutants bioavailability and toxicological risk from microplastics to marine mussels. *Environ Pollut*, 198, 211-222. <https://doi.org/10.1016/j.envpol.2014.12.021>
- Avio, C. G., Gorbi, S., & Regoli, F. (2015). Experimental development of a new protocol for extraction and characterization of microplastics in fish tissues: First observations in commercial species from Adriatic Sea. *Mar Environ Res*, 111, 18-26. <https://doi.org/10.1016/j.marenvres.2015.06.014>

- Bastesen, E., Haave, M., Andersen, G. L., Velle, G., Bødtker, G., & Krafft, C. G. (2021). Rapid landscape changes in plastic bays along the Norwegian coastline. *Frontiers in Marine Science*, 166.
- Bastesen, E., Haave, M., & Neby, S. (2020). Utvikling av kartleggingsmetoder og estimat for oppryddingskostnader for makroplast i strandsonen.
- Bergmann, M., Gutow, L., & Klages, M. (2015). *Marine anthropogenic litter*. Springer Nature.
- Bergmann, M., Wirzberger, V., Krumpfen, T., Lorenz, C., Primpke, S., Tekman, M. B., & Gerdt, G. (2017). High Quantities of Microplastic in Arctic Deep-Sea Sediments from the HAUSGARTEN Observatory. *Environ Sci Technol*, 51(19), 11000-11010. <https://doi.org/10.1021/acs.est.7b03331>
- Bernes, C. (1998). *Persistent organic pollutants*.
- Bhargava, R., Wang, S.-Q., & Koenig, J. L. (2003). FTIR microspectroscopy of polymeric systems. *Liquid chromatography/FTIR microspectroscopy/microwave assisted synthesis*, 137-191.
- Boisvert, G., Sonne, C., Rigét, F. F., Dietz, R., & Letcher, R. J. (2019). Bioaccumulation and biomagnification of perfluoroalkyl acids and precursors in East Greenland polar bears and their ringed seal prey. *Environmental pollution*, 252, 1335-1343.
- Booth, A., Kubowicz, S., Beegle-Krause, C., Skancke, J., Nordam, T., Landsem, E., Throne-Holst, M., & Jahren, S. (2017). Microplastic in global and Norwegian marine environments: Distributions, degradation mechanisms and transport. *Miljødirektoratet M-918*, 1-147.
- Boucher, J., & Friot, D. (2017). *Primary microplastics in the oceans: a global evaluation of sources* (Vol. 10). Iucn Gland, Switzerland.
- Brander, S. M., Renick, V. C., Foley, M. M., Steele, C., Woo, M., Lusher, A., Carr, S., Helm, P., Box, C., & Cherniak, S. (2020). Sampling and quality assurance and quality control: a guide for scientists investigating the occurrence of microplastics across matrices. *Applied spectroscopy*, 74(9), 1099-1125.
- Bråte, I. L., Eidsvoll, D. P., Steindal, C. C., & Thomas, K. V. (2016). Plastic ingestion by Atlantic cod (*Gadus morhua*) from the Norwegian coast. *Marine Pollution Bulletin*, 112(1-2), 105-110. <https://doi.org/10.1016/j.marpolbul.2016.08.034>
- Cameron, J. M., Bruno, C., Parachalil, D. R., Baker, M. J., Bonnier, F., Butler, H. J., & Byrne, H. J. (2020). Vibrational spectroscopic analysis and quantification of proteins in human blood plasma and serum. In *Vibrational Spectroscopy in Protein Research* (pp. 269-314). Elsevier.
- Carpenter, E. J., & Smith, K. L. (1972). Plastics on the Sargasso Sea surface. *Science*, 175(4027), 1240-1241.
- Catarino, A. I., Macchia, V., Sanderson, W. G., Thompson, R. C., & Henry, T. B. (2018). Low levels of microplastics (MP) in wild mussels indicate that MP ingestion by humans is minimal compared to exposure via household fibres fallout during a meal. *Environmental pollution*, 237, 675-684.
- Chain, E. P. o. C. i. t. F. (2016). Presence of microplastics and nanoplastics in food, with particular focus on seafood. *Efsa Journal*, 14(6), e04501.
- Chalmers, J. M. (2006). Infrared spectroscopy in analysis of polymers and rubbers. *Encyclopedia of Analytical Chemistry: Applications, Theory and Instrumentation*.
- Chanda, M., & Roy, S. K. (2006). *Plastics technology handbook*. CRC press.
- Chubarenko, I., Bagaev, A., Zobkov, M., & Esiukova, E. (2016). On some physical and dynamical properties of microplastic particles in marine environment. *Mar Pollut Bull*, 108(1-2), 105-112.

- Clark, N. J., Khan, F. R., Crowther, C., Mitrano, D. M., & Thompson, R. C. (2022). Uptake, distribution and elimination of palladium-doped polystyrene nanoplastics in rainbow trout (*Oncorhynchus mykiss*) following dietary exposure. *Science of The Total Environment*, 158765.
- Cole, M., Lindeque, P., Fileman, E., Halsband, C., & Galloway, T. S. (2015). The impact of polystyrene microplastics on feeding, function and fecundity in the marine copepod *Calanus helgolandicus*. *Environ Sci Technol*, 49(2), 1130-1137. <https://doi.org/10.1021/es504525u>
- Cole, M., Webb, H., Lindeque, P. K., Fileman, E. S., Halsband, C., & Galloway, T. S. (2014). Isolation of microplastics in biota-rich seawater samples and marine organisms. *Sci Rep*, 4, 4528. <https://doi.org/10.1038/srep04528>
- Collard, F., Gilbert, B., Compere, P., Eppe, G., Das, K., Jauniaux, T., & Parmentier, E. (2017). Microplastics in livers of European anchovies (*Engraulis encrasicolus*, L.). *Environ Pollut*, 229, 1000-1005. <https://doi.org/10.1016/j.envpol.2017.07.089>
- Collard, F., Husum, K., Eppe, G., Malherbe, C., Hallanger, I. G., Divine, D. V., & Gabrielsen, G. W. (2021). Anthropogenic particles in sediment from an Arctic fjord. *Science of the Total Environment*, 772, 145575.
- Cunningham, E. M., Ehlers, S. M., Dick, J. T., Sigwart, J. D., Linse, K., Dick, J. J., & Kiriakoulakis, K. (2020). High abundances of microplastic pollution in deep-sea sediments: evidence from Antarctica and the Southern Ocean. *Environmental Science & Technology*, 54(21), 13661-13671.
- de Sousa, F. D. B. (2021). Plastic and its consequences during the COVID-19 pandemic. *Environmental Science and Pollution Research*, 28(33), 46067-46078.
- Dris, R., Gasperi, J., Saad, M., Mirande, C., & Tassin, B. (2016). Synthetic fibers in atmospheric fallout: A source of microplastics in the environment? *Marine Pollution Bulletin*, 104(1-2), 290-293. <https://doi.org/10.1016/j.marpolbul.2016.01.006>
- EFSA. (2016). Presence of microplastics and nanoplastics in food, with particular focus on seafood. *Efsa Journal*, 14(6), e04501. <https://doi.org/10.2903/j.efsa.2016.4501>
- Enders, K., K  ppler, A., Biniash, O., Feldens, P., Stollberg, N., Lange, X., Fischer, D., Eichhorn, K.-J., Pollehne, F., & Oberbeckmann, S. (2019). Tracing microplastics in aquatic environments based on sediment analogies. *Scientific Reports*, 9(1), 1-15.
- Enders, K., Lenz, R., Stedmon, C. A., & Nielsen, T. G. (2015). Abundance, size and polymer composition of marine microplastics $\geq 10 \mu\text{m}$ in the Atlantic Ocean and their modelled vertical distribution. *Mar Pollut Bull*, 100(1), 70-81. <https://doi.org/10.1016/j.marpolbul.2015.09.027>
- Fisheries, D.-G. f. M. A. a. (2021). *The EU fish market* https://www.eumofa.eu/documents/20178/477018/EN_The+EU+fish+market_2021.pdf/27a6d912-a758-6065-c973-c1146ac93d30?t=1636964632989
- Foekema, E. M., De Gruijter, C., Mergia, M. T., van Franeker, J. A., Murk, A. J., & Koelmans, A. A. (2013). Plastic in north sea fish. *Environ Sci Technol*, 47(15), 8818-8824. <https://doi.org/10.1021/es400931b>
- Fowler, C. W., Merrick, R., & Baker, J. D. (1989). Studies of the population level effects of entanglement on northern fur seals. Proceedings of the second international conference on marine debris,
- Gago, J., Galgani, F., Maes, T., & Thompson, R. C. (2016). Microplastics in seawater: recommendations from the marine strategy framework directive implementation process. *Frontiers in Marine Science*, 3, 219.
- Garcia, S. M., & Newton, C. (1995). *Current situation, trends and prospects in world capture fisheries*. FAO, Fisheries Department.

- GESAMP. (2015). Microplastic in the ocean. A global assessment. . *GESAMP, The Joint Group of Experts on Scientific Aspects on Marine Environmental Protection*.
- GESAMP. (2016). *Sources, fate and effects of microplastics in the marine environment: part two of a global assessment*.
- Geyer, R. (2020). A brief history of plastics. In *Mare Plasticum-The Plastic Sea* (pp. 31-47). Springer.
- Geyer, R., Jambeck, J. R., & Law, K. L. (2017). Production, use, and fate of all plastics ever made. *Sci Adv*, 3(7), e1700782. <https://doi.org/10.1126/sciadv.1700782>
- Gomiero, A., Haave, M., Bjørøy, Ø., Herzke, D., Kögel, T., Nikiforov, V., & Øysæd, K. B. (2020a). *Quantification of microplastic in fillet and organs of farmed and wild salmonids-a comparison of methods for detection and quantification (SALMODETECT)* (NORCE report 8-2020, Issue.
- Gomiero, A., Haave, M., Kögel, T., Bjørøy, Ø., Gjessing, M., Berg Lea, T., Horve, E., Martins, C., & Olafsen, T. (2020b). *Tracking of Plastic emissions from aquaculture industry (TrackPlast)* (NORCE report 04-2020, Issue.
- Gomiero, A., Skogerbø, G., & Øysæd, K. B. (2018). Development and application of a fast and sensitive method for micro and nanoplastics characterization in drinking water. *In prep*.
- Gomiero, A., Øysæd, K. B., Agustsson, T., van Hoytema, N., van Thiel, T., & Grati, F. (2019). First record of characterization, concentration and distribution of microplastics in coastal sediments of an urban fjord in south west Norway using a thermal degradation method. *Chemosphere*, 227, 705-714. <https://doi.org/10.1016/j.chemosphere.2019.04.096>
- Hagen, P. E., & Walls, M. P. (2005). The Stockholm Convention on persistent organic pollutants. *Natural Resources & Environment*, 19(4), 49-52.
- Hamilton, A., de Wit, W., Scheer, R., Stakes, T., & Allan, S. (2019). Solving plastic pollution through accountability. *WWF—World Wide Fund For Nature, Gland, Switzerland*.
- Harris, D. C. (2010). *Quantitative chemical analysis*. Macmillan.
- Hartmann, N. B., Huffer, T., Thompson, R. C., Hasselov, M., Verschoor, A., Daugaard, A. E., Rist, S., Karlsson, T., Brennholt, N., Cole, M., Herrling, M. P., Hess, M. C., Ivleva, N. P., Lusher, A. L., & Wagner, M. (2019). Are We Speaking the Same Language? Recommendations for a Definition and Categorization Framework for Plastic Debris. *Environ Sci Technol*, 53(3), 1039-1047. <https://doi.org/10.1021/acs.est.8b05297>
- Hedayati, A. (2016). Liver as a target organ for eco-toxicological studies. *J Coast Zone Manag*, 19(3), e118.
- Heessen, H., Ter Hofstede, R., & Daan, N. (2006). ICES-FishMap.
- Henshaw, D. L., & O'Carroll, M. J. (2009). Scientific Committee on Emerging and Newly Identified Health Risks (SCENIHR). *Brussels: European Commission*.
- Heywood, R. (1981). Target organ toxicity. *Toxicology Letters*, 8(6), 349-358.
- Hidalgo-Ruz, V., Gutow, L., Thompson, R. C., & Thiel, M. (2012). Microplastics in the marine environment: a review of the methods used for identification and quantification. *Environ Sci Technol*, 46(6), 3060-3075. <https://doi.org/10.1021/es2031505>
- Haave, M., Gomiero, A., Schönheit, J., Nilsen, H., & Olsen, A. B. (2021). Documentation of Microplastics in Tissues of Wild Coastal Animals [Original Research]. *Frontiers in Environmental Science*, 9(31). <https://doi.org/10.3389/fenvs.2021.575058>
- Haave, M., Lorenz, C., Primpke, S., & Gerdts, G. (2019). Different stories told by small and large microplastics in sediment - first report of microplastic concentrations in an urban recipient in Norway. *Mar Pollut Bull*, 141, 501-513. <https://doi.org/10.1016/j.marpolbul.2019.02.015>

- International Organization for Standardization. (2013). ISO 472:2013 In *Plastic- Vocabulary* Geneva International Organization for Standardization.
- Ismail, A. A., van de Voort, F. R., & Sedman, J. (1997). Fourier transform infrared spectroscopy: principles and applications. In *Techniques and instrumentation in analytical chemistry* (Vol. 18, pp. 93-139). Elsevier.
- Ivleva, N. P. (2021). Chemical analysis of microplastics and nanoplastics: Challenges, advanced methods, and perspectives. *Chemical Reviews*, *121*(19), 11886-11936.
- Iwamoto, A., & Tokiwa, Y. (1993). Effects of the Blend Ratio and Melt Viscosity on Biodegradability of Plastics Containing an Aliphatic Polyester. *Kobunshi Ronbunshu*, *50*(10), 789-791. <https://doi.org/DOI.10.1295/koron.50.789>
- Jovanović, B. (2017). Ingestion of microplastics by fish and its potential consequences from a physical perspective. *Integrated Environmental Assessment and Management*, *13*(3), 510-515.
- Jovanović, B., Gökdag, K., Güven, O., Emre, Y., Whitley, E. M., & Kideys, A. E. (2018). Virgin microplastics are not causing imminent harm to fish after dietary exposure. *Mar Pollut Bull*, *130*, 123-131.
- Kenyon, K. W., & Kridler, E. (1969). Laysan albatrosses swallow indigestible matter. *The Auk*, *86*(2), 339-343.
- Kershaw, P., Turra, A., & Galgani, F. (2019). Guidelines for the monitoring and assessment of plastic litter and microplastics in the ocean.
- Kirstein, I. V., Hensel, F., Gomiero, A., Iordachescu, L., Vianello, A., Wittgren, H. B., & Vollertsen, J. (2021). Drinking plastics?—Quantification and qualification of microplastics in drinking water distribution systems by μ FTIR and Py-GCMS. *Water Research*, *188*, 116519.
- Knutsen, H., Cyvin, J. B., Totland, C., Lilleeng, Ø., Wade, E. J., Castro, V., Pettersen, A., Laugesen, J., Møskeland, T., & Arp, H. P. H. (2020). Microplastic accumulation by tube-dwelling, suspension feeding polychaetes from the sediment surface: A case study from the Norwegian Continental Shelf. *Marine Environmental Research*, *161*, 105073.
- Kooi, M., & Koelmans, A. A. (2019). Simplifying Microplastic via Continuous Probability Distributions for Size, Shape, and Density. *Environmental Science & Technology Letters*, *6*(9), 551-557. <https://doi.org/10.1021/acs.estlett.9b00379>
- Kwaśniak, J., & Falkowska, L. (2012). Mercury distribution in muscles and internal organs of the juvenile and adult Baltic cod (*Gadus morrhua callarias* Linnaeus, 1758). *Oceanological and Hydrobiological Studies*, *41*(2), 65-71.
- Käppler, A., Fischer, D., Oberbeckmann, S., Schernewski, G., Labrenz, M., Eichhorn, K.-J., & Voit, B. (2016). Analysis of environmental microplastics by vibrational microspectroscopy: FTIR, Raman or both? *Analytical and Bioanalytical Chemistry*, *408*(29), 8377-8391. <https://doi.org/10.1007/s00216-016-9956-3>
- Lambert, S., & Wagner, M. (2016). Characterisation of nanoplastics during the degradation of polystyrene. *Chemosphere*, *145*, 265-268. <Go to ISI>://WOS:000369196300033
- Lassen, C., Hansen, S. F., Magnusson, K., Norén, F., Hartmann, N. I. B., Jensen, P. R., Nielsen, T. G., & Brinch, A. (2012). Microplastics-Occurrence, effects and sources of. *Significance*, *2*, 2.
- Lebreton, L., & Andrady, A. (2019). Future scenarios of global plastic waste generation and disposal. *Palgrave Communications*, *5*(1), 6. <https://doi.org/10.1057/s41599-018-0212-7>
- Letcher, R. J., Gebbink, W. A., Sonne, C., Born, E. W., McKinney, M. A., & Dietz, R. (2009). Bioaccumulation and biotransformation of brominated and chlorinated contaminants and their metabolites in ringed seals (*Pusa hispida*) and polar bears

- (*Ursus maritimus*) from East Greenland. *Environment International*, 35(8), 1118-1124.
- Li-Chan, E., Chalmers, J. M., & Griffiths, P. R. (2010). *Applications of Vibrational Spectroscopy in Food Science, 2 Volume Set*. John Wiley & Sons.
- Link, J. S., Bogstad, B., Sparholt, H., & Lilly, G. R. (2009). Trophic role of Atlantic cod in the ecosystem. *Fish and Fisheries*, 10(1), 58-87.
- Lithner, D., Larsson, Å., & Dave, G. (2011). Environmental and health hazard ranking and assessment of plastic polymers based on chemical composition. *Science of The Total Environment*, 409(18), 3309-3324. <https://doi.org/10.1016/j.scitotenv.2011.04.038>
- Liu, G.-L., & Kazarian, S. (2022). Recent advances in studies of cultural heritage using ATR-FTIR spectroscopy and ATR-FTIR spectroscopic imaging. *Analyst*.
- Lobelle, D., & Cunliffe, M. (2011). Early microbial biofilm formation on marine plastic debris. *Marine Pollution Bulletin*, 62(1), 197-200. <https://doi.org/10.1016/j.marpolbul.2010.10.013>
- Lorenz, C., Dolven, J. K., Værøy, N., Stephansen, D., Olsen, S. B., & Vollertsen, J. (2020). Microplastic pollution in three rivers in south eastern Norway.
- Lorenz, C., Roscher, L., Meyer, M. S., Hildebrandt, L., Prume, J., Löder, M. G. J., Primpke, S., & Gerds, G. (2019). Spatial distribution of microplastics in sediments and surface waters of the southern North Sea. *Environmental Pollution*, 252, 1719-1729. <https://doi.org/10.1016/j.envpol.2019.06.093>
- Lusher, A., Brate, I. L. N., Munno, K., Hurley, R. R., & Welden, N. A. (2020). Is It or Isn't It: The Importance of Visual Classification in Microplastic Characterization. *Appl Spectrosc*, 74(9), 1139-1153. <https://doi.org/10.1177/0003702820930733>
- Lusher, A., Buenaventura, N. T., Eidsvoll, D., Thrane, J.-E., Økelsrud, A., & Jartun, M. (2018). Freshwater microplastics in Norway: A first look at sediment, biota and historical plankton samples from Lake Mjøsa and Lake Femunden. *NIVA-rapport*.
- Lusher, A., Hollman, P., & Mendoza-Hill, J. (2017). *Microplastics in fisheries and aquaculture: status of knowledge on their occurrence and implications for aquatic organisms and food safety*. FAO.
- Lusher, A., Hurley, R., Arp, H. P. H., Booth, A. M., Brate, I. L. N., Gabrielsen, G. W., Gomiero, A., Gomes, T., Grosvik, B. E., Green, N., Haave, M., Hallanger, I. G., Halsband, C., Herzke, D., Joner, E. J., Kogel, T., Rakkestad, K., Ranneklev, S. B., Wagner, M., & Olsen, M. (2021). Moving forward in microplastic research: A Norwegian perspective. *Environ Int*, 157, 106794. <https://doi.org/10.1016/j.envint.2021.106794>
- Lusher, A., Welden, N. A., Sobral, P., & Cole, M. (2017). Sampling, isolating and identifying microplastics ingested by fish and invertebrates. *Analytical Methods*, 9(9), 1346-1360. <Go to ISI>://WOS:000395999600005
- Lusher, A. L., Tirelli, V., O'Connor, I., & Officer, R. (2015). Microplastics in Arctic polar waters: the first reported values of particles in surface and sub-surface samples. *Scientific Reports*, 5. <https://doi.org/ARTN1494710.1038/srep14947>
- Löder, M. G. J., Imhof, H. K., Ladehoff, M., Loschel, L. A., Lorenz, C., Mintenig, S., Piehl, S., Primpke, S., Schrank, I., Laforsch, C., & Gerds, G. (2017). Enzymatic purification of microplastics in environmental samples. *Environ Sci Technol*. <https://doi.org/10.1021/acs.est.7b03055>
- Maes, T., McGlade, J., Fahim, I. S., Green, D. S., Landrigan, P., Andrady, A. L., Costa, M. F., Geyer, R., Gomes, R., & Hwai, A. T. S. (2021). From Pollution to Solution: A Global Assessment of Marine Litter and Plastic Pollution.
- McIlwraith, H. K., Kim, J., Helm, P., Bhavsar, S. P., Metzger, J. S., & Rochman, C. M. (2021). Evidence of Microplastic Translocation in Wild-Caught Fish and Implications

- for Microplastic Accumulation Dynamics in Food Webs. *Environ Sci Technol*, 55(18), 12372-12382. <https://doi.org/10.1021/acs.est.1c02922>
- McKeen, L. W. (2014). *The effect of temperature and other factors on plastics and elastomers* (3rd ed.). William Andrew.
- Meikle, J. L. (1995). *American plastic: a cultural history*. Rutgers University Press.
- Mekonnen, T., Mussone, P., Khalil, H., & Bressler, D. (2013). Progress in bio-based plastics and plasticizing modifications. *Journal of Materials Chemistry A*, 1(43), 13379-13398.
- Miller, M. E., Hamann, M., & Kroon, F. J. (2020). Bioaccumulation and biomagnification of microplastics in marine organisms: a review and meta-analysis of current data. *Plos One*, 15(10), e0240792.
- Muir, D. C., Backus, S., Derocher, A. E., Dietz, R., Evans, T. J., Gabrielsen, G. W., Nagy, J., Norstrom, R. J., Sonne, C., & Stirling, I. (2006). Brominated flame retardants in polar bears (*Ursus maritimus*) from Alaska, the Canadian Arctic, East Greenland, and Svalbard. *Environmental Science & Technology*, 40(2), 449-455.
- Napper, I. E., & Thompson, R. C. (2020). Plastic Debris in the Marine Environment: History and Future Challenges. *Global Challenges*, 4(6), 1900081. <https://doi.org/10.1002/gch2.201900081>
- Nerheim, M. S., & Lusher, A. L. (2020). Investigating microsized anthropogenic particles in Norwegian fjords using opportunistic nondisruptive sampling. *Anthropocene Coasts*, 3(1), 76-85.
- Novotna, K., Cermakova, L., Pivokonska, L., Cajthaml, T., & Pivokonsky, M. (2019). Microplastics in drinking water treatment—current knowledge and research needs. *Science of the total environment*, 667, 730-740.
- Pavia, D. L., Lampman, G. M., & Kriz, G. S. (2001). Introduction to spectroscopy a guide for student of organic chemistry. *London: Brooks/Cole*.
- Peeken, I., Primpke, S., Beyer, B., Gutermann, J., Katlein, C., Krumpfen, T., Bergmann, M., Hehemann, L., & Gerdt, G. (2018). Arctic sea ice is an important temporal sink and means of transport for microplastic. *Nature Communications*, 9. <https://doi.org/ARTN150510.1038/s41467-018-03825-5>
- Pipkin, W., Belganeh, R., Robberson, W., Allen, H., Cook, A.-M., & Watanabe, A. (2021). Identification of Microplastics in Environmental Monitoring Using Pyrolysis–GC–MS Analysis.
- PlasticsEurope. (2021). *Plastics- The facts 2021; An analysis of European plastic production, demand and waste data* Retrieved Feb 1, 2022 from <https://plasticseurope.org/wp-content/uploads/2021/12/Plastics-the-Facts-2021-web-final.pdf>
- Prata, J. C. (2018). Airborne microplastics: Consequences to human health? *Environ Pollut*, 234, 115-126. <https://doi.org/10.1016/j.envpol.2017.11.043>
- Primpke, S., Cross, R. K., Mintenig, S. M., Simon, M., Vianello, A., Gerdt, G., & Vollertsen, J. (2020). Toward the Systematic Identification of Microplastics in the Environment: Evaluation of a New Independent Software Tool (siMPle) for Spectroscopic Analysis. *Appl Spectrosc*, 74(9), 1127-1138. <https://doi.org/10.1177/0003702820917760>
- Primpke, S., Lorenz, C., Rascher-Friesenhausen, R., & Gerdt, G. (2017). Automated Analysis of μ FTIR Imaging Data for Microplastic Samples. In *Fate and Impact of Microplastics in Marine Ecosystems* (pp. 90-91). Elsevier. <https://doi.org/http://dx.doi.org/10.1016/B978-0-12-812271-6.00092-2>
- Provencher, J., Ammendolia, J., Rochman, C., & Mallory, M. (2019). Assessing plastic debris in aquatic food webs: what we know and don't know about uptake and trophic transfer. *Environmental Reviews*, 27(3), 304-317.

- Ruus, A., Daae, I. A., & Hylland, K. (2012). Accumulation of polychlorinated biphenyls from contaminated sediment by Atlantic cod (*Gadus morhua*): direct accumulation from resuspended sediment and dietary accumulation via the polychaete *Nereis virens*. *Environmental Toxicology and Chemistry*, 31(11), 2472-2481.
- Shaw, S. D., Berger, M. L., Brenner, D., Kannan, K., Lohmann, N., & Pöpke, O. (2009). Bioaccumulation of polybrominated diphenyl ethers and hexabromocyclododecane in the northwest Atlantic marine food web. *Science of the Total Environment*, 407(10), 3323-3329.
- Shaw, S. D., Brenner, D., Berger, M. L., Fang, F., Hong, C.-S., Addink, R., & Hilker, D. (2008). Bioaccumulation of polybrominated diphenyl ethers in harbor seals from the northwest Atlantic. *Chemosphere*, 73(11), 1773-1780.
- Simpson, S. L. (2005). Exposure– Effect Model for Calculating Copper Effect Concentrations in Sediments with Varying Copper Binding Properties: A Synthesis. *Environmental science & technology*, 39(18), 7089-7096.
- Sintim, H. Y., & Flury, M. (2017). Is biodegradable plastic mulch the solution to agriculture’s plastic problem? In: ACS Publications.
- Sivertsvik, M., Rosnes, J. T., & Jeksrud, W. K. (2004). Solubility and absorption rate of carbon dioxide into non-respiring foods. Part 2: Raw fish fillets. *Journal of Food Engineering*, 63(4), 451-458.
- Subramanian, A., & Rodriguez-Saona, L. (2009). Fourier transform infrared (FTIR) spectroscopy. *Infrared spectroscopy for food quality analysis and control*, 145-178.
- Summers, J. (2014). *Dildo Found in Cod's Stomach By Norwegian Fisherman*. Retrieved June 13, 2022 from https://www.huffingtonpost.co.uk/2014/04/12/dildo-found-in-cods-stomach_n_5139217.html
- Sørmo, E. G., Salmer, M. P., Jenssen, B. M., Hop, H., Bæk, K., Kovacs, K. M., Lydersen, C., Falk-Petersen, S., Gabrielsen, G. W., & Lie, E. (2006). Biomagnification of polybrominated diphenyl ether and hexabromocyclododecane flame retardants in the polar bear food chain in Svalbard, Norway. *Environmental Toxicology and Chemistry: An International Journal*, 25(9), 2502-2511.
- Tagg, A. S., Sapp, M., Harrison, J. P., & Ojeda, J. s. J. (2015). Identification and quantification of microplastics in wastewater using focal plane array-based reflectance micro-FT-IR imaging. *Analytical chemistry*, 87(12), 6032-6040.
- Thermo Fisher (2022). *Nicolet™ iN10 MX Infrared Imaging Microscope*. Retrieved June 13, 2022 from <https://www.thermofisher.com/order/catalog/product/IQLAADGAAGFAHDMAPE>
- Thompson, R. C., Olsen, Y., Mitchell, R. P., Davis, A., Rowland, S. J., John, A. W., McGonigle, D., & Russell, A. E. (2004). Lost at sea: where is all the plastic? *Science*, 304(5672), 838. <https://doi.org/10.1126/science.1094559>
- UNEP. (2017). Combating marine plastic litter and microplastics: An assessment of the effectiveness of relevant international, regional and subregional governance strategies and approaches (No./EA. 3/INF/5). *United Nations Environment Assembly of the United Nations Environment Programme, Nairobi*.
- UNEP. (2021). *From Pollution to Solution: A Global Assessment of Marine Litter and Plastic Pollution* (928073881X).
- Urban, R. C., & Nakada, L. Y. K. (2021). COVID-19 pandemic: Solid waste and environmental impacts in Brazil. *Science of the Total Environment*, 755, 142471.
- Van Mourik, L., Crum, S., Martinez-Frances, E., van Bavel, B., Leslie, H., de Boer, J., & Cofino, W. (2021). Results of WEPAL-QUASIMEME/NORMANs first global interlaboratory study on microplastics reveal urgent need for harmonization. *Science of the Total Environment*, 772, 145071.

- van Raamsdonk, L. W., van der Zande, M., Koelmans, A. A., Hoogenboom, R. L., Peters, R. J., Groot, M. J., Peijnenburg, A. A., & Weesepeel, Y. J. (2020). Current insights into monitoring, bioaccumulation, and potential health effects of microplastics present in the food chain. *Foods*, 9(1), 72.
- Veerasingam, S., Ranjani, M., Venkatachalapathy, R., Bagaev, A., Mukhanov, V., Litvinyuk, D., Mugilarasan, M., Gurumoorthi, K., Gunganathan, L., & Aboobacker, V. (2021). Contributions of Fourier transform infrared spectroscopy in microplastic pollution research: A review. *Critical reviews in environmental science and technology*, 51(22), 2681-2743.
- Vianello, A., Jensen, R. L., Liu, L., & Vollertsen, J. (2019). Simulating human exposure to indoor airborne microplastics using a Breathing Thermal Manikin. *Scientific reports*, 9(1), 1-11.
- Volkheimer, G. (1993). Persorption of microparticles. *Pathologie*, 14(5), 247-252. (Persorption von Mikropartikeln.)
- Watts, A. J., Urbina, M. A., Goodhead, R. M., Moger, J., Lewis, C., & Galloway, T. S. (2016). Effect of microplastic on the gills of the Shore Crab *Carcinus maenas*. *Environ Sci Technol*. <https://doi.org/10.1021/acs.est.6b01187>
- Weisser, J., Beer, I., Hufnagl, B., Hofmann, T., Lohninger, H., Ivleva, N. P., & Glas, K. (2021). From the well to the bottle: identifying sources of microplastics in mineral water. *Water*, 13(6), 841.
- Welden, N. A., & Lusher, A. L. (2017). Impacts of changing ocean circulation on the distribution of marine microplastic litter. *Integrated Environmental Assessment and Management*, 13(3), 483-487.
- Woods, M. N., Stack, M. E., Fields, D. M., Shaw, S. D., & Matrai, P. A. (2018). Microplastic fiber uptake, ingestion, and egestion rates in the blue mussel (*Mytilus edulis*). *Marine Pollution Bulletin*, 137, 638-645. <https://doi.org/10.1016/j.marpolbul.2018.10.061>
- Worm, B., Lotze, H. K., Jubinville, I., Wilcox, C., & Jambeck, J. (2017). Plastic as a persistent marine pollutant. *Annual Review of Environment and Resources*, 42(1), 1-26.
- Wright, S. L., & Kelly, F. J. (2017). Plastic and human health: a micro issue? *Environmental science & technology*, 51(12), 6634-6647.
- Wright, S. L., Thompson, R. C., & Galloway, T. S. (2013). The physical impacts of microplastics on marine organisms: a review. *Environmental pollution*, 178, 483-492.
- Xu, J.-L., Thomas, K. V., Luo, Z., & Gowen, A. A. (2019). FTIR and Raman imaging for microplastics analysis: State of the art, challenges and prospects. *TrAC Trends in Analytical Chemistry*, 119, 115629.
- Yousif, E., & Haddad, R. (2013). Photodegradation and photostabilization of polymers, especially polystyrene: review. *SpringerPlus*, 2(1), 398. <https://doi.org/10.1186/2193-1801-2-398>
- Zarfl, C. (2019). Promising techniques and open challenges for microplastic identification and quantification in environmental matrices. *Analytical and Bioanalytical Chemistry*, 411(17), 3743-3756.
- Zeytin, S., Wagner, G., Mackay-Roberts, N., Gerdt, G., Schuirmann, E., Klockmann, S., & Slater, M. (2020). Quantifying microplastic translocation from feed to the fillet in European sea bass *Dicentrarchus labrax*. *Mar Pollut Bull*, 156, 111210.
- Aalborg University, A. W. I. (n.d.). *Systematic Identification of Microplastic in the Environment* <https://simple-plastics.eu/>

Appendices

Appendix A - Material and suppliers

Table 1A- List over enzymes used in this study

Enzymes	Code	EC-number	Application field	Supplier
Protease from Bacillus sp.	P3111	232-752-2	Protein	Sigma Aldrich
Lipase from <i>Aspergillus oryzae</i>	LO777	232-619-9	Hydrolysis	Sigma Aldrich

Table 2A- List over chemicals used in this study

Chemicals	Formula	#CAS	Supplier
Glycine	C2H5NO2	56-40-6	Sigma Aldrich
Hydrogenchloric acid 37%	HCL	7647-01-0	Sigma Aldrich
Hydrogen peroxide 30%	H2O2	7722-84-1	Sigma Aldrich
Phosphate buffered saline tablets	C12H3K2Na3O8P2	-	Sigma Aldrich
Sodium dodecyl sulfate (SDS)	NaC12H25SO4	200-578-6	ACROS ORGANICS
Sodium hydroxide pellets	NaOH	1310-73-2	Sigma Aldrich
Ethanol	C2H6O	-	Antibac
MilliQ-water	H2O	-	Q-pod purelab prima

Table 3A- List over buffers used in this study

Buffer	Chemical	Amount
Glycine	Glycine	7.5 g
	NaOH pellets	3.7 g
	MilliQ-water	1 L
	HCL (Adjusting pH to 10.0)	
Phosphate buffered saline (PBS)	PBS tablets	2 tablets
	MilliQ water	1 L
	NaOH (Adjusting pH to)	

Table 4A- List over equipment used for sample preparation in this study

Equipment	Application	Supplier
Glass fibre filter	Filtration of solutions and buffers	Whatman
Anodisc filter	Filtration of sample for μ FTIR analysis	Whatman
Stainless steel filter, 10 μ m	Filtration of samples	Rolf Kørner GmbH
Glass wear	Sample preparation	Schott Duran and VWR
Glass wear	Filtration equipment	Millipore
Finnpipette Digital ACL 1-5mL	Pipette	Labsystems Finland

Table 5A- List over instruments used in this study

Instrument	Application	Supplier
Branson 200	Ultrasonic cleaner	Branson
Muffle oven	Equipment cleaning	L3/12 Nabertherm GmbH
Nicolet iN10 MX Infrared Imaging Microscope	μ FTIR-Analysis	Thermo Fisher
Flameboy	Preparation of equipment, bruner	Integra
Chemical duty pump, 220 V750 Hz	Vacuum dump for filtration	Millipore
Mettler PB3002 weight	Weight (g)	Mettler Toledo
Drying oven	Optimization of enzymatic treatments	Termaks
Zymark TurboVap 500	Evaporation of samples	Zymark

Table 6A- List over software used in this study

Software	Application	Supplier
Excel	Calculations	Microsoft
SPSS statistics 27	Statistical analysis	IBM
OMNIC Picta	FTIR analysis	ThermoFisher Science
SiMPLe 1.0	Reference database	SiMPLe

Appendix B- Filter images, heat maps and spectra maps

Sample #1

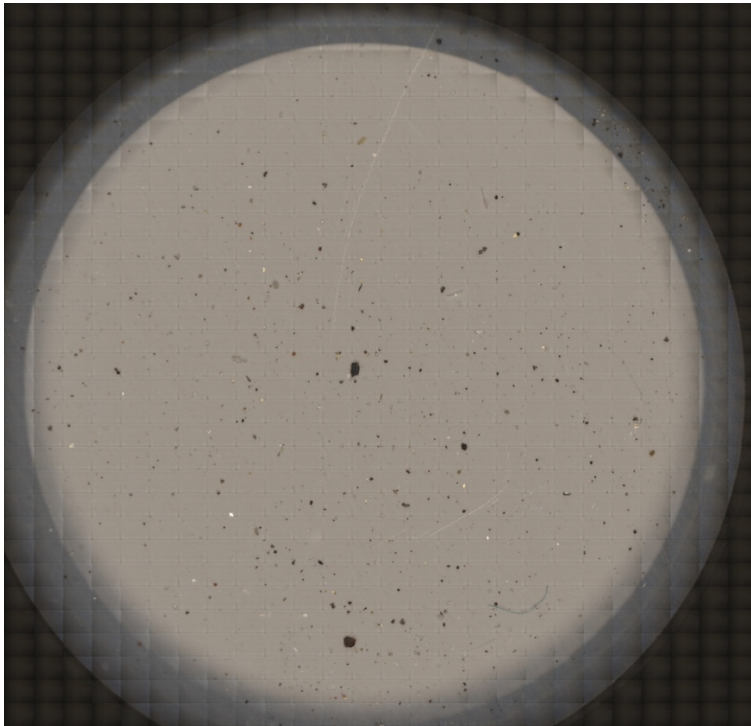


Figure 1B- Sample #1, containing 4 MP-particles (2 PE, PET and PS polymers). 2 PE particles subtracted due to similar particles in blank.

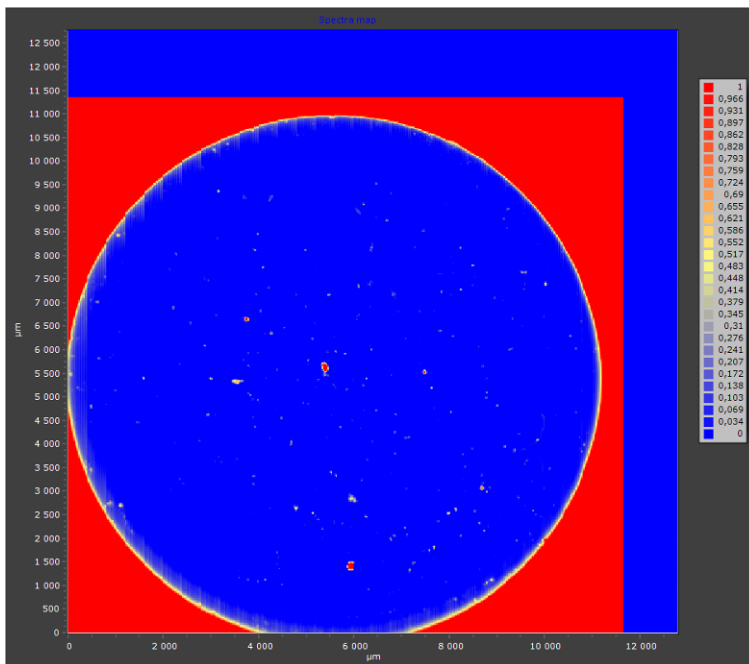


Figure 2B- Heat map for sample #1

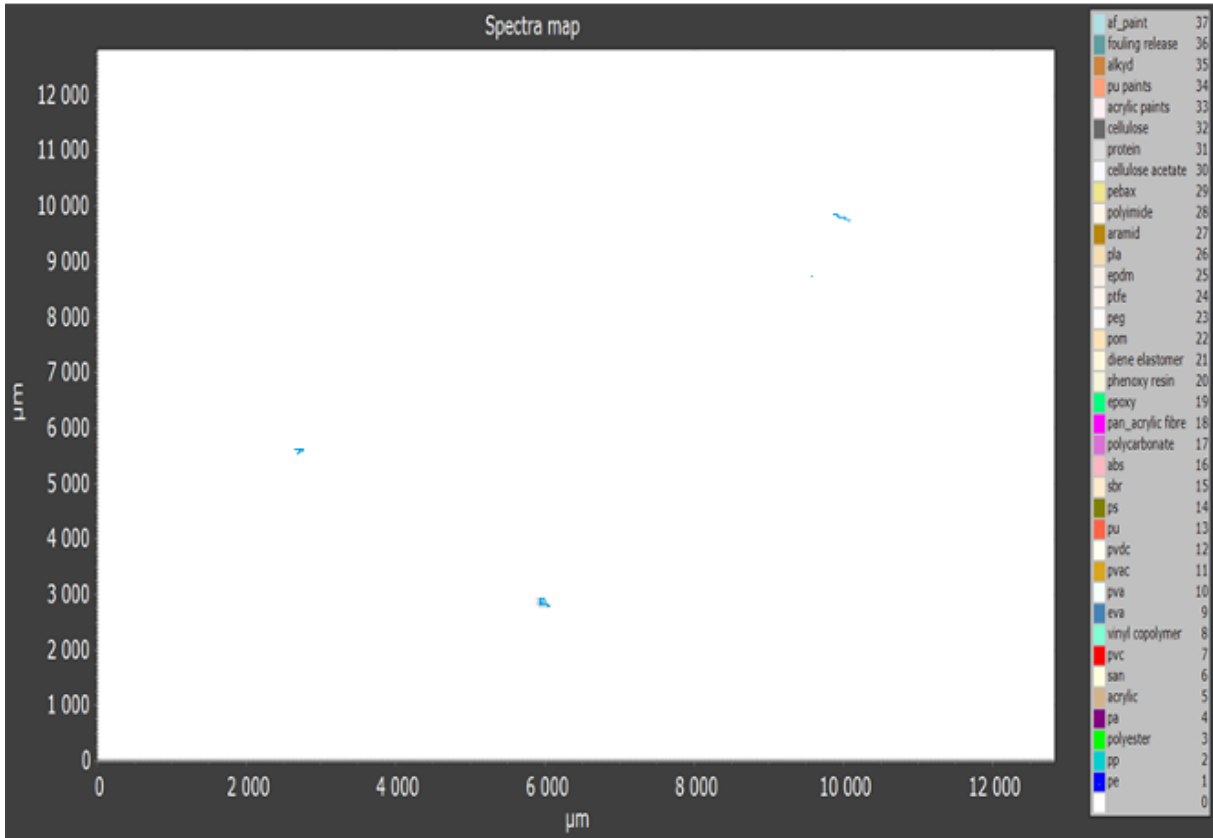


Figure 3B- Spectra map for sample #1.

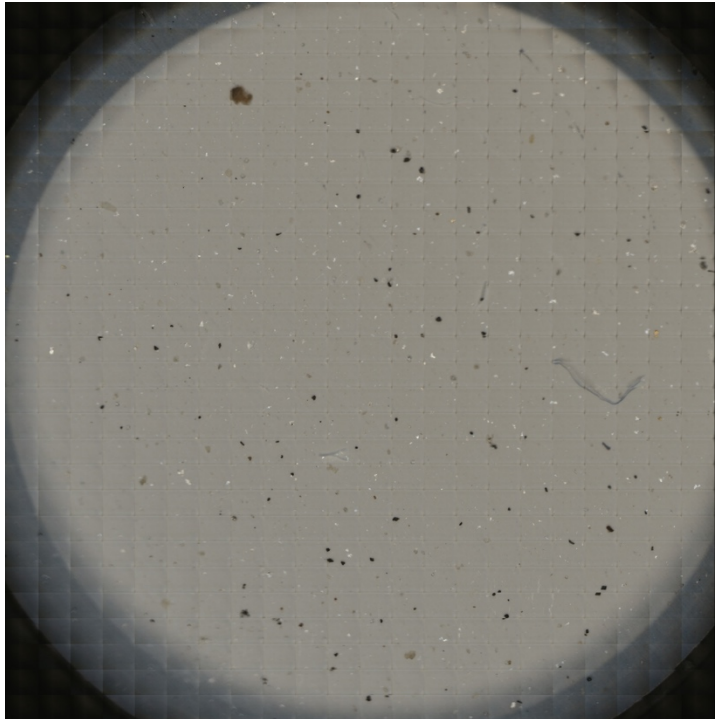


Figure 4B- Filter image for sample #1 blank.

Sample #2

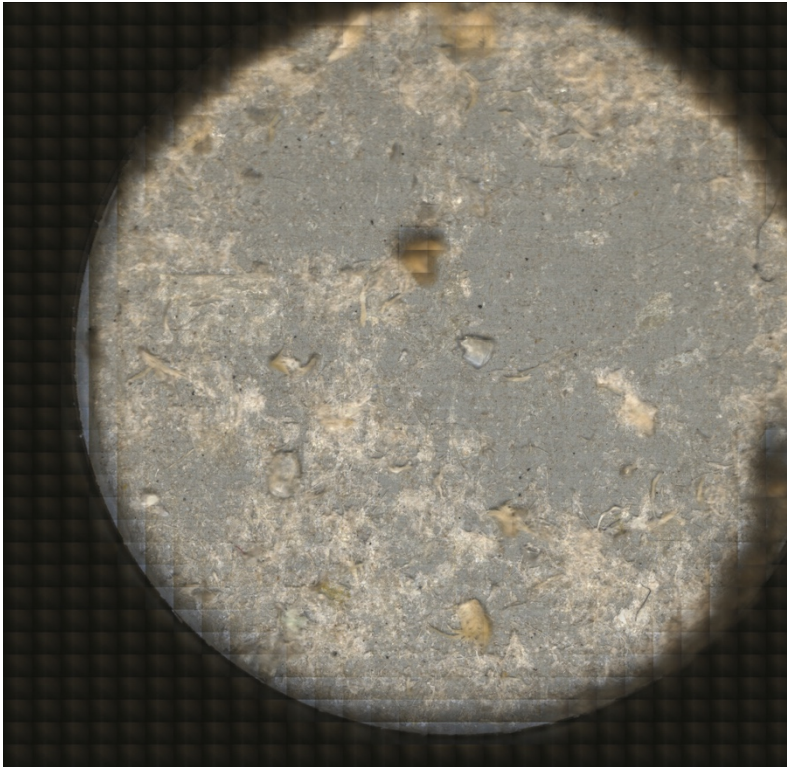


Figure 5B- Filter image of sample #2.

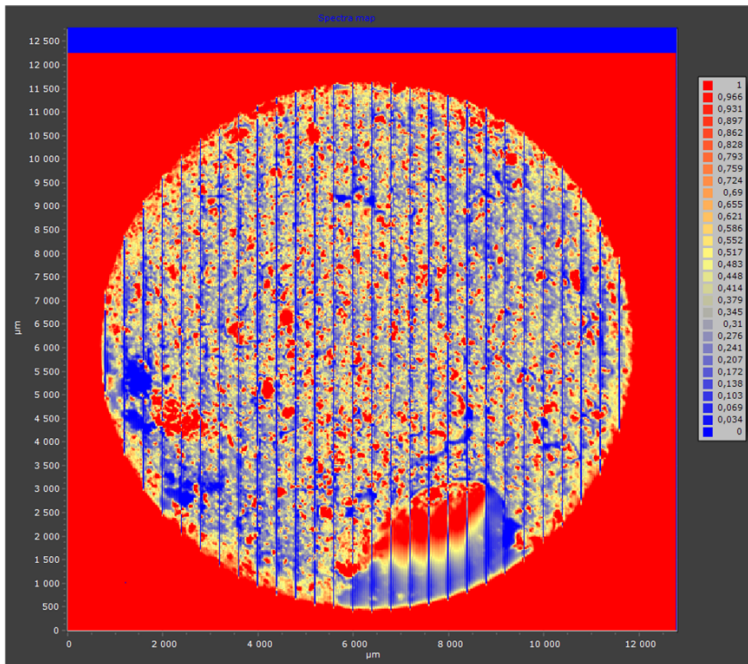


Figure 6B- Heat map of sample #2. Due to interferences no spectra map could be received.

Sample #3

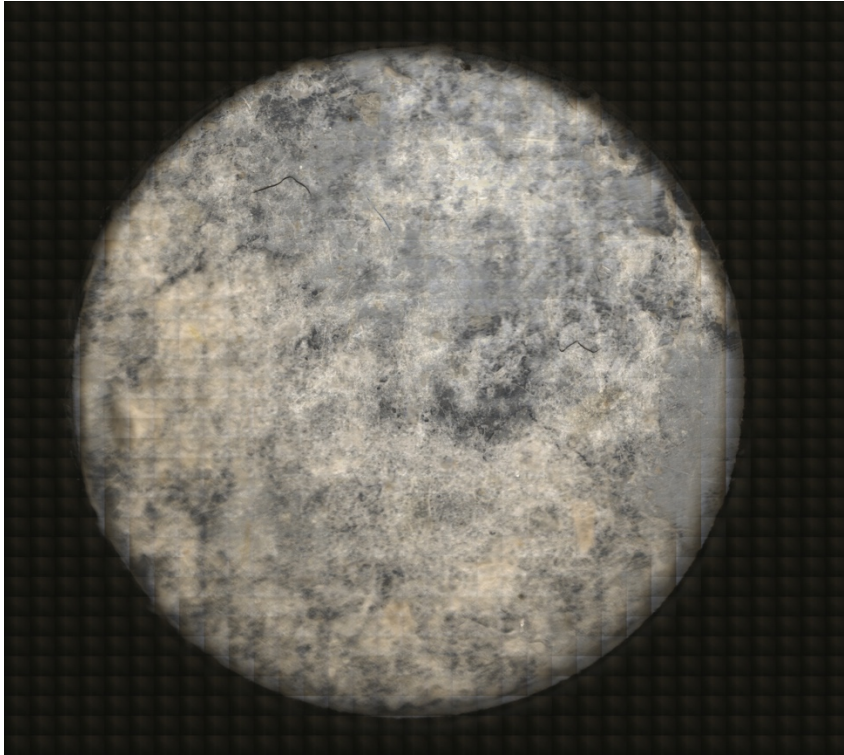


Figure 7B- Filter image of sample #3.

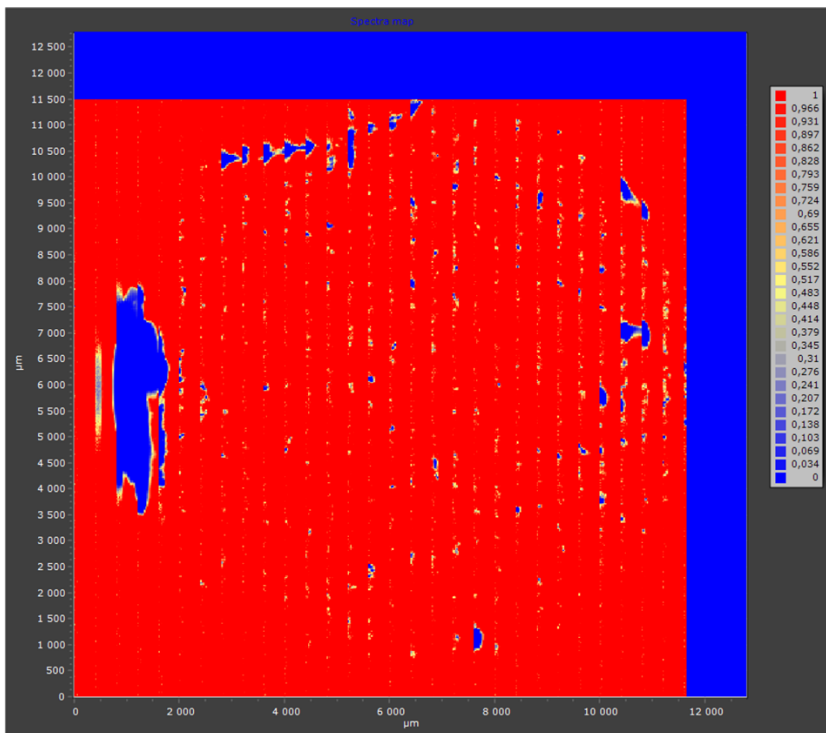


Figure 8B- Heat map of sample #3. Due to interference no spectra map could be received.

Sample #4

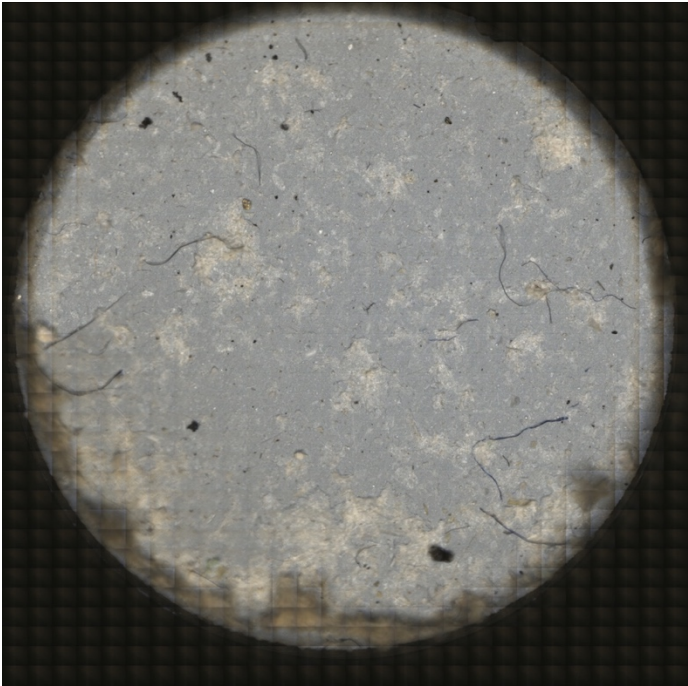


Figure 9B- Filter image of sample #4, contains 7 MP-particles (PP-polymers).

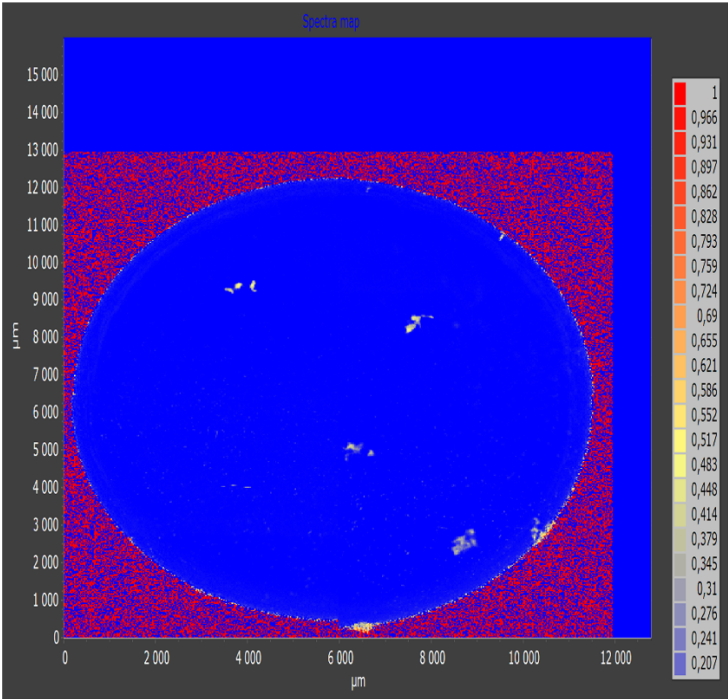


Figure 10B- Heat map of sample #4

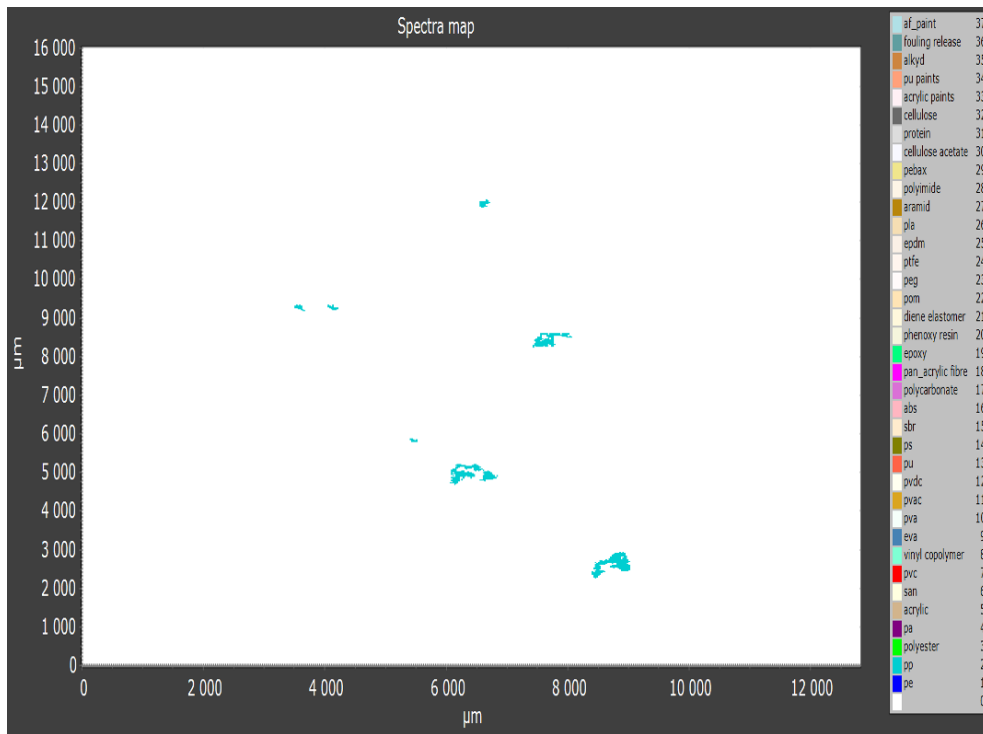


Figure 11B- Spectra map of sample #4.

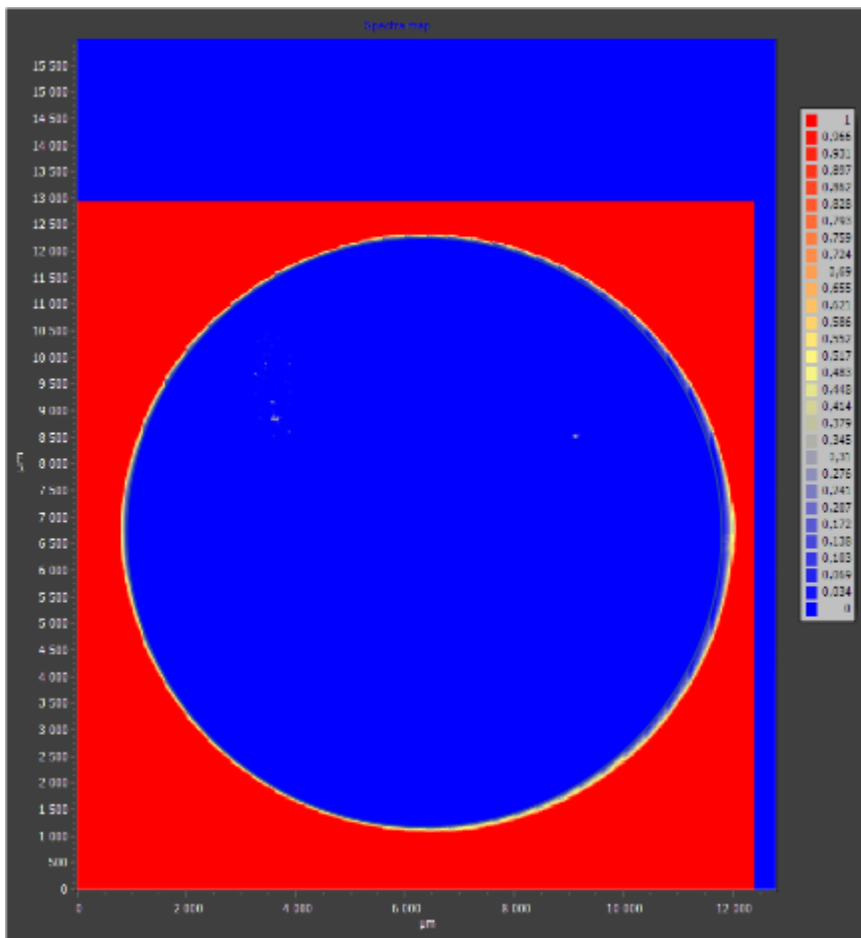


Figure 12B- Heat map over sample #4-blank.

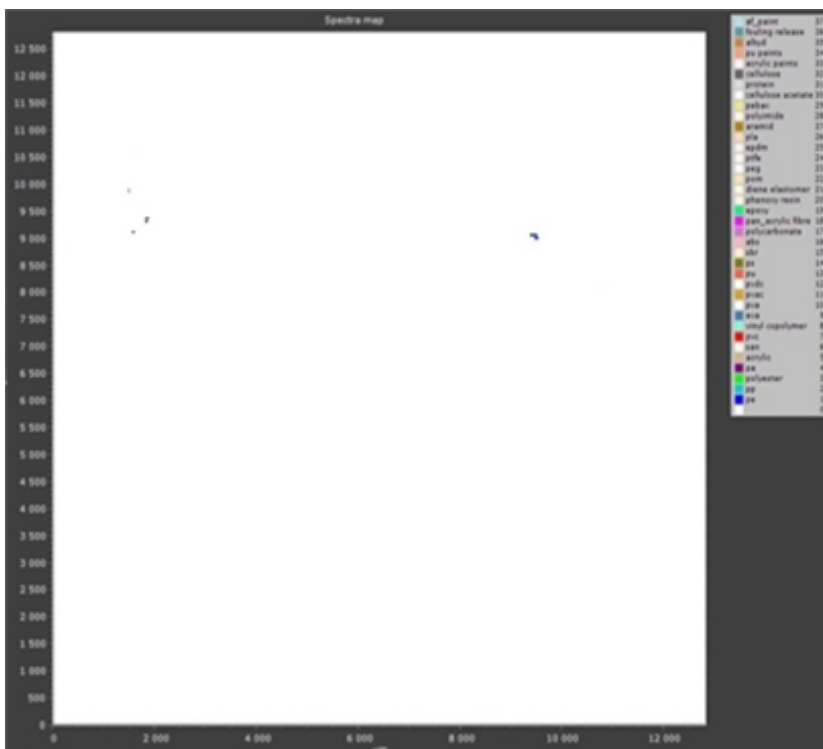


Figure 13B- Spectra map over sample #4-blank.

Sample #5

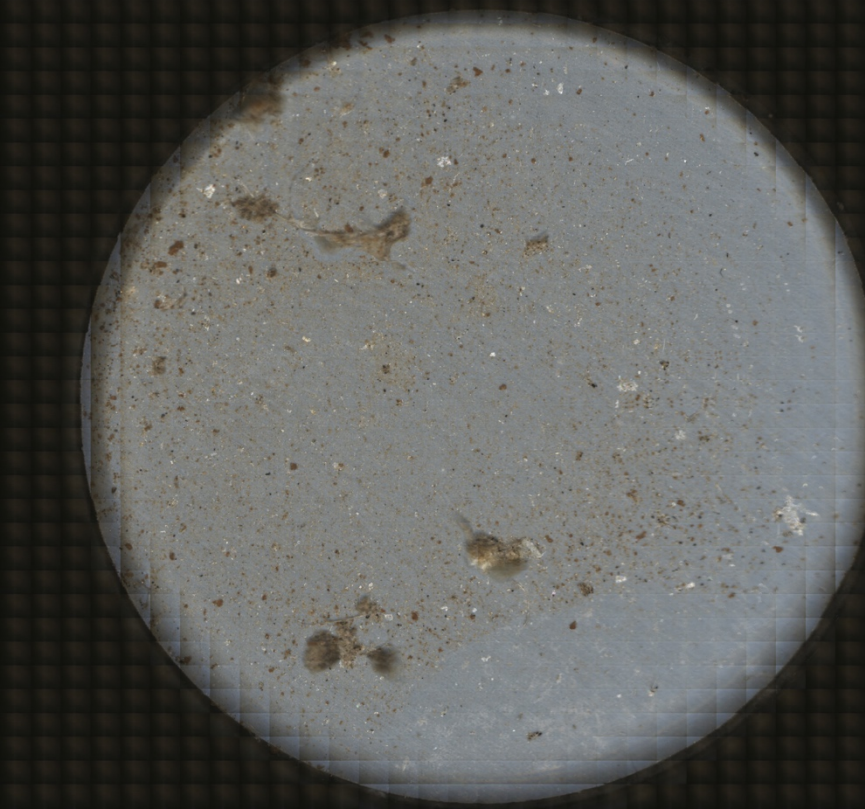


Figure 14B- Filter image of sample #5

Sample #6

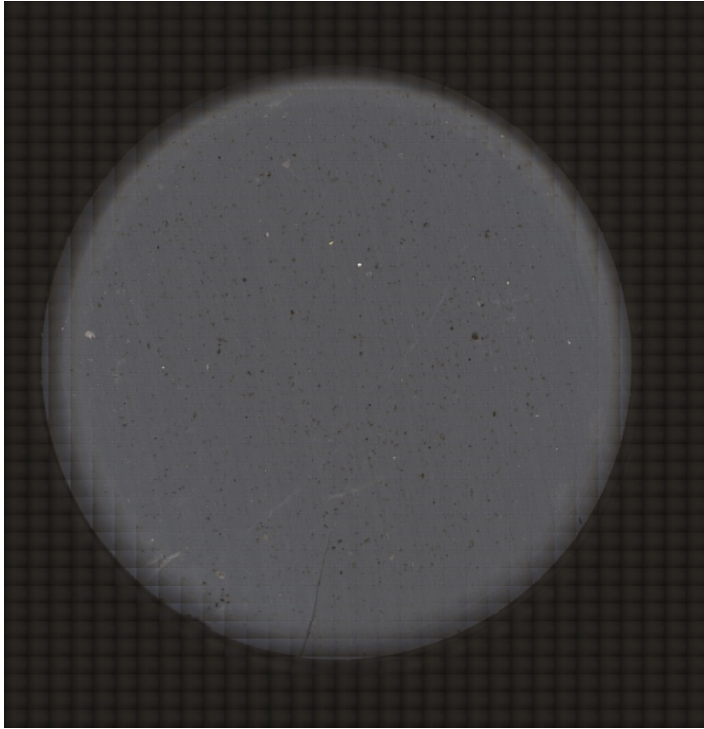


Figure 17B- Filter image of sample #6.

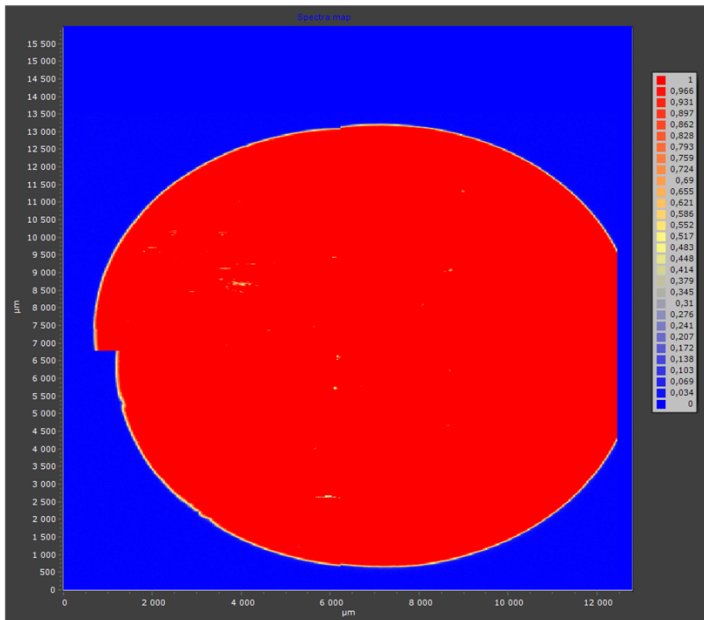


Figure 18B- Heat map of sample #6.

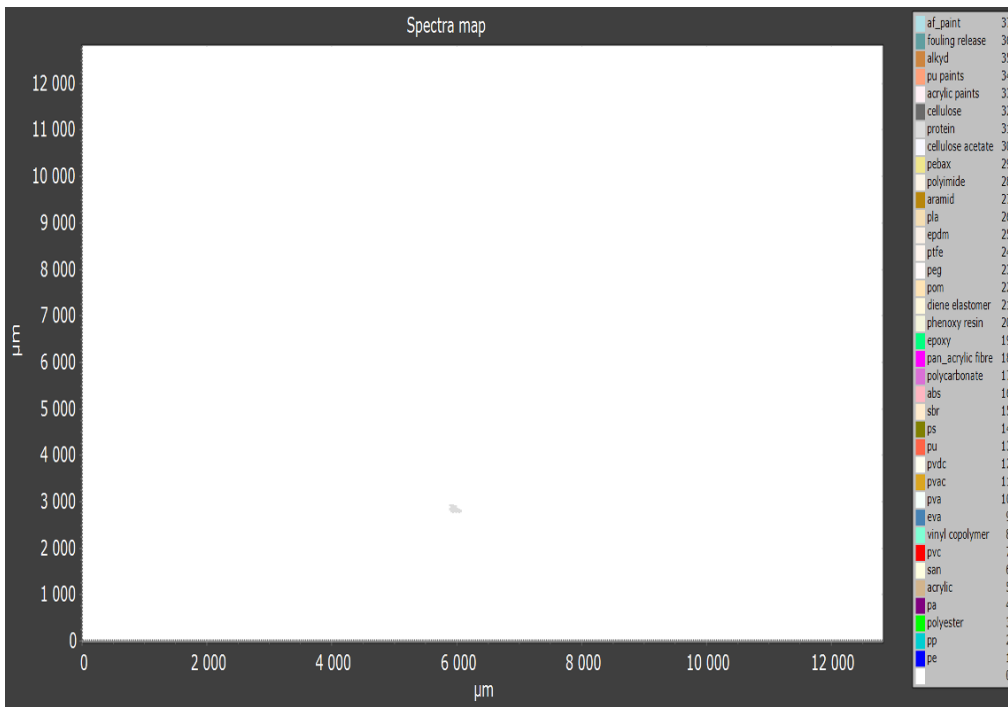


Figure 19B- Spectra map of sample #6.

Sample #7

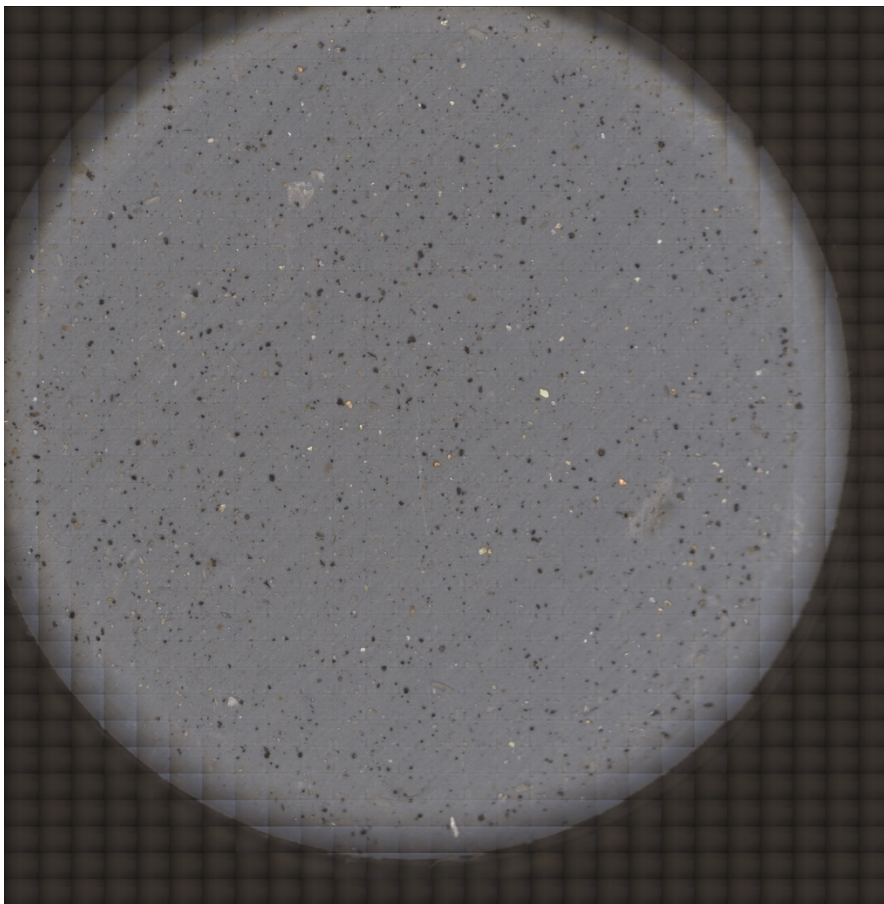


Figure 20B- Filter image of sample #7.

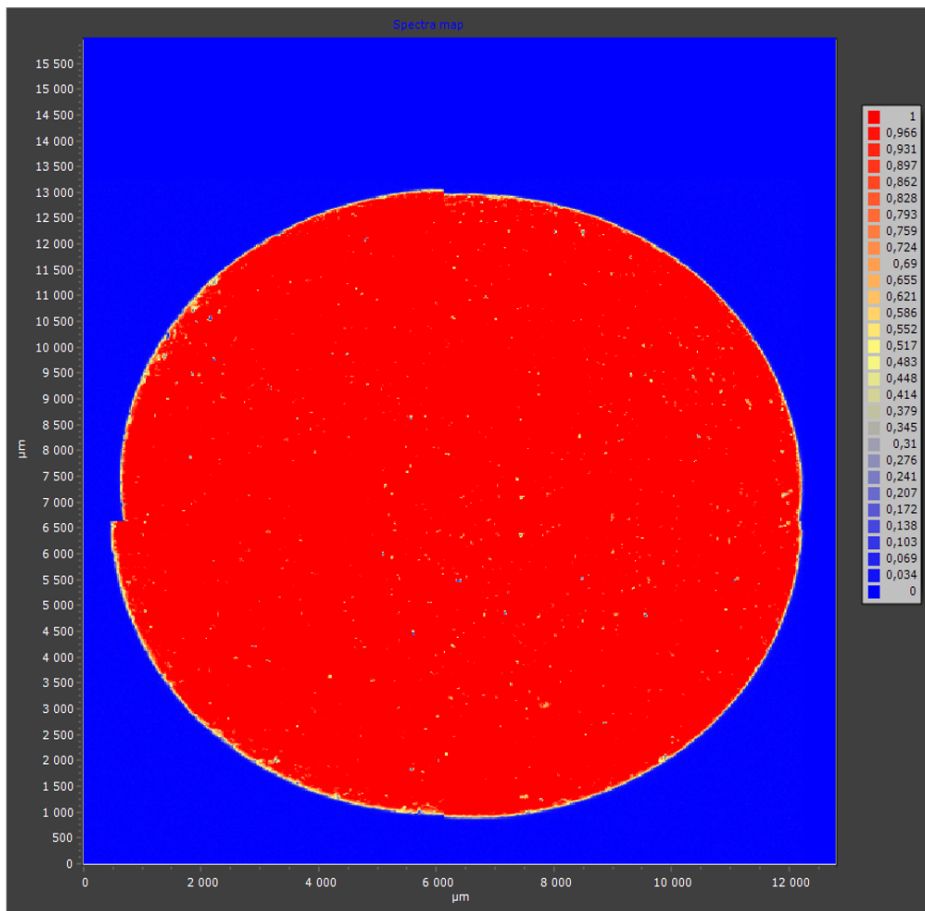


Figure 21B- Heat map of sample #7.

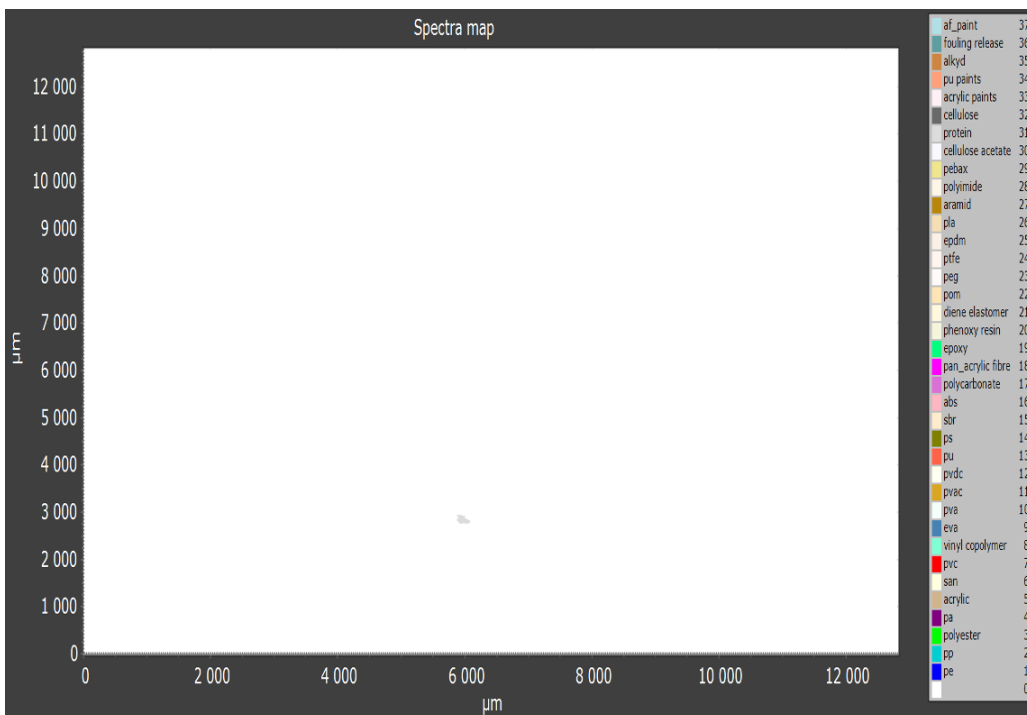


Figure 22B- Spectra map of sample #7.

Sample #8

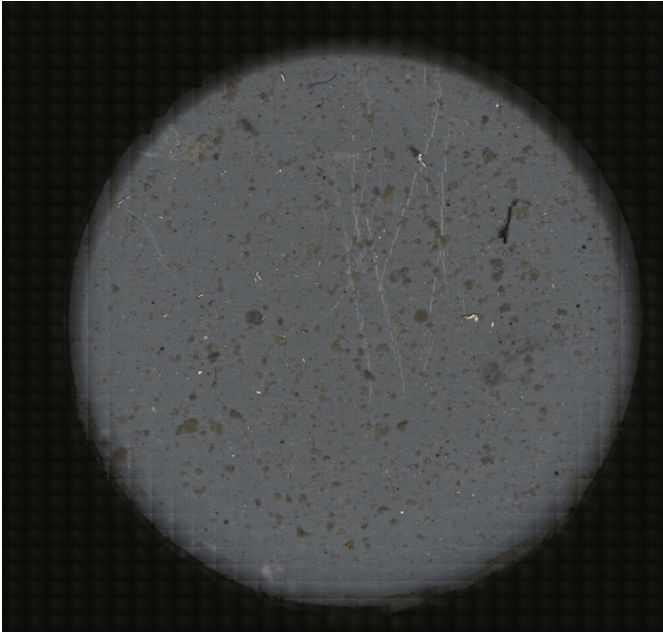


Figure 23B- Filter image of sample #8.

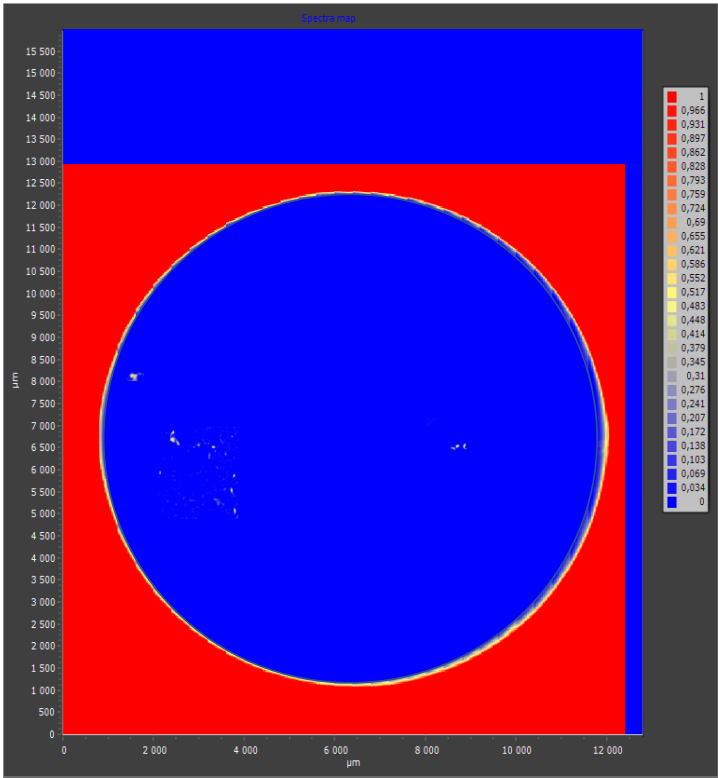


Figure 24B- Heat map for sample #8.

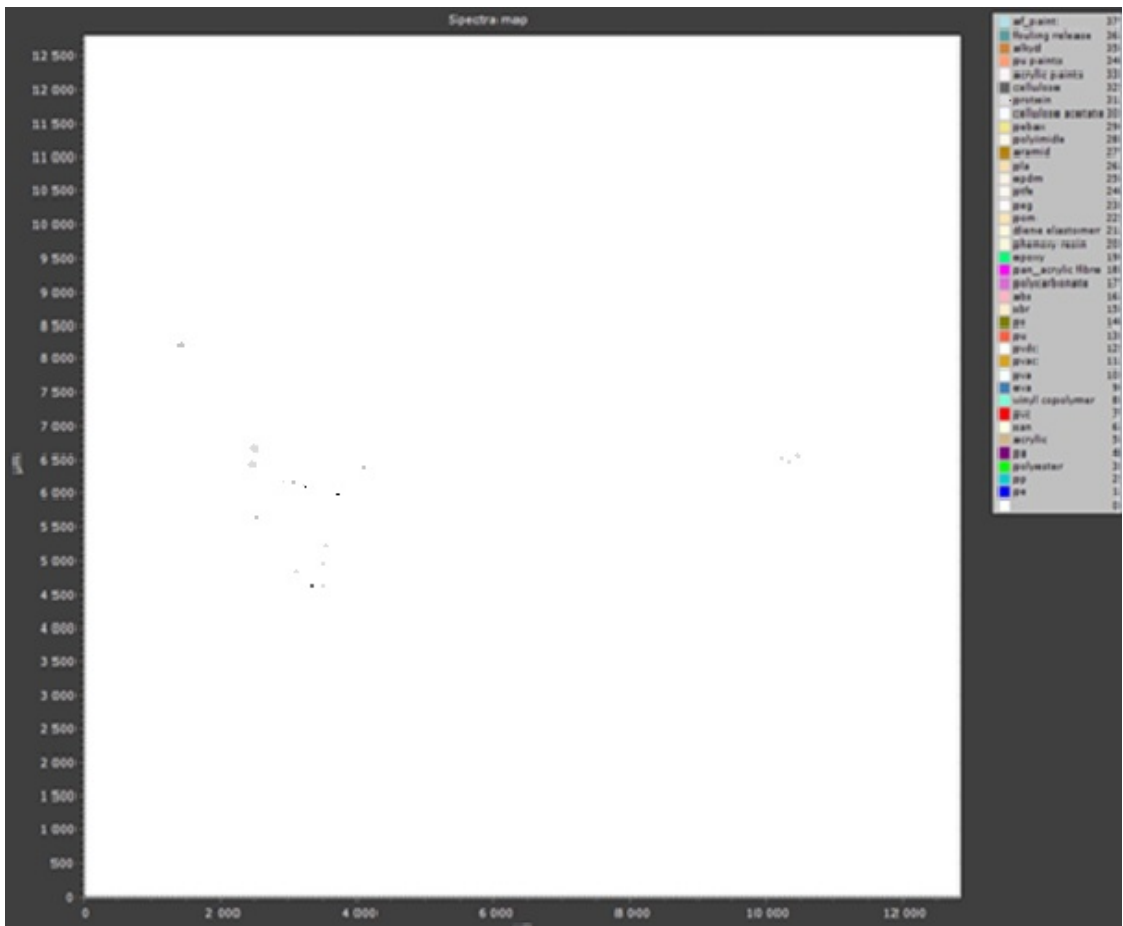


Figure 25B- Spectra map of sample #8.

Sample #9

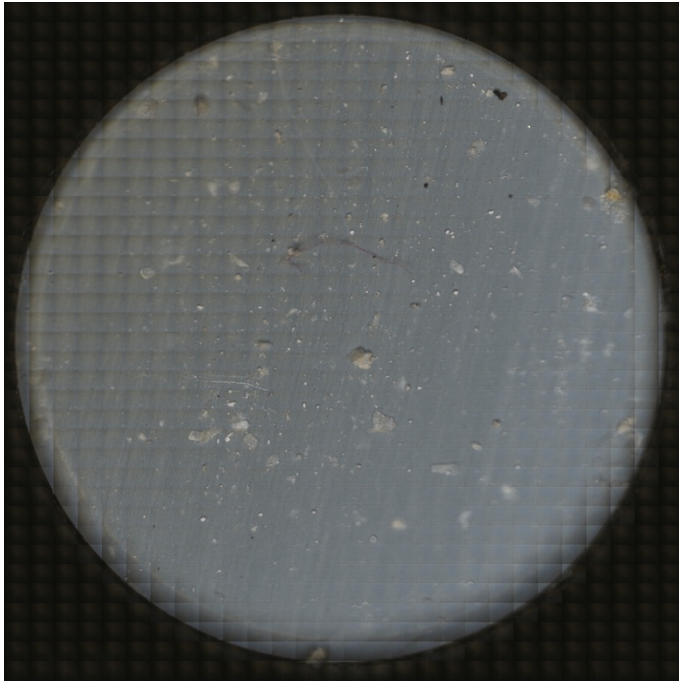


Figure 26B- Filter image of #sample 9

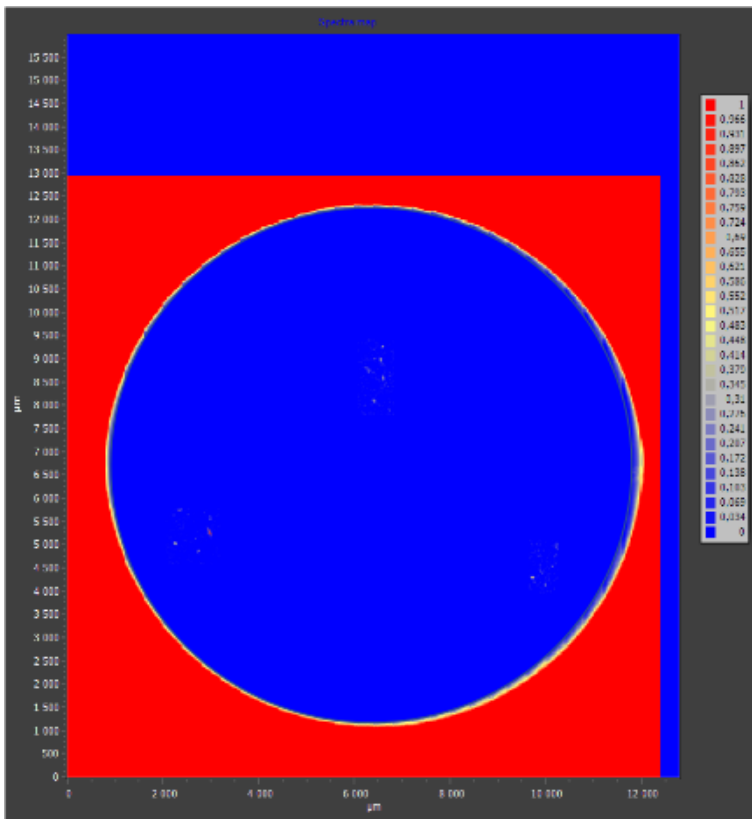


Figure 27B- Heat map of sample #9

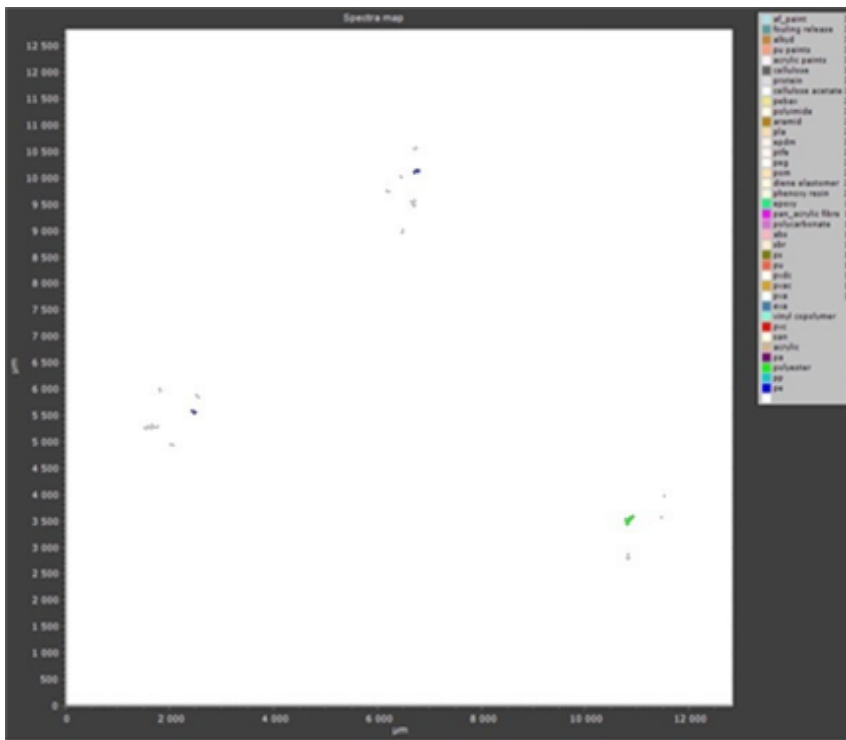


Figure 28B- Spectra image of sample #9

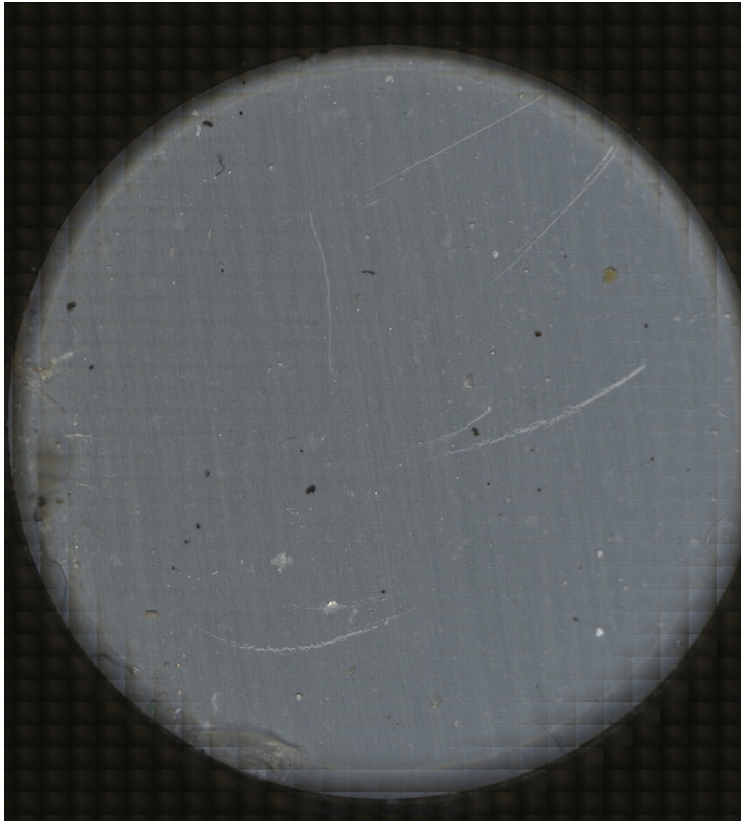


Figure 29B- Filter image for sample #9 blank

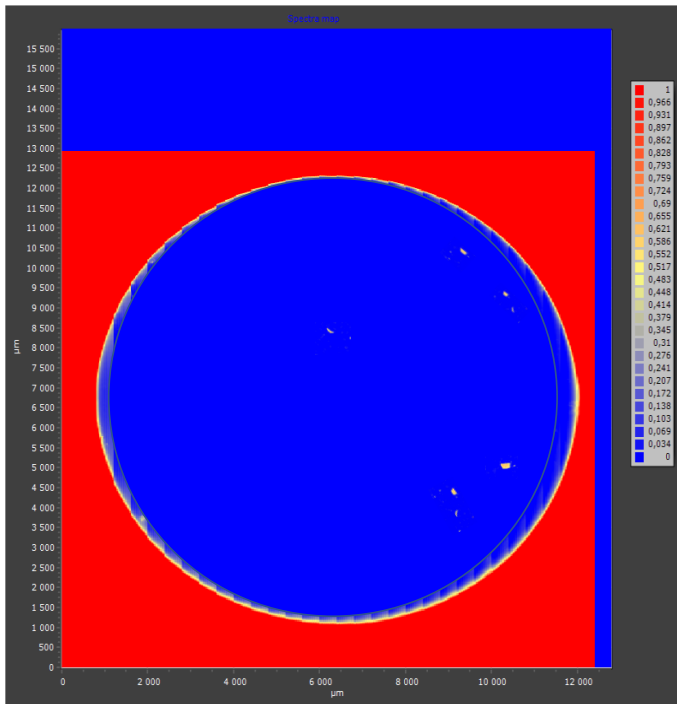


Figure 30B- Heat map for sample #9 blank

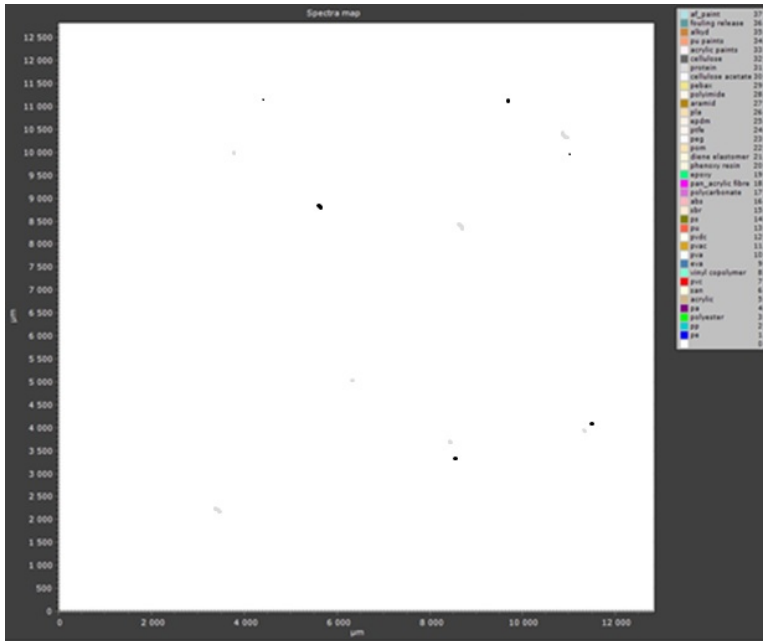


Figure 31B- Spectra map for sample #9 blank.

Sample #10

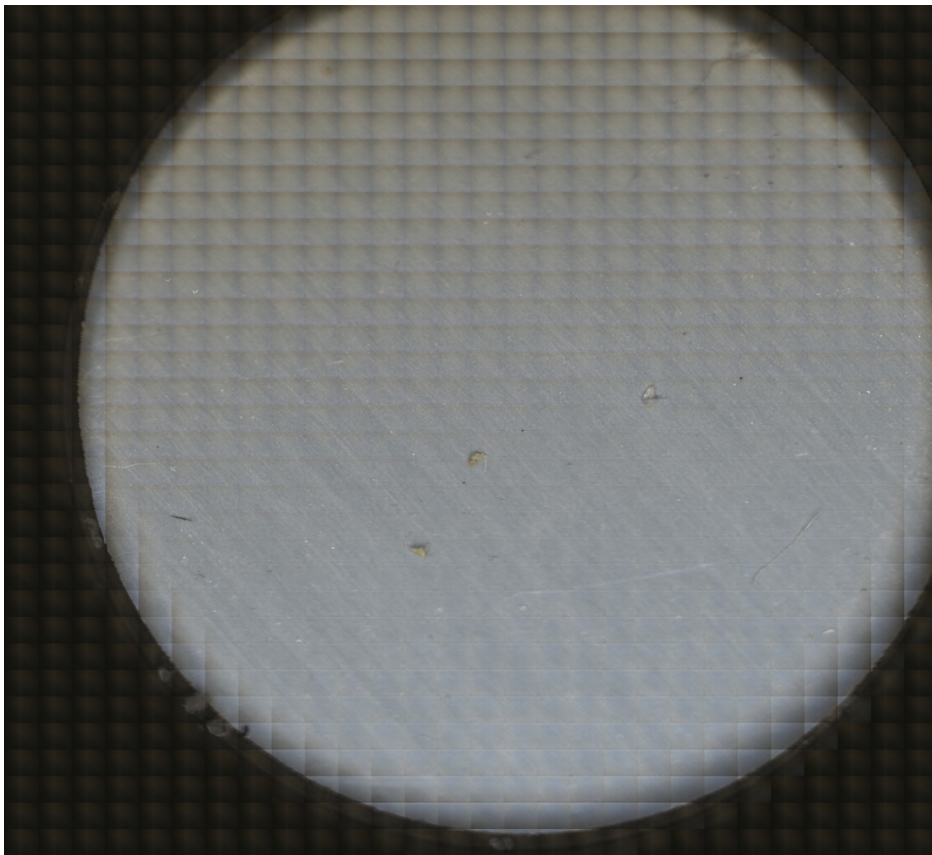


Figure 32B- Filter image of sample #10

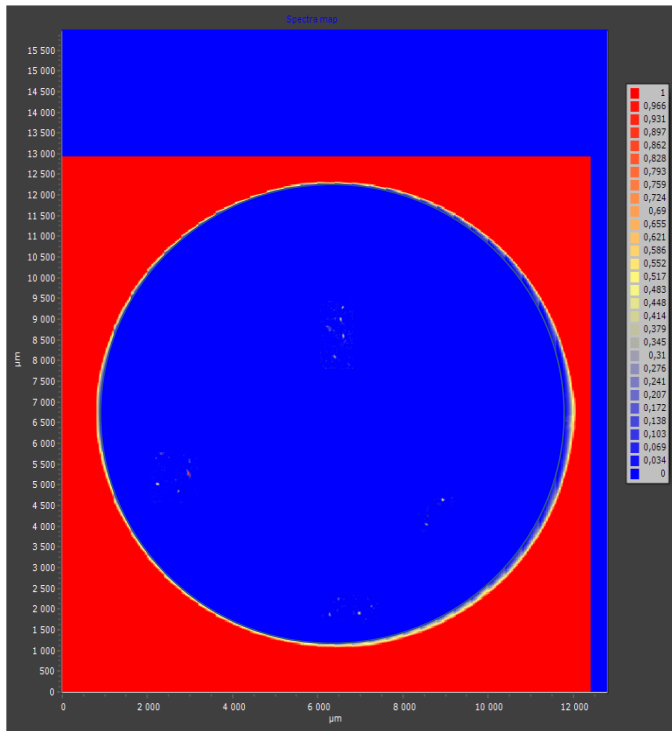


Figure 33B- Heat map for sample #10.

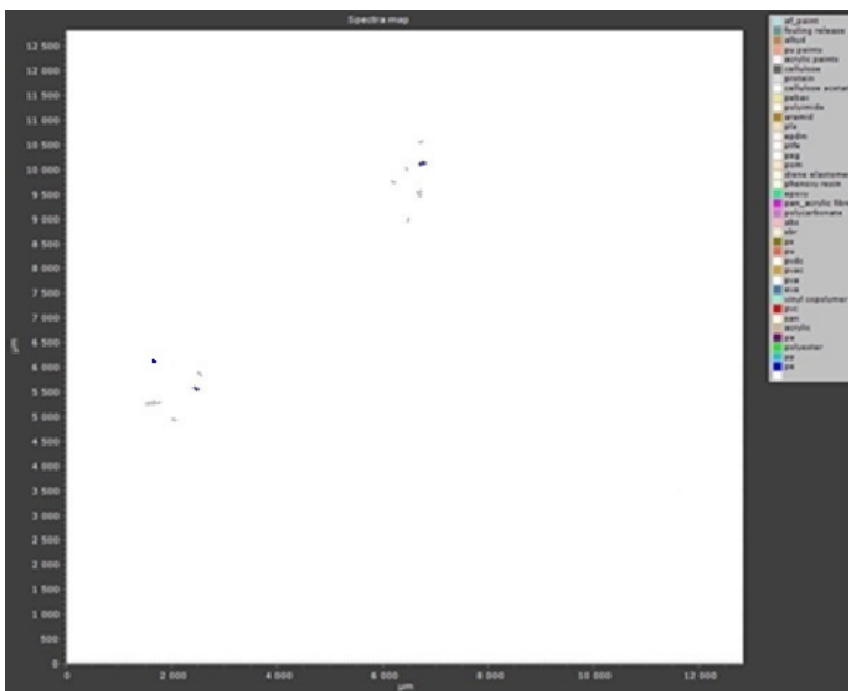


Figure 34B- Spectra map for sample #10.

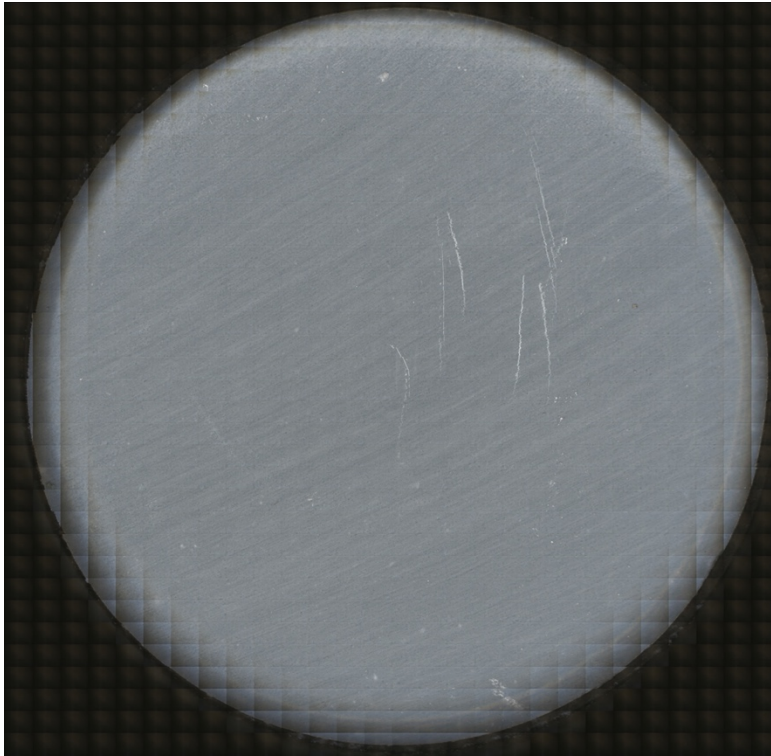


Figure 35B- Filter image sample #10 blank

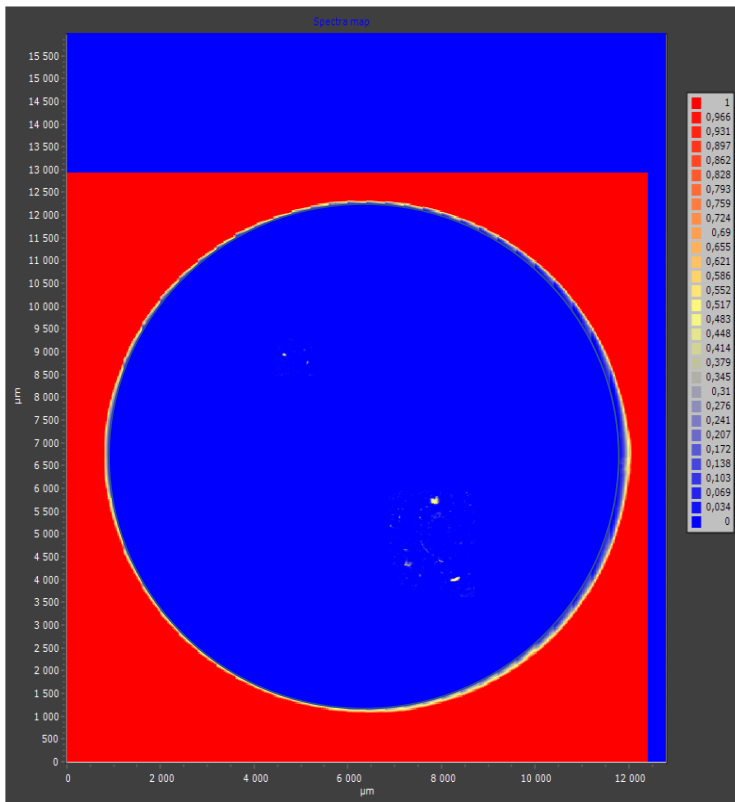


Figure 36B- Heat mat for sample #10 blank.

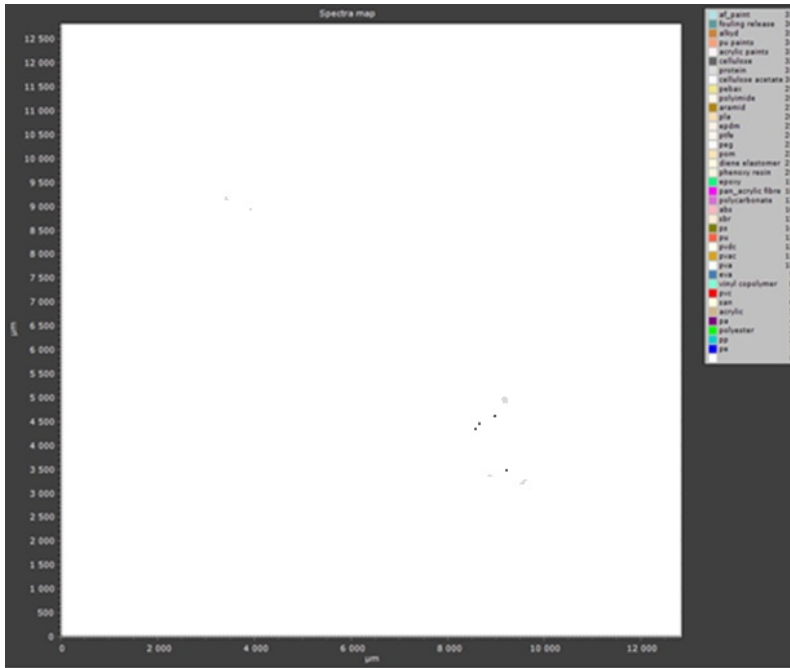


Figure 37B- Spectra map for sample #10 blank

Sample #11

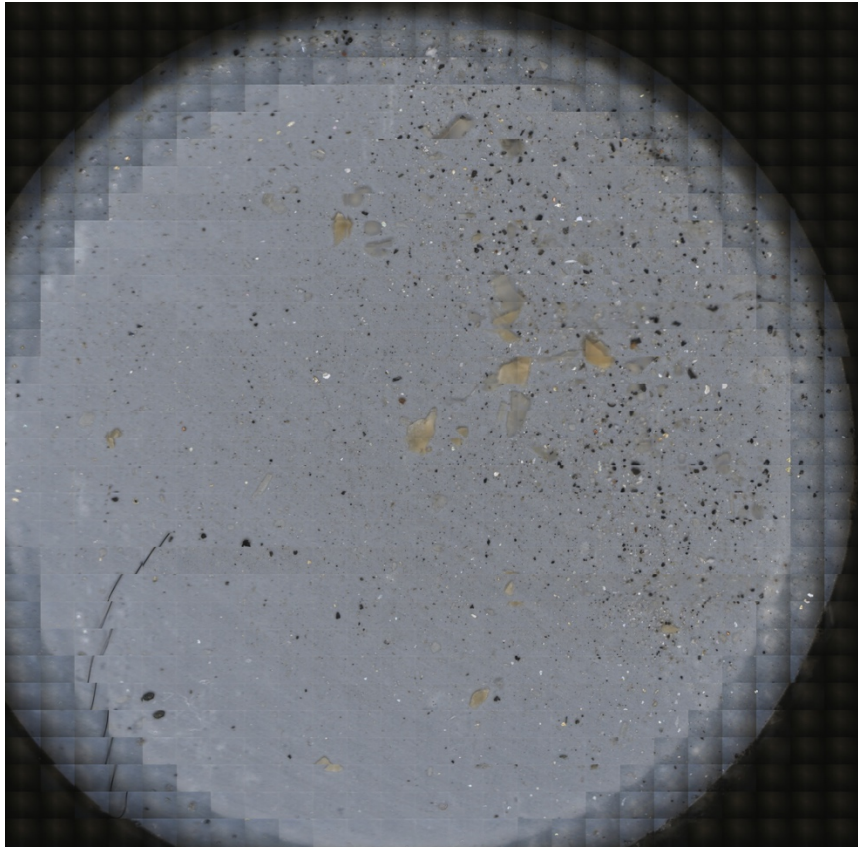


Figure 38B- Filter image of sample #11

F C39- Heat map

F C40- Spectra

F C41- Blank

F C42- Heat blank

F C43- Spectra

Sample #12

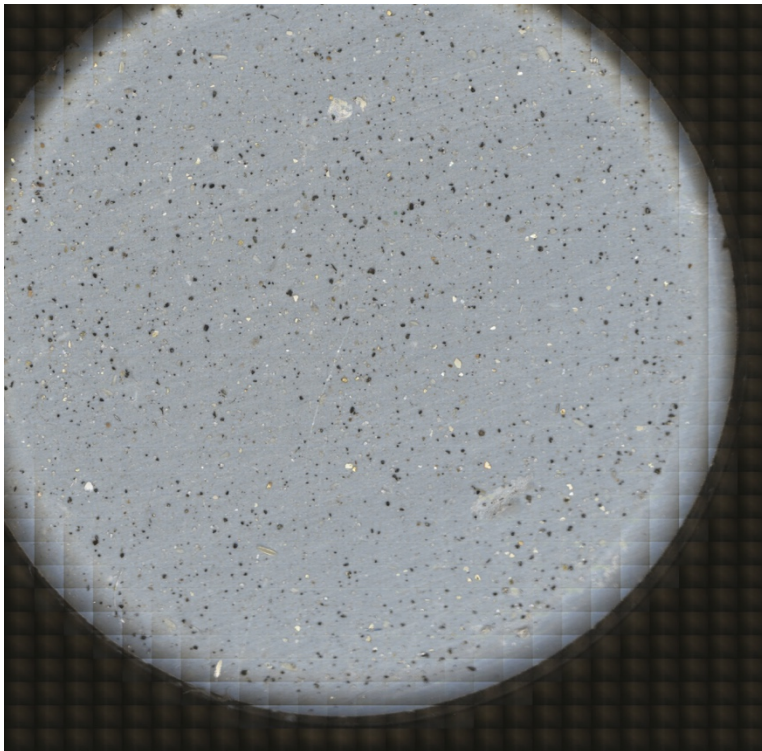


Figure 44B- Filter image of sample #12

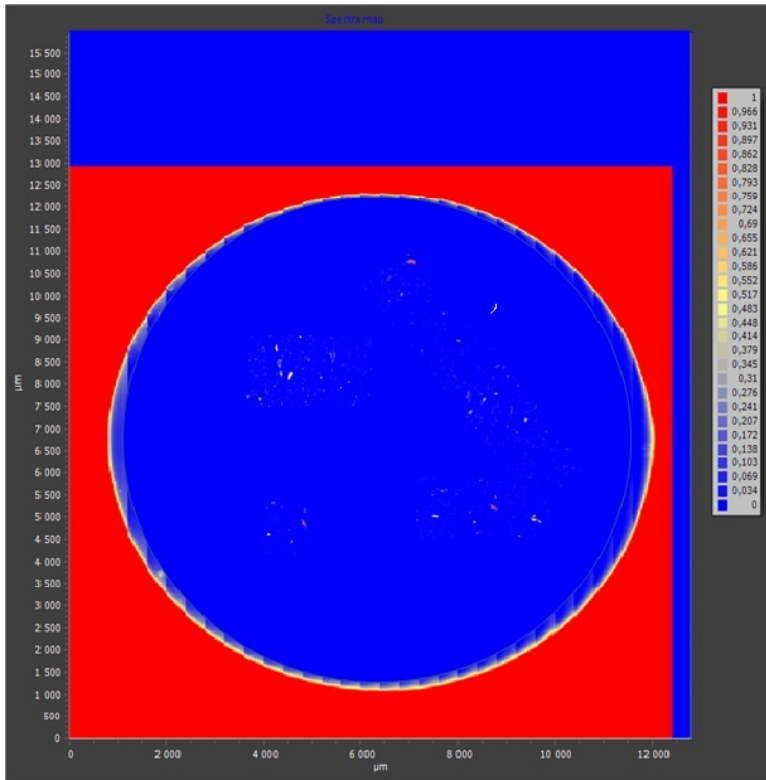


Figure 45B- Heat map for sample #12

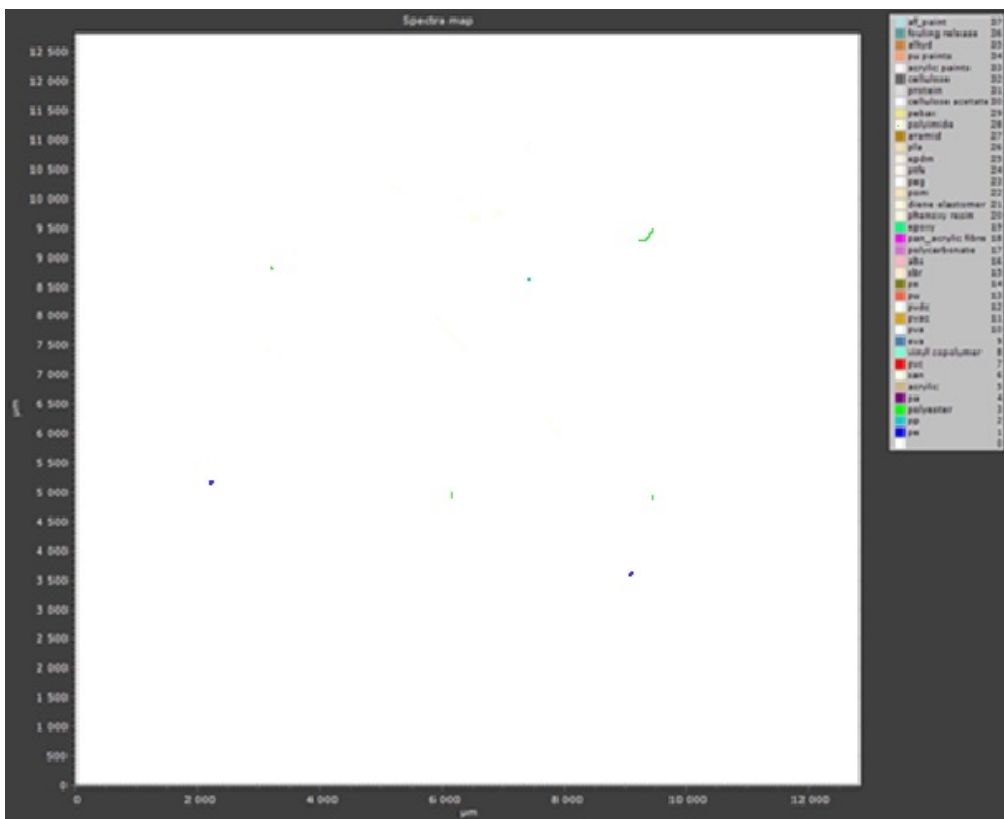


Figure 46B- Spectra image for sample #12.

Sample #13



Figure 47B- Filter image of sample #13

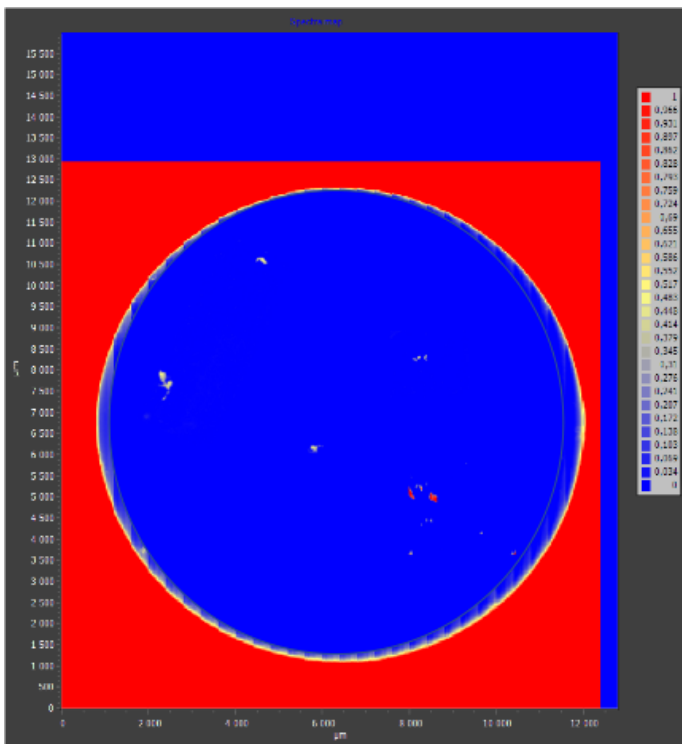


Figure 48B- Heat map of sample #13

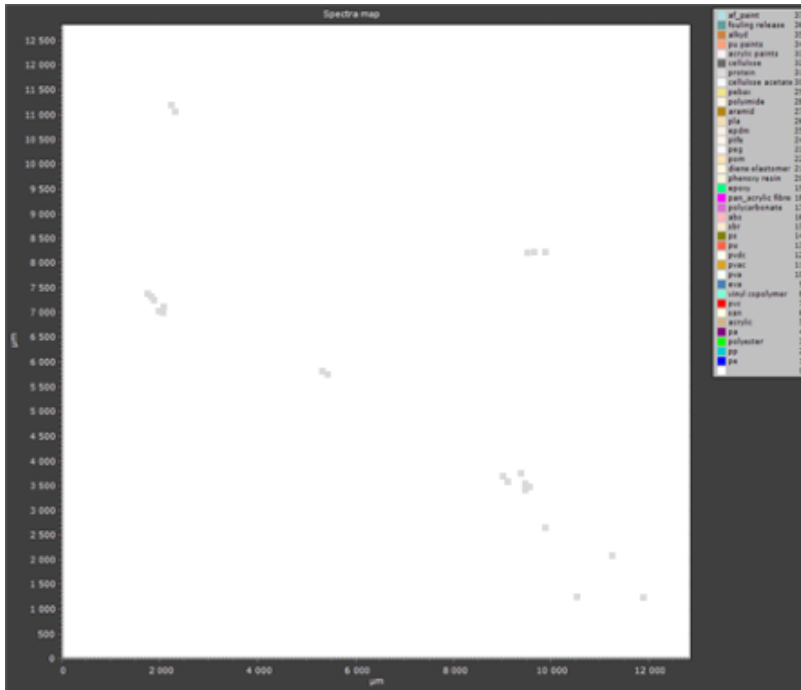


Figure 49B- Spectra map of sample #13

Sample #14

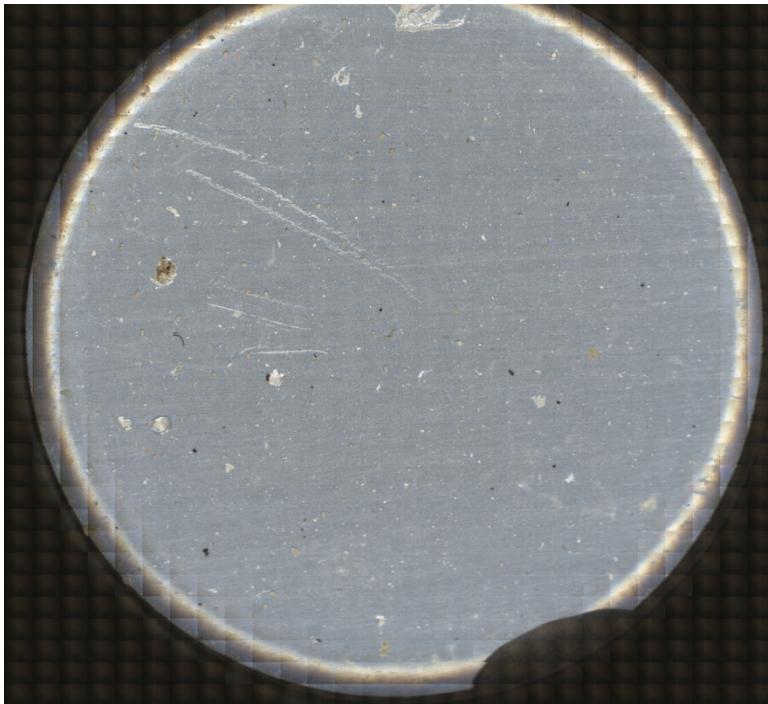


Figure 50B- Filter image of sample #14

Sample #15



Figure 53B- Filter image over sample #15

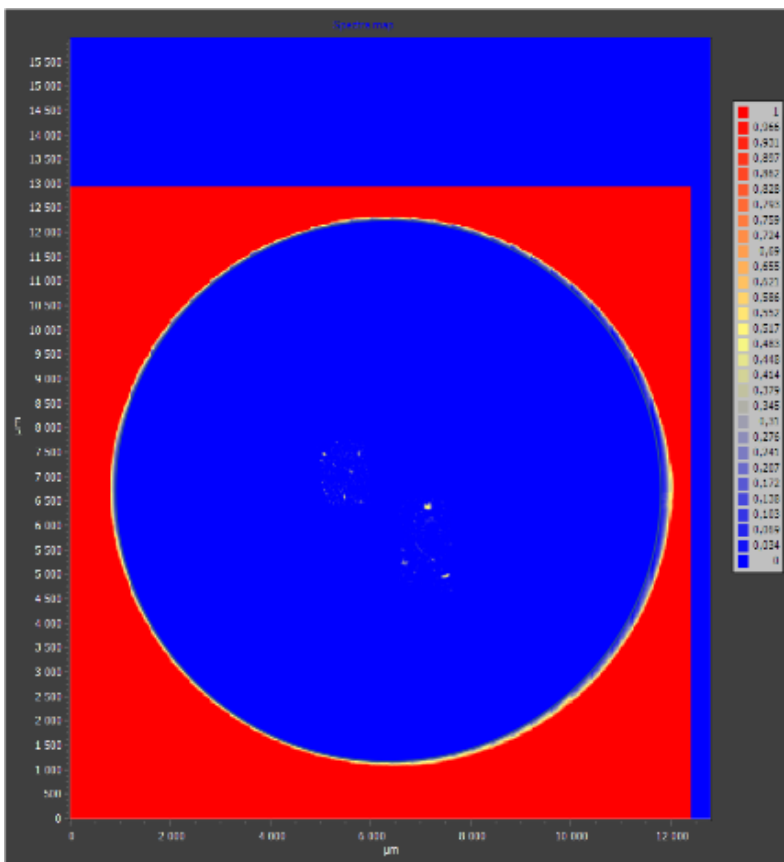


Figure 54B- Heat map over sample #15

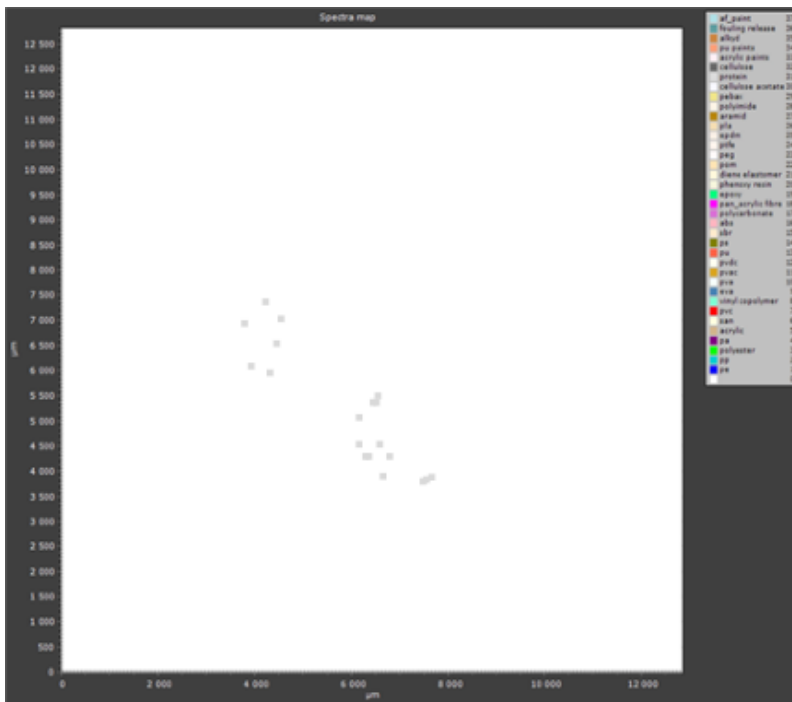


Figure 55B- Spectra map over sample #15

Sample #16

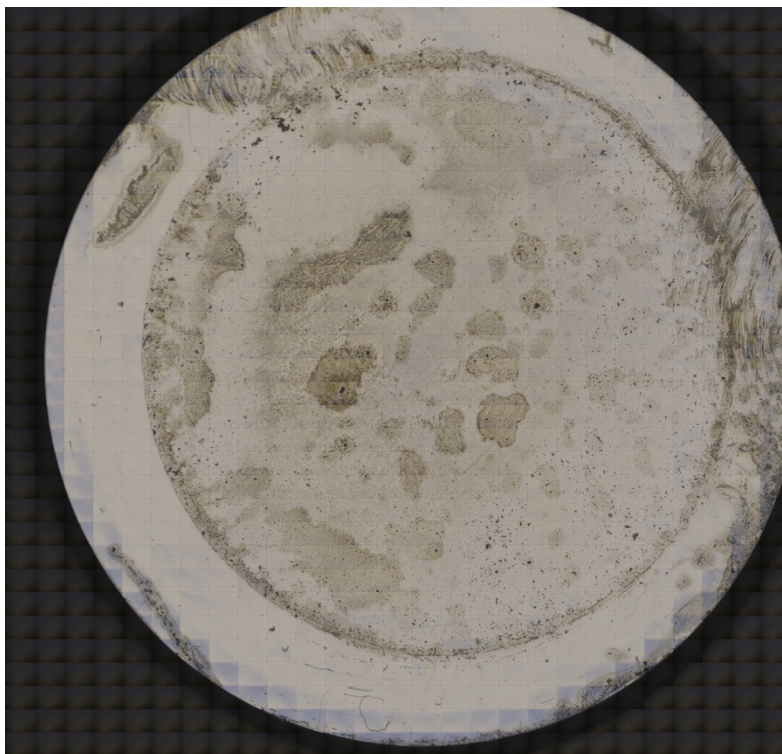


Figure 56B- Filter image of sample #16

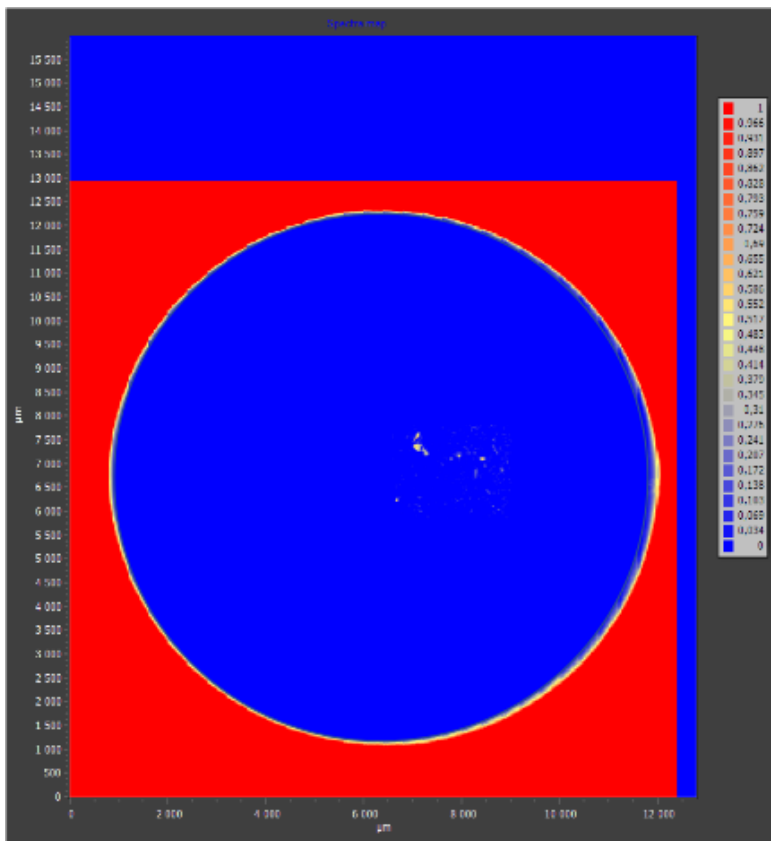


Figure 57B- Heat map of sample #16

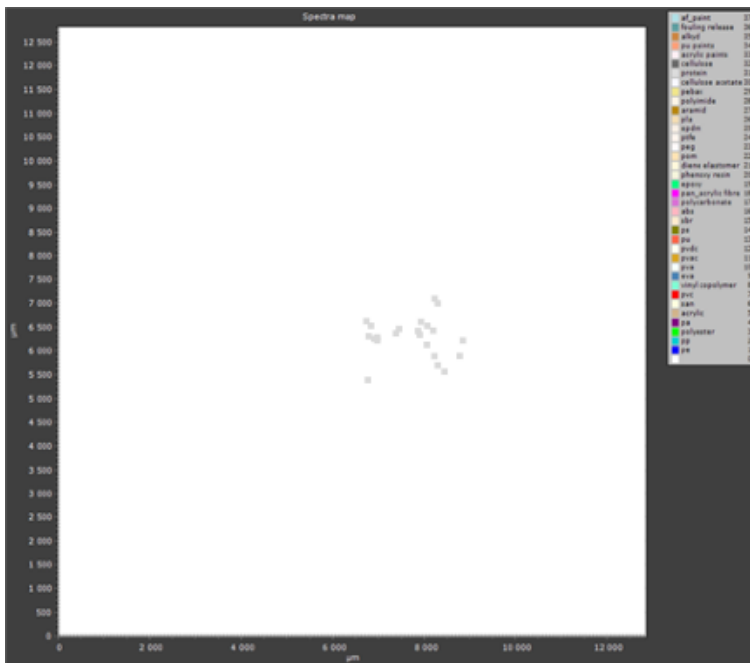


Figure 58B- Spectra map of sample #16

Sample #17

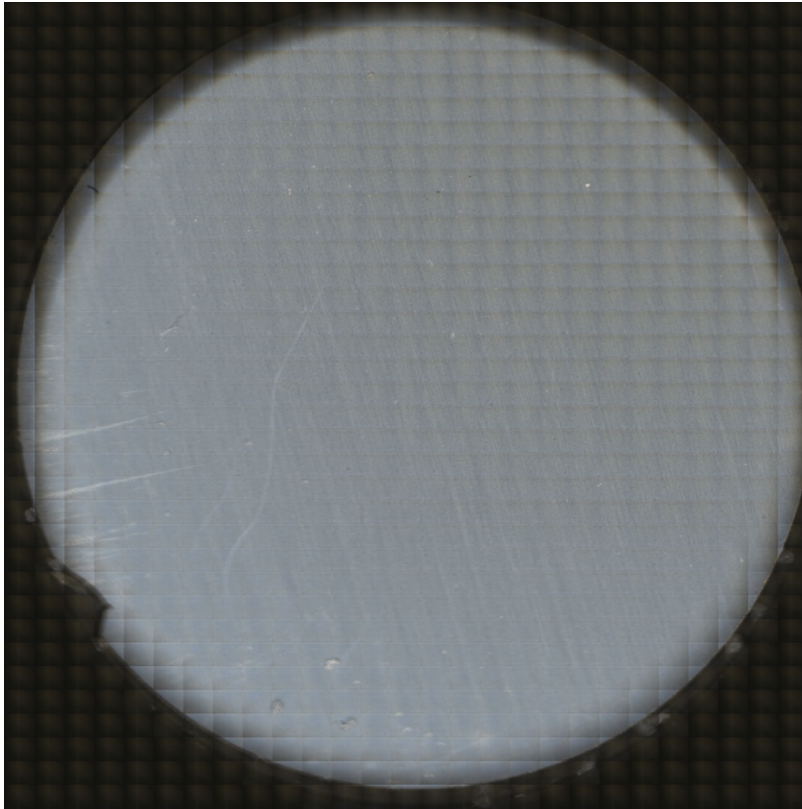


Figure 59B- Filter image of sample #17

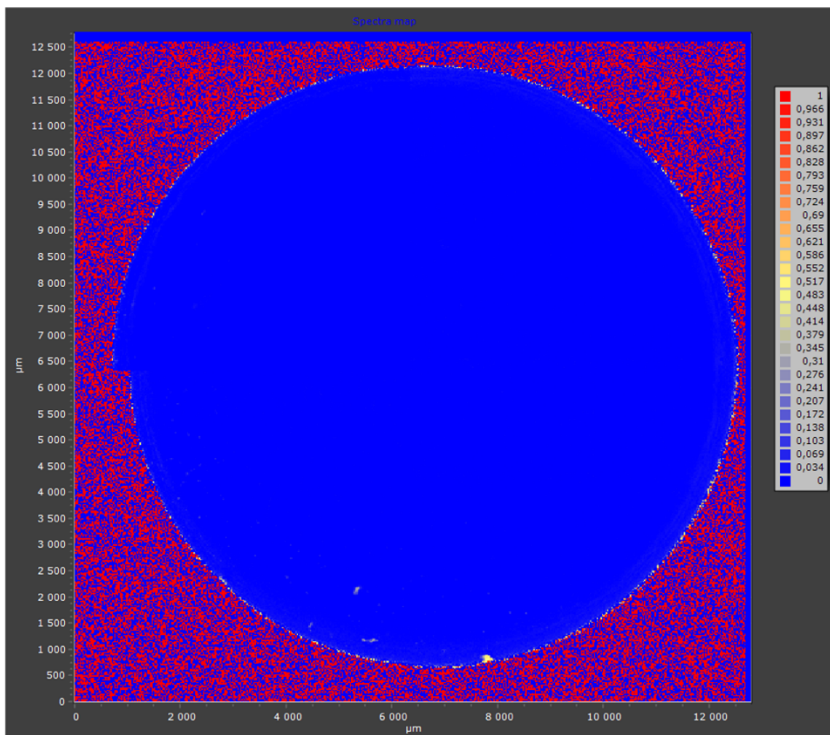


Figure 60B- Heat map of sample #17

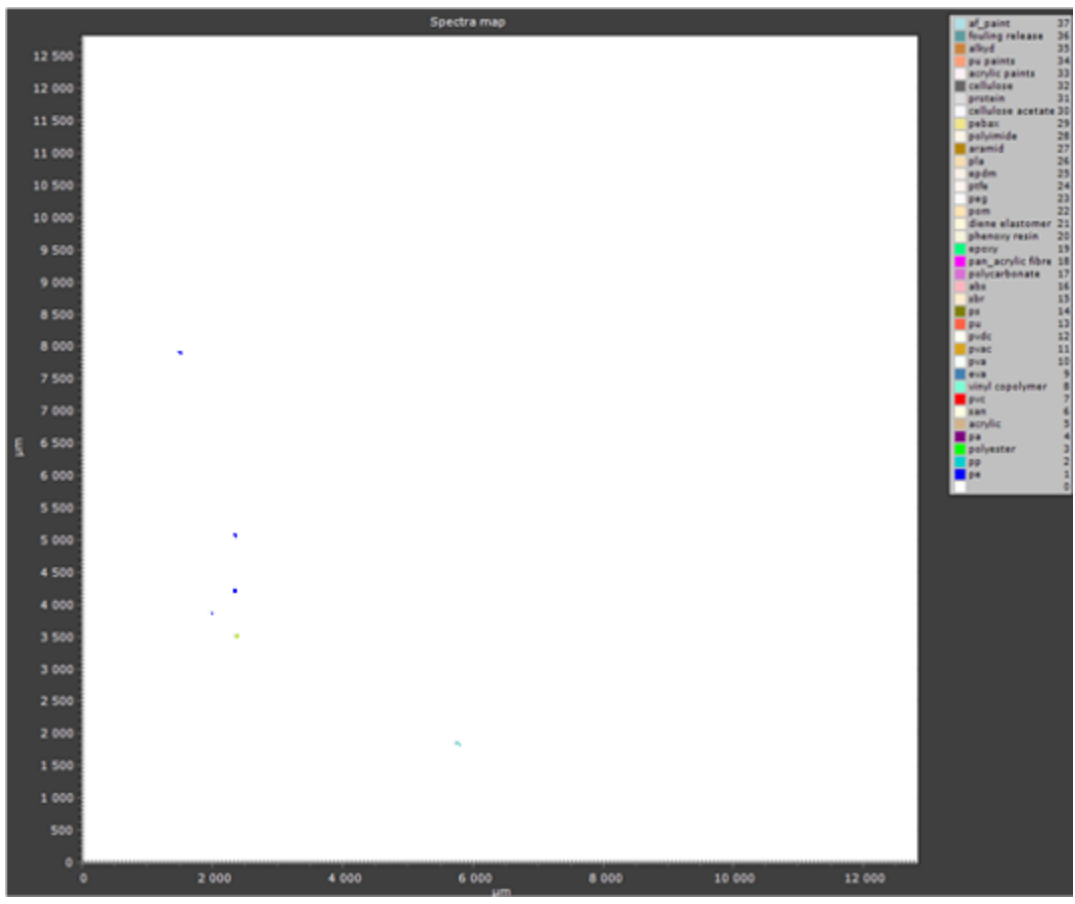


Figure 61B- Spectra map of sample #17

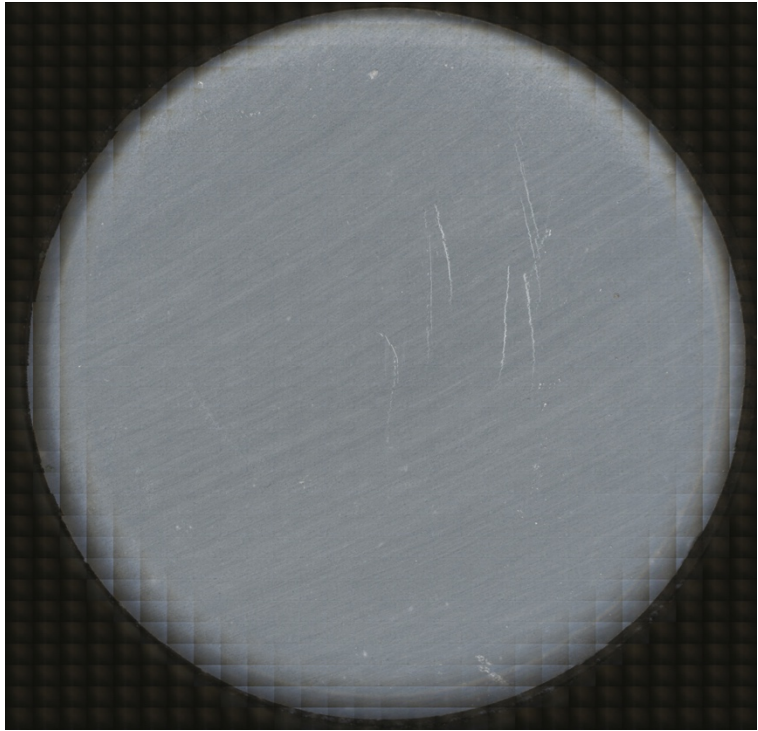


Figure 62B- Filter image of sample #17 blank

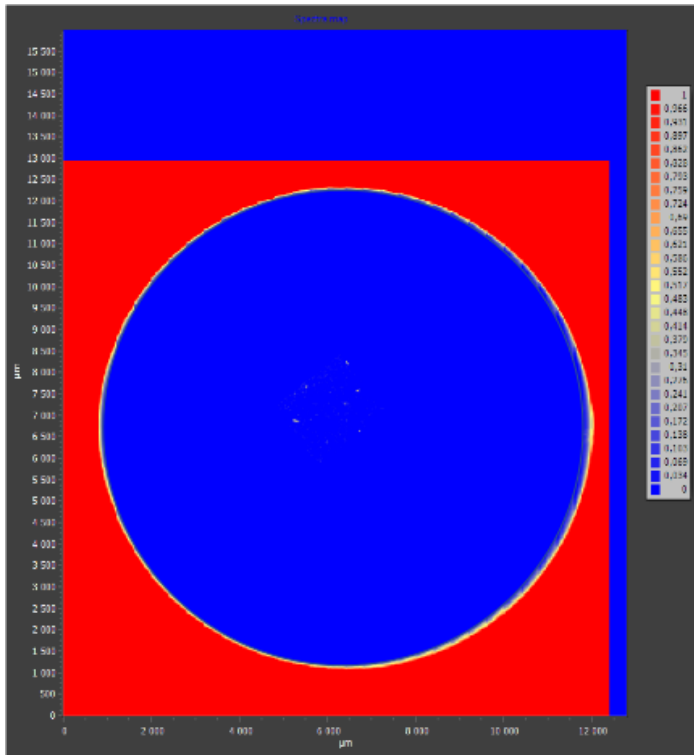


Figure 63B- Heat map of sample #17 blank

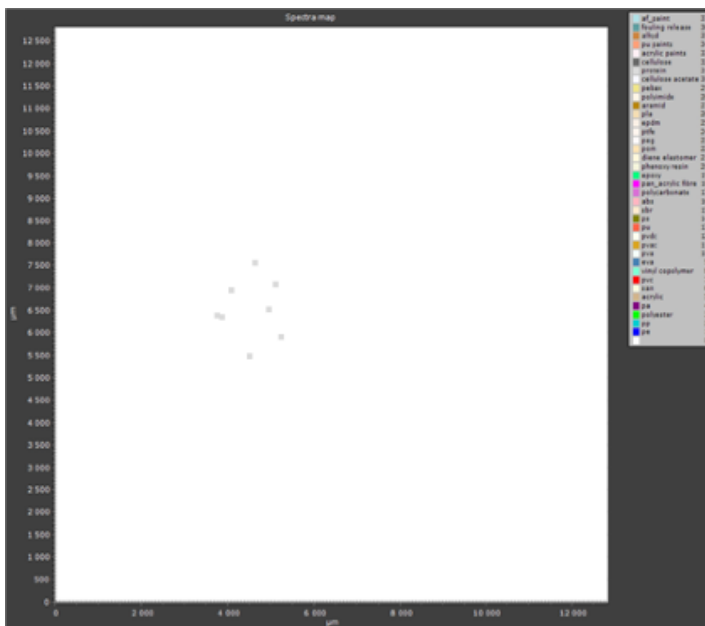


Figure 64B- Spectra map of sample #17 blank

Sample #18

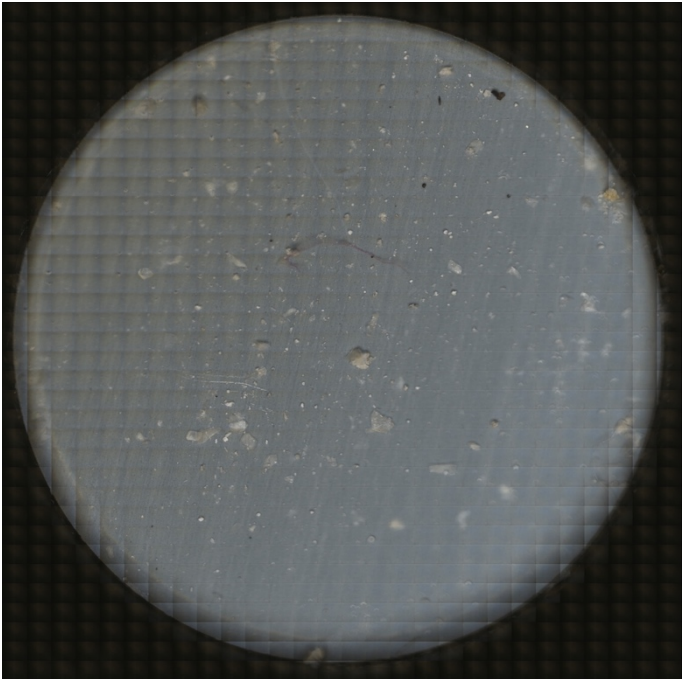


Figure 65B- Filter image of sample #18

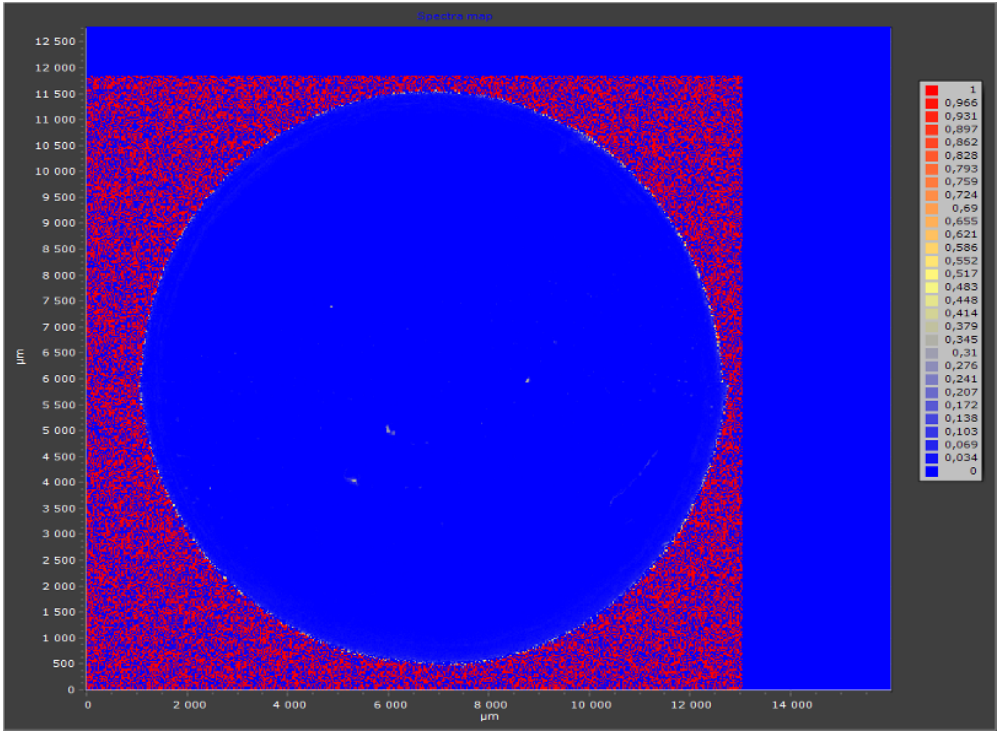


Figure 66B- Heat map of sample #18

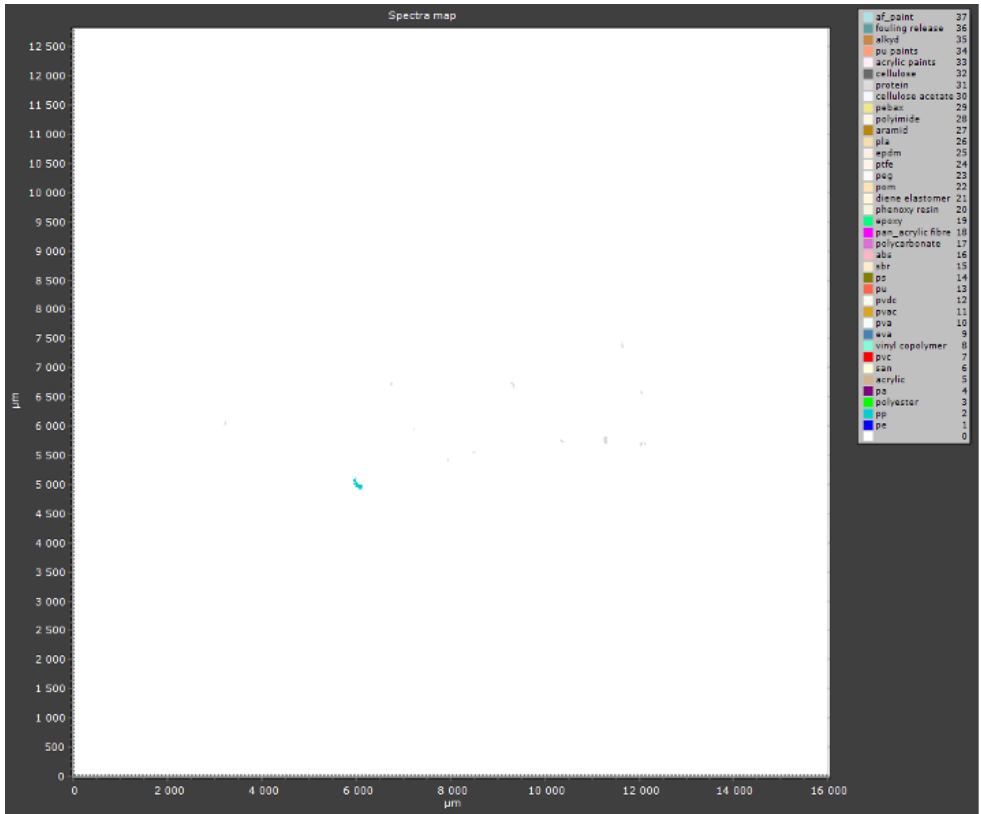


Figure 67B- Spectra image of sample #18

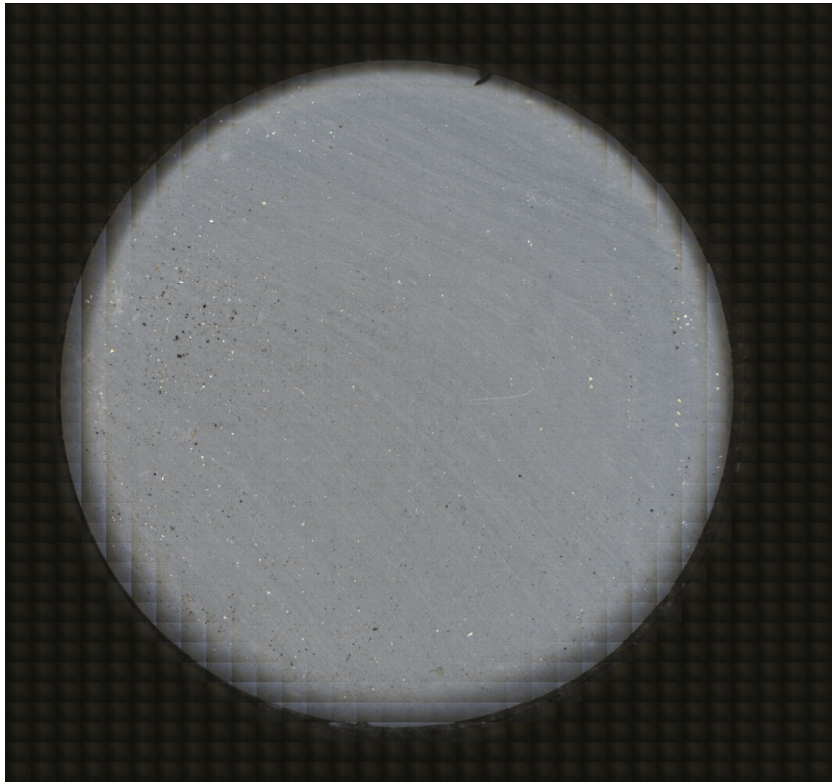


Figure C68- Filter image of sample #18 blank.

Sample #19

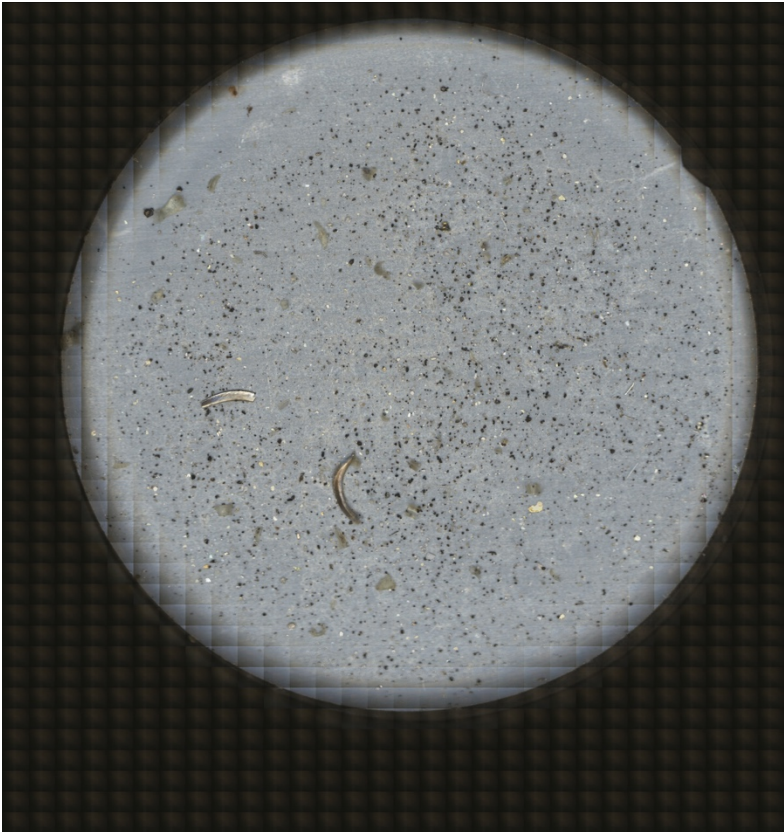


Figure 71B- Filter image of sample #19

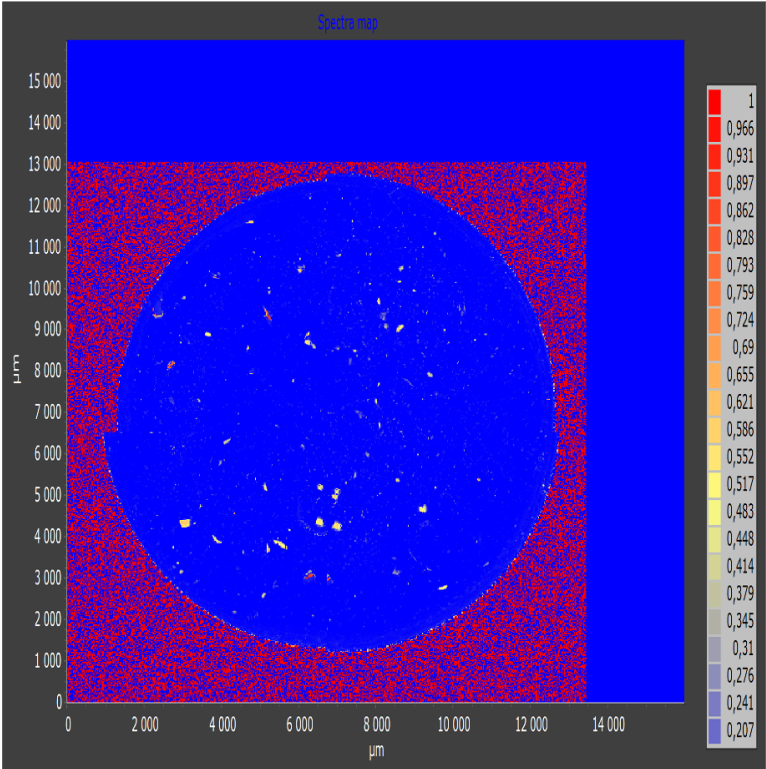


Figure 72B- Heat map of sample #19

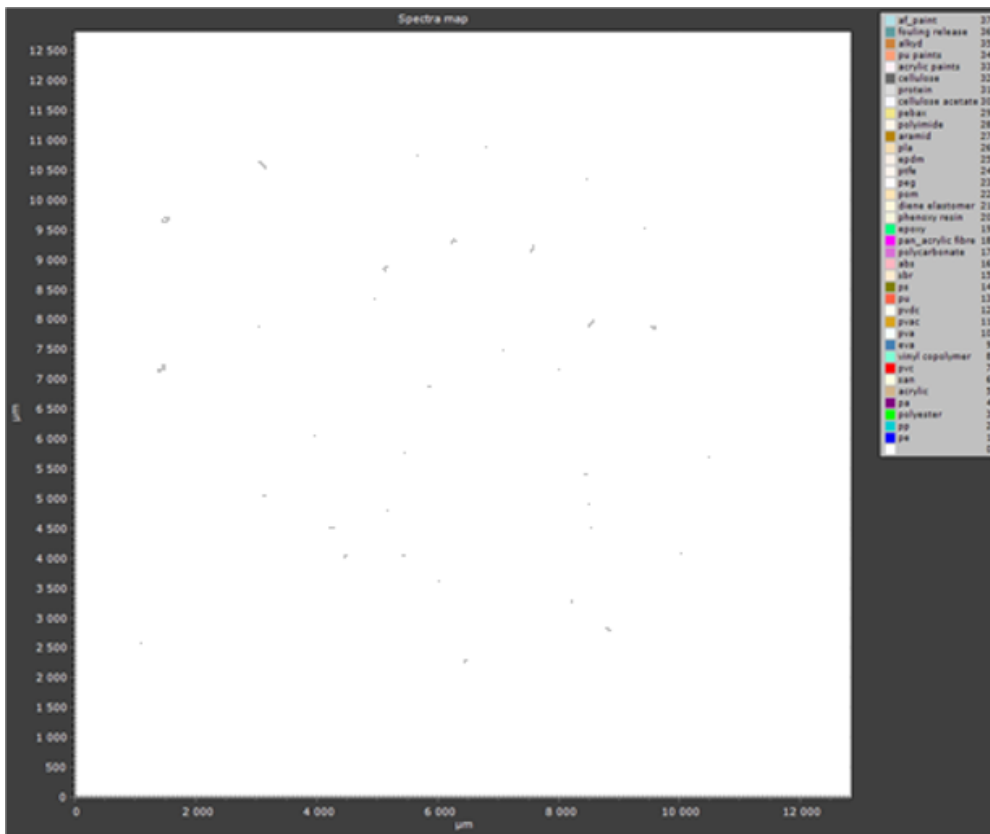


Figure 73B- Spectra map of sample #19

Sample #20

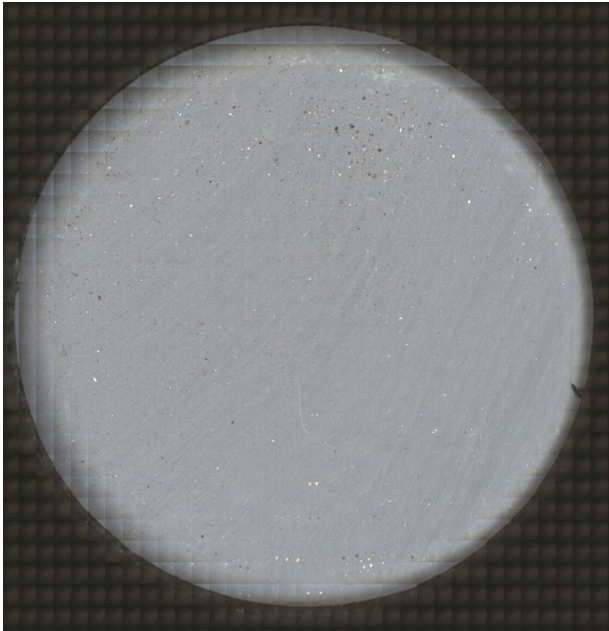


Figure 74B- Filter image of sample #20.

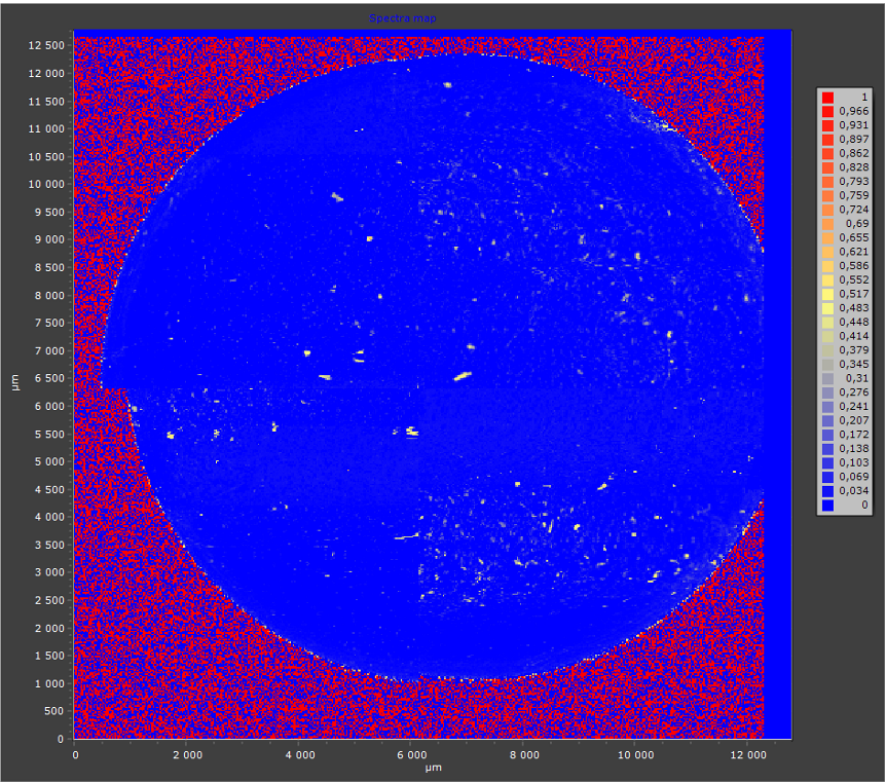


Figure 75B- Heat map of sample #20

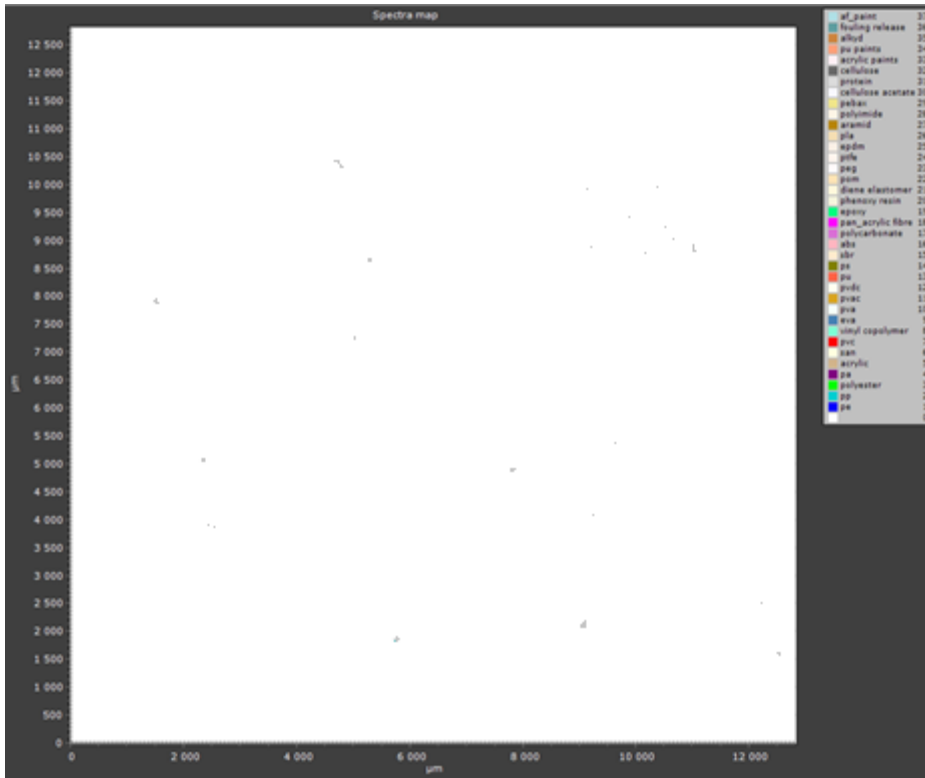


Figure 76B- Spectra map of sample #20.

Sample #21

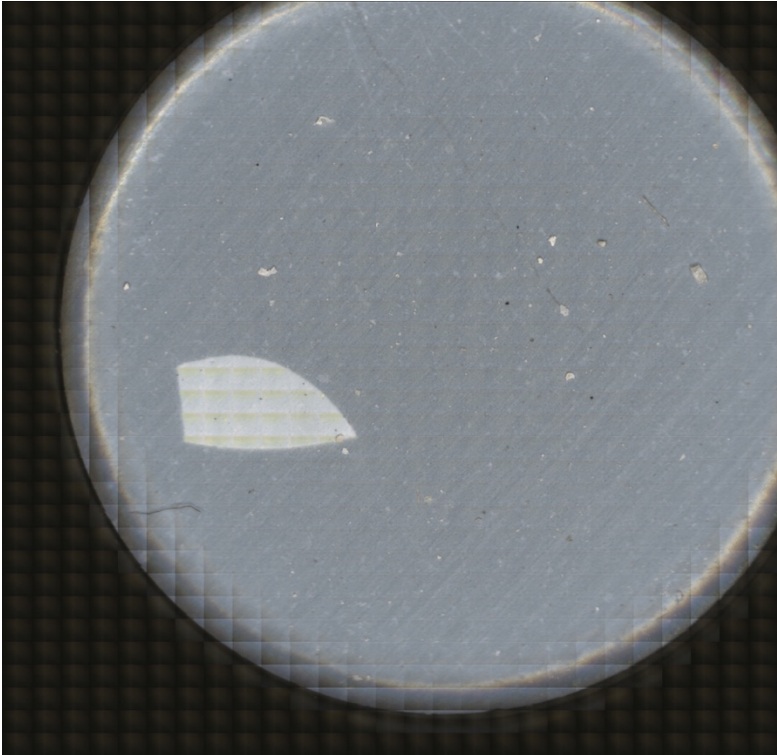


Figure 77B- Filter image of sample #21

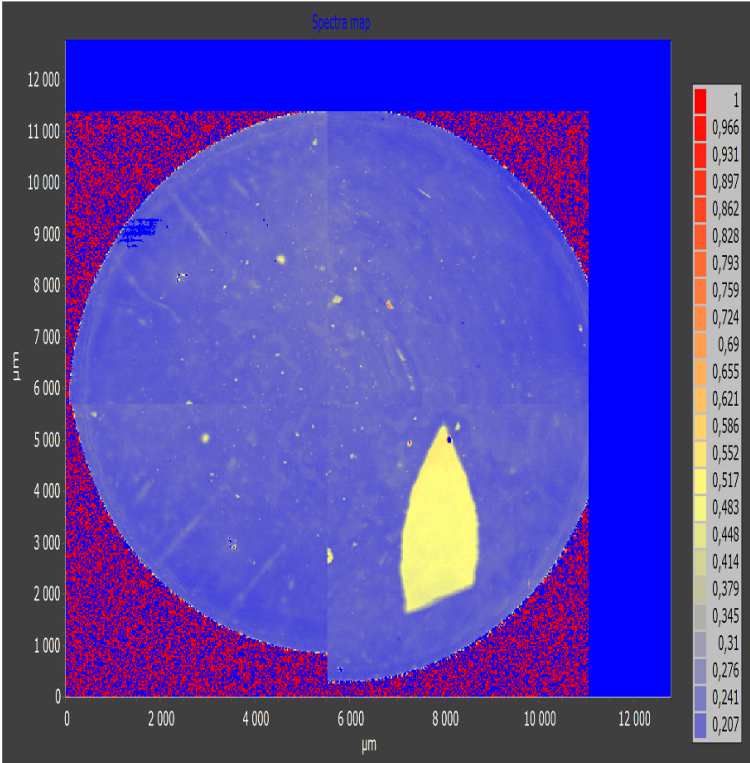


Figure 78B- Heat map of sample #21

Sample #22

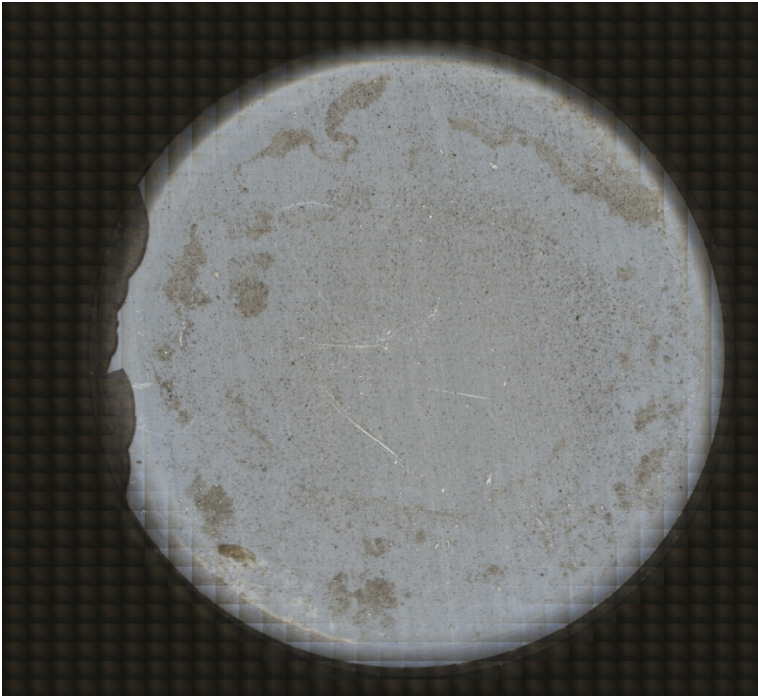


Figure 79B- Filter image of sample #22.

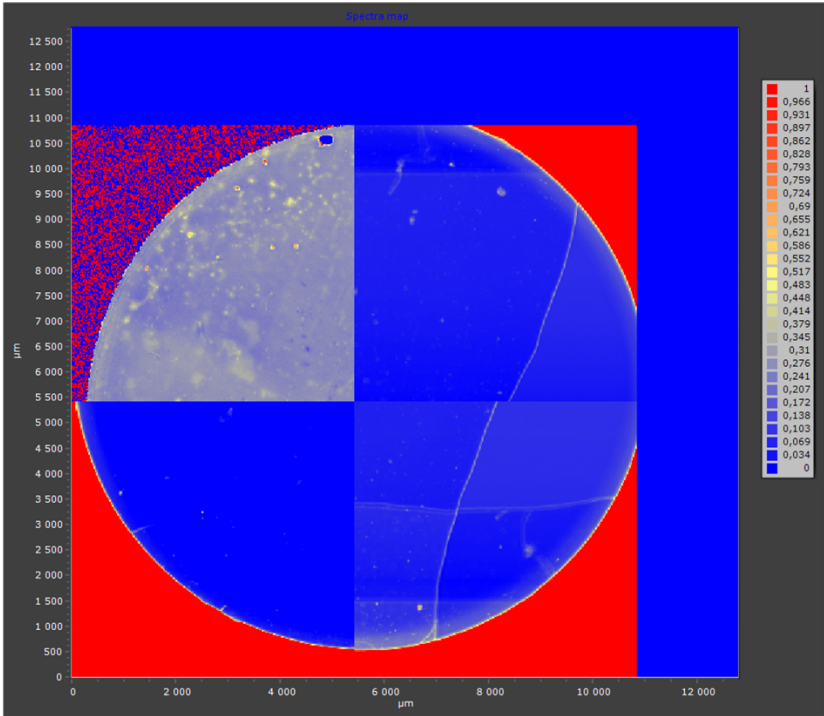


Figure 80B- Heat map of sample #22

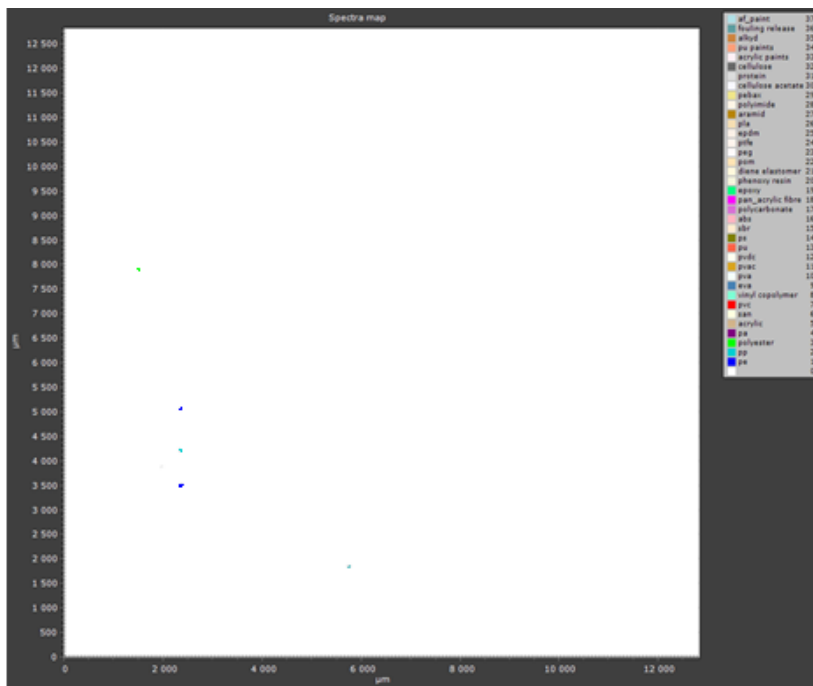


Figure 81B- Spectra map of sample #22

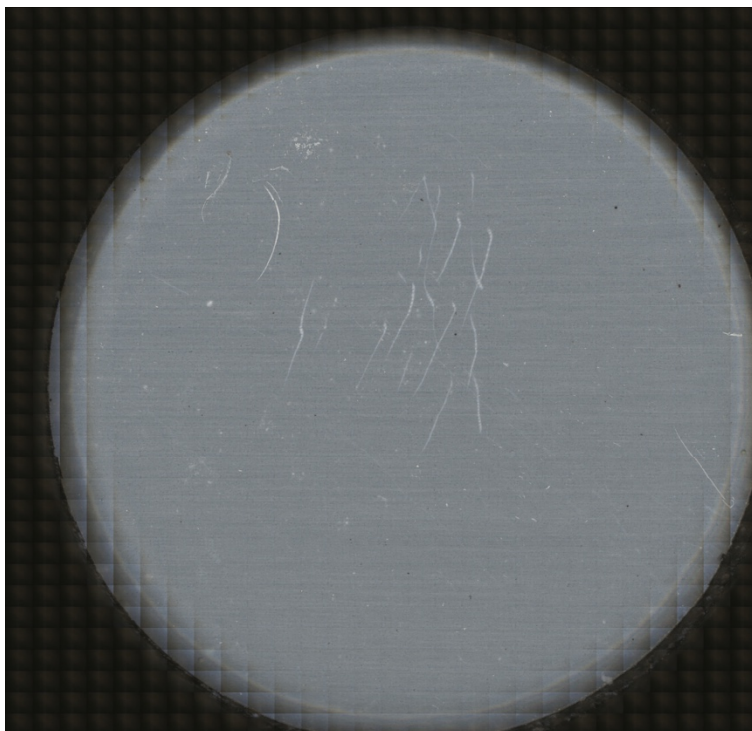


Figure 82B- Filter image of sample #22 blank

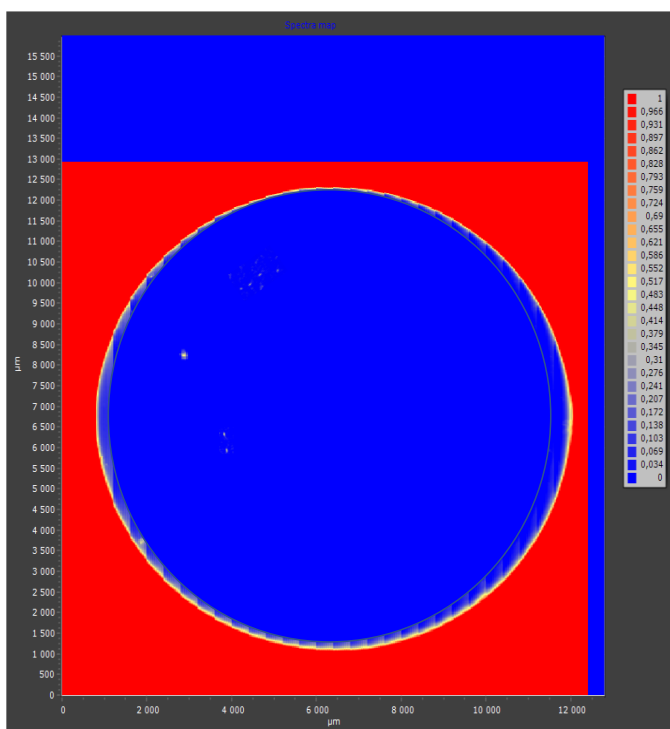


Figure 83B- Heat map of sample #22 blank

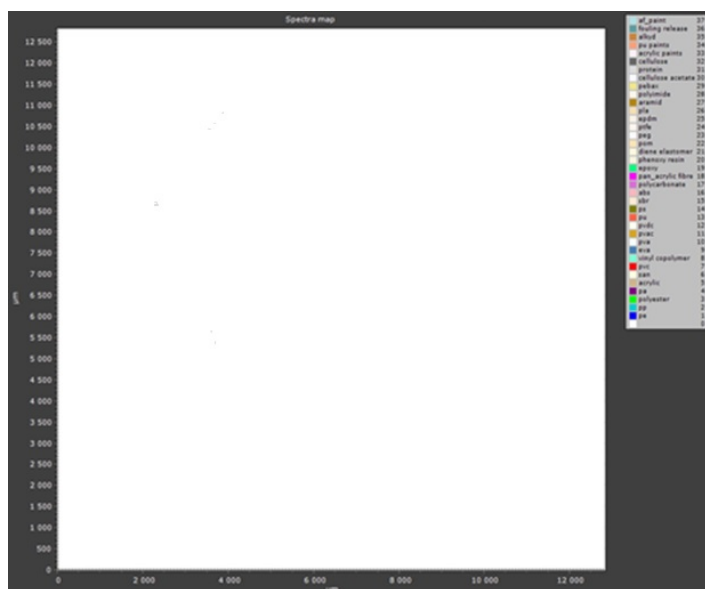


Figure 84B- Spectra map of sample #22 blank

Sample #23

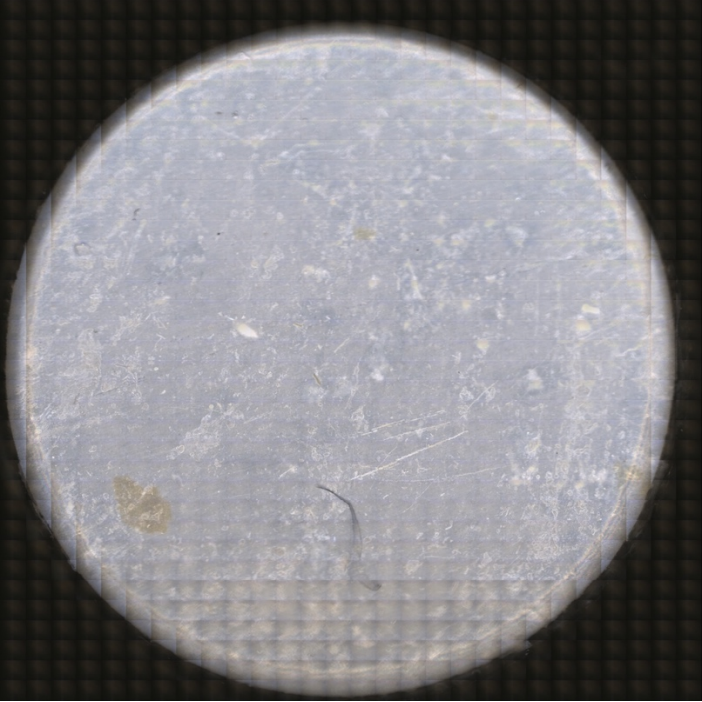


Figure 85B- Filter image of sample #23.

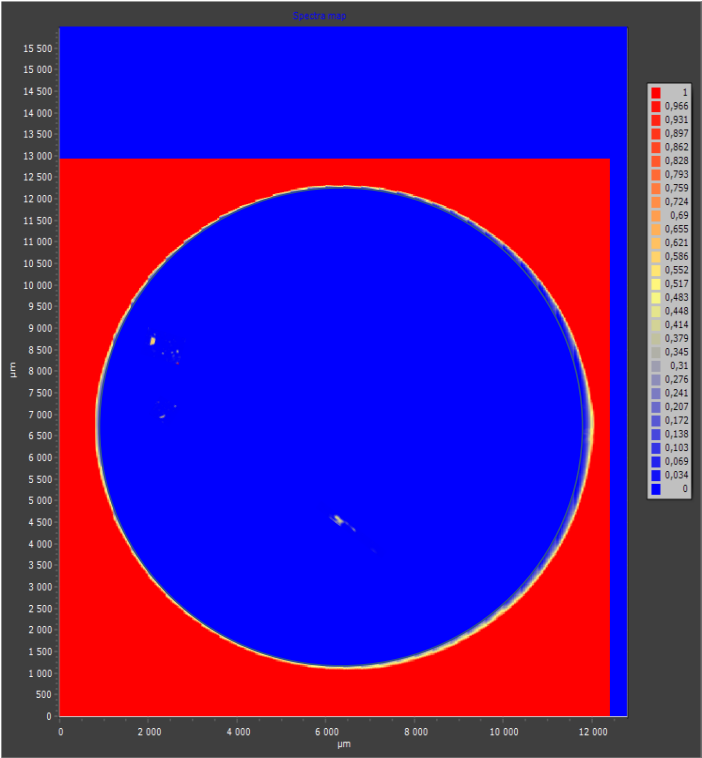


Figure 86B- Heat map for sample #23

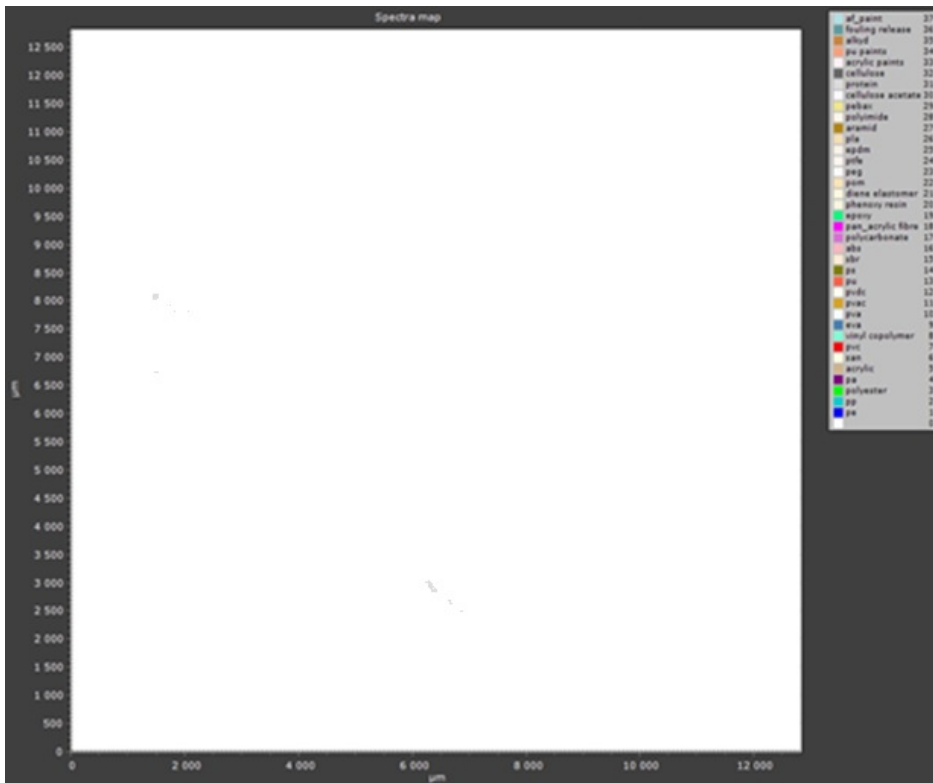


Figure 87B- Spectra map for sample #23.



Figure 88B- Comparison spectra using SiMPle reference library with PE polymers found in the sample (orange) to the standard (blue).

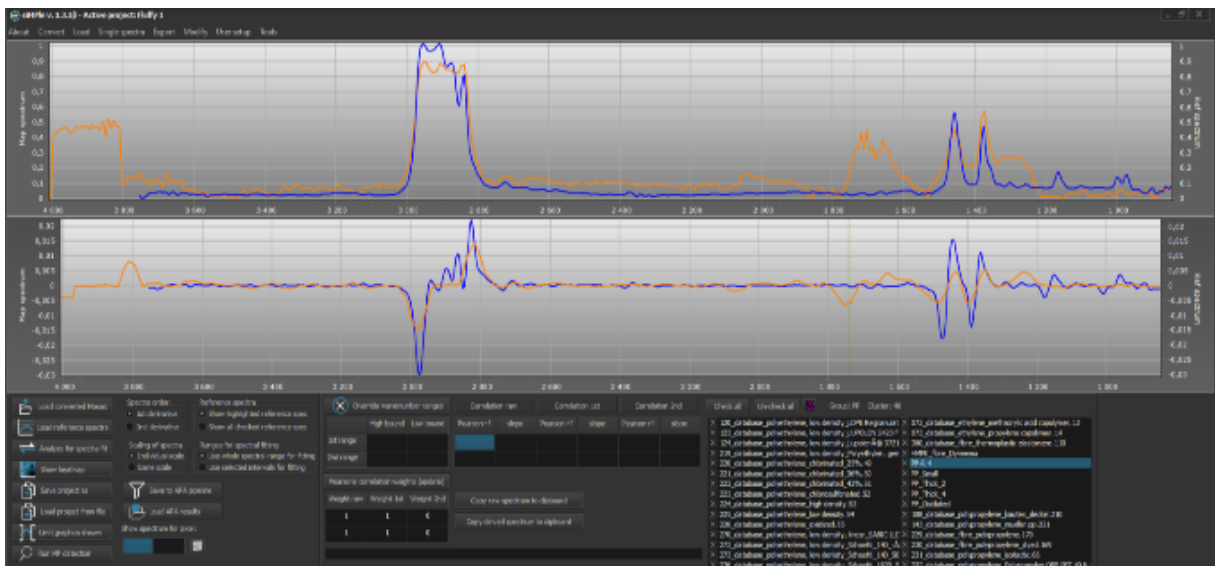


Figure 89B- Comparison spectra using SiMPle reference library with PP polymers found in the sample (orange) to the standard (blue).

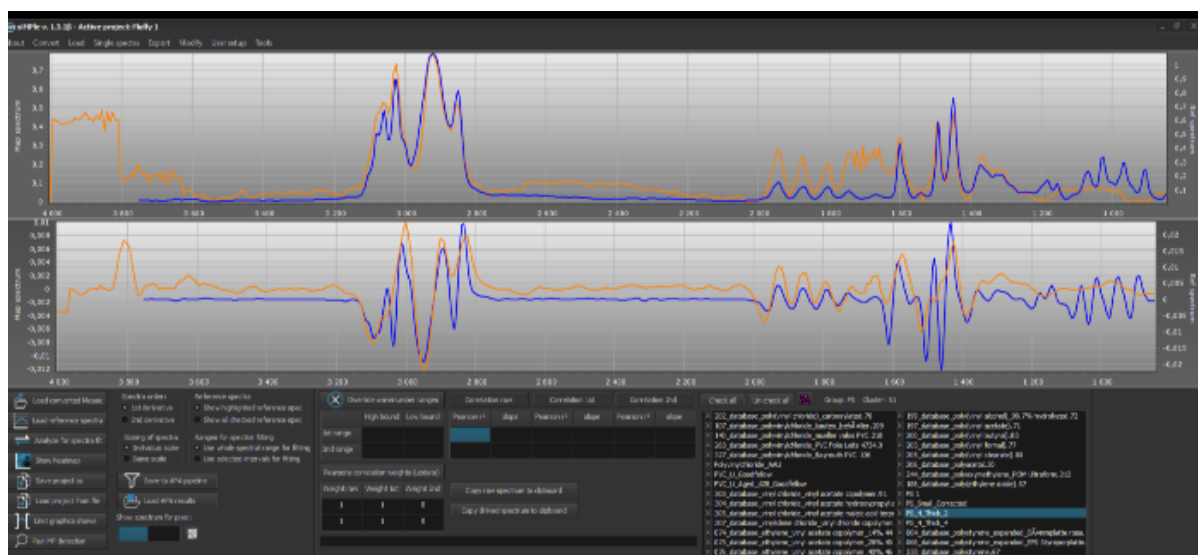


Figure C90- Comparison spectra using SiMPLe reference library with PS polymers found in the sample (orange) to the standard (blue).

No evidence of Microplastic bioaccumulation in muscle tissue



Emilie Hæggernes
University of Bergen
emiliehaeggernes@student.uib.no



Marte Haave
NORCE/UiB
Marte.haave@uib.no
maha@norce-research.no



Alessio Gomiero
NORCE Norwegian Research Centre
algo@norce-research.no

In this novel study, Microplastics (MP, <1mm) were quantified in muscle tissue of wild caught cod resident in a plastic polluted region in Western Norway. The relationship between size/age and MP in muscle tissues were investigated to assess the bioaccumulation and biomagnification potential of MP in the marine food web. The result show no evidence of bioaccumulation of microplastic in muscle tissue.

Highlights

- MP were detected in muscle tissue from 8 of 23 cod from plastic polluted area in Western Norway.
- Particles under 100µm were most abundant
- No apparent accumulation of MP in cod related to size/age
- The size distribution corresponds to previous studies of MP uptake in fish tissue
- Wet traps for QA/QC, used for detecting airborne contamination shows a low number of particles.

Results

- The majority of the 27 microplastic particles were below 100µm and varied from 32-830 µm (Figure 3).
- The highest nMP was 10,3 MP/100g muscle tissue (3,30±1,60 nMP/100g).
- Fragments were the dominant particle shape in both locations.
- Dominating polymers were PP (70%) and PE (64%). The Six polymers identified by µFTIR, are commonly produced worldwide, and include PP > PE > PS > PET > PA > PES (Figure 3).
- 2 PE particles in one wet trap were removed from a sample result.

Sample preparation and analysis

- Dissection of fish and extraction of MP was done in a plastic free environment at NORCE PlastLab (Figure 1C) to limit contamination.
- MP was extracted by gentle enzymatic and oxidative treatments (Figure 1D,E), described in Gomiero et al 2020.
- A spectroscopic method for identification, µFTIR, was applied determining size, shape and polymer.
- SIMPLEx software was used as reference library (Primpke et al 2018).

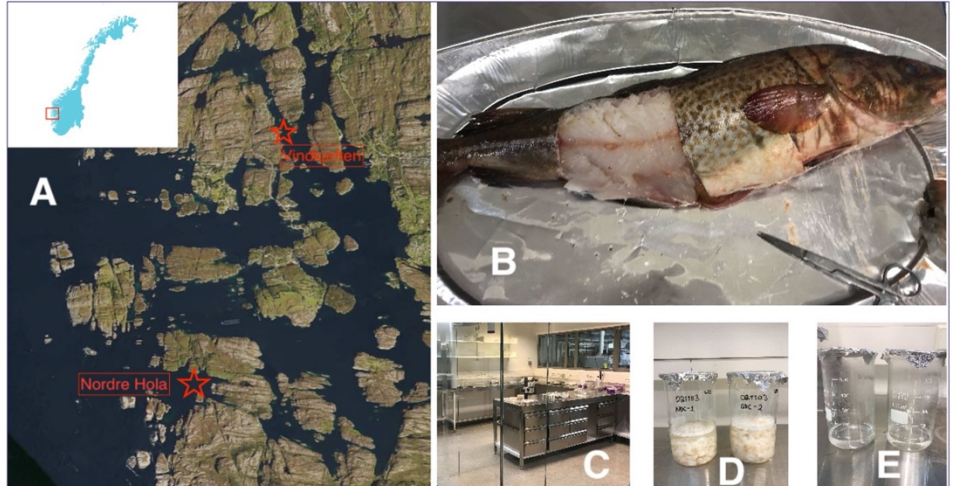


Figure 1. A) Sampling locations on the west coast of Norway, B) Muscle tissue dissection of cod (*Gadus morhua*), C) NORCE PlastLab, D-E) Sample preparation for purification and isolation method, from pre-treatment in SDS (D) to enzymatic oxidative treatment to remove proteins and fats (E).

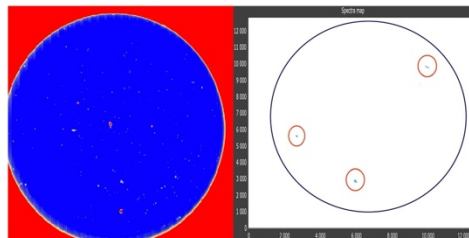


Figure 2. µFTIR filter image and spectra map for detected PP polymers

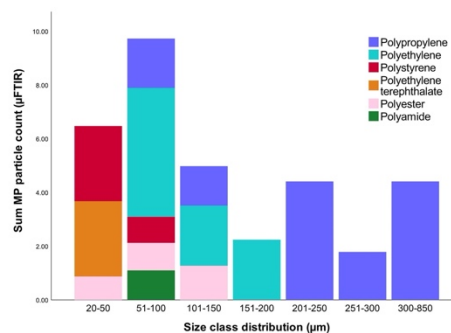


Figure 3. Sum of MP particles in cod (nMP/100g) after µFTIR analysis per size class

Observed MP in cod was not related to size and age

There was no relationship between the number of isolated microplastic particles per fish and the length of the fish (as a proxy for age).

This indicates no bioaccumulation or potential biomagnification.

The number of fish with MP are however low, which hampers statistical analyses.

Conclusion

- The present study demonstrated that current µFTIR methods are sufficient to identify MP (>20µm) in cod muscle tissue.
- Current methods indicate that MP is not present in all cod.
- Results show that MP is not related to size/age, indicating no bioaccumulation of MP in cod.
- A larger sample size is needed to fully elucidate the potential bioaccumulation of MP in marine wild-life.
- More research is needed to assess the risk of MP in the marine environment and its fate in the food web

Gomiero, A., Haave, M., Kågel, T., Bjørøy, Ø., Gjessing, M., Berg Lea, T., Horve, E., Martins, C., & Olafsen, T. (2020b). Tracking of Plastic emissions from aquaculture industry (TrackPlast) (NORCE report 04-2020).
Primpke, S., Wirth, M., Lorenz, C., & Gerdt, G. (2018). Reference database design for the automated analysis of microplastic samples based on Fourier transform infrared (FTIR) spectroscopy. *Anal Bioanal Chem*, 410(21), 5131-5141.

Thanks to Kenneth Bruvik (Norwegian Hunters and Anglers' Association/ NJFF) for providing samples and essential local knowledge for this study and pupils from NJFF/TAM for catching cod for the project. Thanks to Veslemøy Narvestad and Adrián Jaén-Gil (NORCE) for general contribution and assistance during laboratory work. Thanks to all involved personnel from NORCE for valuable assistance.



NORCE Norwegian Research Centre AS
www.norce-research.no